Mesenchymal Stem Cells Induce Recovery After Stroke by Regulation of Inflammation and Oligodendrogenesis

BY

MATTHEW KYLE TOBIN
B.S., University of Michigan, Ann Arbor, MI, 2011

THESIS

Submitted as partial fulfillment of the requirements
for the degree of Doctor of Philosophy in Neuroscience
in the Graduate College of the
University of Illinois at Chicago, 2020

Chicago, Illinois

Defense Committee:

John Larson, Psychiatry – Chair
Orly Lazarov, Anatomy and Cell Biology – Advisor
Richard Minshall, Anesthesiology, Pharmacology
Fernando Testai, Neurology and Rehabilitation Medicine
Larry Tobacman, Medicine

DEDICATION

To my grandparents, Earl and Elaine Liff and Cal and Joan Tobin. Through 60+ years of marriage, they have shown me what unbridled love and support is both for each other and for their families. They have always supported and encouraged my goals and aspirations and for that I will be forever grateful.

ACKNOWLEDGMENTS

I would first like to acknowledge several of my high school science teachers, Cheryl Byrnes, Barb Obinger, and Heather (Heidorn) Hernandez, all three of whom first introduced me to the world of chemistry and biology and started me down this path to a career as a physician scientist. Without their enthusiasm for teaching and genuine care and interest for their students I may never have thought about spending a lifetime learning about all science and medicine have to offer.

Next, I would like to thank all of the academic mentors I have had throughout the years. First, Drs. John Fink and Shirley Rainier, my two mentors as an undergraduate at the University of Michigan. From them I learned the foundations of scientific inquiry and the fundamentals to build a career in academic medicine. I would also like to thank the UIC MSTP for taking a chance on me as a first-year medical student applying to the MSTP. I would next like to acknowledge the entire Department of Neurosurgery at the University of Illinois at Chicago, specifically Drs. Fady Charbel, Konstantin Slavin, Sergey Neckrysh, and Ankit Mehta, all of whom have been incredibly generous mentors to me allowing me to be an active participant both in research and clinical care during my tenure as a student at UIC.

Next, I want to thank Dr. Amelia Bartholomew for allowing me to work with and learn from her during my first two years of medical school. She showed me that it is possible to be a successful scientist, physician, and educator. I next want to thank my graduate advisor, Dr. Orly Lazarov, for her patience and support during my time in the lab. She gave me the opportunities to pursue research interests that were difficult and

pushed me both mentally and physically. I am incredibly grateful and fortunate to have had the opportunity to grow and learn under her mentorship during my training. I want to thank the members of my thesis committee, Drs. John Larson, Fernando Testai, Rich Minshall, and Larry Tobacman for their advice during my committee meetings, and for their continued support outside of those meetings. Their guidance has been instrumental in developing this dissertation.

I would also like to acknowledge the other members of the Lazarov lab, past and present, who helped foster a productive and supportive lab environment: Jacqueline Bonds, Caryn Davis, Ahmed Disouky, Aashu Shetti, Kianna Musaraca, Dr. Carolyn Hollands, Dr. Nancy Bartolotti, Dr. Rachana Mishra, and Dr. Yeshwant Kurhe. I would also especially like to thank Kyra Lopez, an undergraduate student in the lab, who spent countless hours performing data acquisition for me, without whom, large portions of this dissertation would not exist. I would also like to acknowledge the entire Department of Anatomy and Cell Biology, especially the lab of Dr. Ernesto Bongarzone which has been generous enough to provide materials used in this dissertation and guidance and advice about experimental questions.

I next want to thank Dr. Weiguo Li, the director of the Preclinical Imaging Core in the UIC Research Resources Center and his graduate student, Jin Gao, for their help with the MRI studies. I would like to also thank Dr. Stephanie Cologna, and her student Melissa Pergande, from the Department of Chemistry, for their help and collaboration with the mass spectrometry studies. I want to also thank our funding sources that supported this work including the National Institute of Aging, the National Institute of Allergy and

Infectious Disease, the National Heart, Lung, and Blood Institute, the UIC Center for Clinical and Translational Science, and the American Heart Association.

Finally, and most importantly, I would like to thank my friends and family for their unconditional love throughout my life. They have been a constant source of support through the good and the bad and, without them, I may never have finished.

MKT

TABLE OF CONTENTS

LIST OF TABLES

LIST OF FIGURES

FIGURE PAGE

LIST OF FIGURES (continued)

FIGURE PAGE

LIST OF FIGURES (continued)

FIGURE PAGE

LIST OF ABBREVIATIONS

µg	microgram
µL	microliter
µm	micrometer
µM	micromolar
7-AAD	7-aminoactinomycin D
Å	ångström
aMSCγ	interferon-gamma-activated mesenchymal stem cell
ANOVA	analysis of variance
BBB	blood brain barrier
BCA	bicinchoninic acid
BDNF	brain-derived neurotrophic factor
bFGF	basic fibroblast growth factor
BrdU	5-bromo-2'-deoxyuridine
BSA	bovine serum albumin
CAx	cornu ammonis region (e.g. CA1, CA3)
CCA	common carotid artery
CD	cluster of differentiation (e.g. CD29, CD90, etc)
CFSE	carboxyfluorescein succinimidyl ester
cm	centimeter
CNPase	2',3'-cyclic-nucleotide 3'-phosphodiesterase
CNS	central nervous system
CP	choroid plexus

LIST OF ABBREVIATIONS (continued)

DAPI	4’,6-diamidino-2-phenylindole
DCX	doublecortin
DDA	data dependent acquisition
DG	dentate gyrus
$DiIC_{18}(5)$-DS acid	1,1’-dioctadecyl-3,3,3’,-3’-tetramethylindodicarbocyanine-5,5’-disulfonic
DMEM	Dulbecco’s modified Eagle’s medium
DNase I	deoxyribonuclease I
DPBS	Dulbecco’s phosphate buffered saline
DTT	dithiothreitol
DWI	diffusion weighted imaging
ECA	external carotid artery
ECM	extracellular matrix
EDTA	ethylenediaminetetraacetic acid
EGF	epidermal growth factor
FBS	fetal bovine serum
FDR	false discovery rate
FITC	fluorescein isothiocyanate
FOV	field of view
GCL	granule cell layer
GDNF	glial cell line-derived neurotrophic factor
GFAP	glial fibrillary acidic protein

LIST OF ABBREVIATIONS (continued)

HBSS	Hank's balanced salt solution
HCD	higher-energy collisional dissociation
HCl	hydrochloric acid
ID	inner diameter
Iba1	ionized calcium-binding adapter molecule 1
ICA	internal carotid artery
ICAM-1	intercellular cell adhesion molecule 1
IFN-γ	interferon-gamma
IL-x	Interleukin (e.g. IL-4, IL-6, etc)
iNOS	inducible nitric oxide synthase
I-R	ischemia-reperfusion
IV	intravenous
kDa	kilodalton
kg	kilogram
LC-MS/MS	liquid chromatography tandem mass spectrometry
LPS	lipopolysaccharide
LV	lateral ventricle
M	molar
MBP	myelin basic protein
MCA	middle cerebral artery
MCAO	middle cerebral artery occlusion
MEMα	minimal essential medium alpha

LIST OF ABBREVIATIONS (continued)

MFGE8	milk fat globule-EFG factor 8 protein
MHC-II	major histocompatibility complex II
mL	milliliter
MMP	matrix metalloproteinase
mNSS	modified neurological severity score
MPO	myeloperoxidase
MRI	magnetic resonance imaging
MS	multiple sclerosis
MSC	mesenchymal stem cell
NGF	nerve growth factor
nMSC	naïve mesenchymal stem cell
NO	nitric oxide
NPC	neural progenitor cell
NSC	neural stem cell
NT3	neurotrophin-3
OGD	oxygen-glucose deprivation
OPC	oligodendrocyte progenitor cell
PAGE	polyacrylamide gel electrophoresis
PBS	phosphate buffered saline
PDGF	platelet-derived growth factor
PDGFRα	platelet-derived growth factor receptor alpha
PFA	paraformaldehyde

LIST OF ABBREVIATIONS (continued)

qRT-PCR	quantitative reverse transcription polymerase chain reaction
RF	radiofrequency
RMS	rostral migratory stream
ROS	reactive oxygen species
SAE	serious adverse events
SCID	severe combined immunodeficiency
SDS	sodium dodecyl sulfate
SEM	standard error of the mean
SEMS	spin echo multi slice
SGL	subgranular layer
SHH	sonic hedgehog
SVZ	subventricular zone
T	Tesla
T3	triiodothyronine
TBS	tris buffered saline
TE	echo time
TEAB	trethylammonium bicarbonate
TGF-β	transforming growth factor beta
T_H	Helper T cell
TIA	transient ischemic attack
TMT	tandem mass tag
TNF-α	tumor necrosis factor alpha

LIST OF ABBREVIATIONS (continued)

t-PA	tissue plasminogen activator
TR	repetition time
U	units
VAP-1	vascular adhesion protein 1
VCAM	vascular cell adhesion molecule
γδ	gamma delta

1. INTRODUCTION

1.1. Summary

Stroke is the fourth leading cause of death annually in the United States and is the most common cause of permanent disability in adults worldwide. Nearly 90% of all stroke victims experience an ischemic event with this percentage increasing if one includes hemorrhagic stroke patients who may experience delayed ischemic events resulting from vasospasm. Current treatment options for ischemic stroke patients is limited with only one FDA-approved drug, the thrombolytic agent tissue plasminogen activator (t-PA). Tissue plasminogen activator has several shortcomings including limited efficacy, short therapeutic window, and the potential risk of hemorrhagic transformation. Furthermore, only 4% to 7% of all acute ischemic stroke patients are treated with t-PA, a statistic highlighting the urgency for development on novel and effective treatment strategies.

While the exact mechanism(s) responsible for the brain damage occurring after an ischemic insult is/are not fully elucidated, there is an increasing amount of evidence demonstrating that post-ischemia inflammation contributes to the pathogenic process. Ischemia not only acutely damages the ischemic core but causes more long-term damage in the surrounding ischemic penumbra. The last decade has produced significant amounts of evidence supporting the existence of neurogenesis in the adult mammalian brain. The participation of neural stem cells (NSC) in adult neurogenesis has garnered interest to the members of the scientific community about the ability to utilize these cells for brain repair. How post-ischemia inflammation interacts with neurogenesis has not been fully studied and gaining a better understanding of this relationship could help develop new therapeutic options for brain recovery. Modulation of post-ischemia

inflammation and neurogenesis may provide novel strategies to promote brain repair after ischemic stroke. Mesenchymal stem cells (MSC) offer a unique tool for studying brain repair mechanisms because of their unique ability to regulate the phenotype of microglia and to promote neural stem cell survival and proliferation via secretion of neurotrophic factors. Investigating the utility of MSCs in a stroke setting may offer an exciting new treatment option for stroke patients.

1.2. Significance

With the increasing number of aging adults, the incidence and prevalence of stroke is only going to go up. Current therapeutic options for these patients, especially in the acute setting, is extremely limited and are often ineffective at promoting long-term functional recovery. Therefore, it is essential that new strategies be developed to treat this ever-expanding patient population. The work in this proposal offers a novel, exciting treatment approach for this patients that could promote functional brain repair in stroke victims. If successful, the therapies proposed would have long-lasting impact for both the patients themselves and the families of these patients.

1.3. Statement of Hypothesis

The central hypothesis for this dissertation is that mesenchymal stem cells can promote functional recovery following ischemic stroke by reducing proinflammatory signaling and by enhancing neurogenesis.

1.4. Specific Aims

Specific Aim 1: Determine the effect of ischemia-induced reactive microglia on neurogenesis.

1.1 Hypoxia and ischemia induce microglia towards an inflammatory phenotype. Experiments will examine ischemia-induced microglia phenotype *in vivo and in vitro*, including examination of morphologic characteristics, expression of the pro-inflammatory markers CD11b, MHC-II, CD40, and CD86, levels of secreted TNF-α, IL-1β, IL-6, IL-10, and IL-4, and phagocytic capacity.

1.2 Release of soluble factors by activated microglia following ischemia negatively regulates neurogenesis and brain repair. Using co-culture of NSCs with microglia under both OGD and normoxia, experiments will examine the effect on NSC proliferation, survival, and differentiation. Additionally, experiments will attempt to identify the effect of microglial secreted cytokines on NSC proliferation, survival, and differentiation by culturing NSCs in OGD-preconditioned microglia media. Spatial activation of microglia and their phenotype following ischemia will be examined in rat brain sections following MCAO.

Specific Aim 2: Determine the potential for MSC-induced regeneration following ischemic stroke.

2.1 Treatment with IFN-γ activated mesenchymal stem cells reduces infarct volume and increases functional recovery following stroke and promotes

the conversion of activated microglia from the inflammatory phenotype to the regenerative phenotype following stroke. Examination of infarct volume will serve as an indicator for extent of brain damage following intravenous MSC treatment. Functional recovery will be assessed via numerous neurobehavioral tests including the modified neurological severity score and open field analysis. Co-culture experiments of MSCs and microglia will be utilized to assess *in vitro* phenotypic change in microglia activation under OGD conditions.

2.2 Treatment with IFN-γ activated mesenchymal stem cells promotes the survival of neural progenitor cells following stroke and enhances brain repair. These experiments will examine the effect of intravenous MSC treatment on neurogenesis following MCAO. In addition, MSCs will be co-cultured with NSCs to examine the effect on survival and proliferation of NSCs *in vitro* following OGD.

2. BACKGROUND

2.1. Ischemic Stroke

Stroke is the fourth leading cause of death annually in the United States (Towfighi and Saver 2011) and is the most common cause of permanent disability in adults worldwide (Donnan, Fisher et al. 2008, Go, Mozaffarian et al. 2014). Nearly 90% of all stroke victims suffer from an ischemic event caused by the sudden blockage of blood flow from a thrombus or embolism (Lakhan, Kirchgessner et al. 2009, Towfighi and Saver 2011). This percentage is even higher if one includes hemorrhagic stroke patients who may experience delayed ischemic events arising from arterial or arteriolar vasospasms associated with subarachnoid hemorrhage. Although the exact mechanism(s) responsible for the brain damage occurring following an ischemic insult is/are not fully understood, there is an increasing amount of evidence suggesting that post-ischemia inflammation is a significant contributing factor to the pathogenic process. Ischemia is accompanied by a rapid increase in inflammatory mediators causing irreversible damage to neurons in the ischemic core, with more long-term consequences ultimately appearing in the ischemic penumbra. However, those pathologies can be largely ameliorated via prompt restoration of blood flow. Clinically, this reperfusion can occur spontaneously or via the use of either pharmacological thrombolysis or endovascular thrombectomy. At the present time, the thrombolytic agent tissue plasminogen activator (t-PA) constitutes the only FDA-approved therapy for acute ischemic stroke. However, t-PA has several shortcomings including the potential risk of hemorrhagic transformation, therapeutic window limited to 3 hours from time of symptom onset, and limited efficacy, among others. Data obtained from the Get With The Guidelines-Stroke database shows that only 4-7%

of all the acute ischemic stroke patients are treated with t-PA (Schwamm, Ali et al. 2013), an observation that highlights the need for novel and effective therapeutic approaches.

The last decade or so has produced large amounts of evidence supporting the existence of neurogenesis in adult mammals. Mammalian brains contain neural stem cells (NSCs) that have the ability to self-renew, proliferate, and differentiate into multiple lineages (Lazarov, Mattson et al. 2010). The participation of these cells in the process of adult neurogenesis has attracted interest among members of the research community, especially with respect to their use as possible therapeutic options for brain repair. Both transplantation of NSCs and the utilization of endogenous progenitor cells appear to be plausible strategies for brain injury repair. Exploring the interactions between inflammation and neurogenesis has not been fully studied, and gaining a better understanding of the relationship between these two processes could help in the development of new and exciting therapeutic options for brain repair.

Ischemic stroke causes damage as a result of primary and secondary insults mediated by ischemia and inflammation. Primary injury results from the initial ischemic period, which deprives the brain of oxygen and vital nutrients, such as glucose, critical for survival of CNS cells. Neurons in the infarcted tissue die as a result of the initial injury whereas cells in the penumbra are affected by the rapid influx of immune cells, reactive oxygen species, and toxic inflammatory mediators (Borgens and Liu-Snyder 2012). Current therapeutic options for ischemic stroke, and the less damaging transient ischemic attack (TIA), are aimed at dissolving the clot, which is causing the blockage of blood flow and reestablishing perfusion of the infarcted area. While these strategies are beneficial, reperfusion can also further the injury by increasing local inflammation and inducing

chronic changes in axonal structure and function which can increase neuronal damage (Zhang, Gao et al. 2012).

There are a number of strategies currently under investigation in the preclinical setting aimed at restoring brain function following ischemic insult. These strategies concentrate not at blood flow restoration but rather at inducing neuroprotection and salvaging brain function following the initial injury. Pharmacologic hypothermia, induced by the TRPV1 channel agonist dihydrocapsaicin, has been shown to be neuroprotective if given within 90 minutes of reperfusion following transient middle cerebral artery occlusion (MCAO) in mice (Cao, Balasubramanian et al. 2014). Furthermore, the pharmacologic agent, LJP-1586, which targets and inhibits leukocyte trafficking has been shown to confer neuroprotection following MCAO in a rat model of ischemic stroke (Watcharotayangul, Mao et al. 2012). Additionally, by preventing interactions of the Receptor for Advanced Glycation Endproducts (RAGE) with its ligands (e.g., High-Mobility Group Box-1 [HMGB-1] and S100B), one can promote corresponding reductions in post-ischemic neuroinflammation and neuropathology (Thored, Heldmann et al. 2009).

2.2. Neuroinflammation

2.2.1. Inflammation in the Mammalian Brain

In the intact brain, trafficking of cellular and molecular components from the peripheral circulation is regulated by the blood brain barrier (BBB). However, following brain injury, the tight junctions between endothelial cells of the BBB become permeable, allowing peripheral immune cells to infiltrate brain parenchyma. These cells, along with the proinflammatory cytokines they secrete, contribute to the inflammatory response that

follows brain injury. Acute inflammation arises both from responses of resident immune cells, the microglia, as well as from infiltrating immune cells of the peripheral circulation (Aktas, Ullrich et al. 2007). Inflammation of the mammalian brain, however, is not only a response mechanism that follows CNS injury, such as from traumatic brain injury, spinal cord injury, and stroke. It is also often a large contributing factor to neurological diseases such as Alzheimer's disease, amyotrophic lateral sclerosis, multiple sclerosis, and Parkinson's disease (Minghetti 2005, Eikelenboom, Veerhuis et al. 2006). Chronic inflammation and the release of proinflammatory molecules from immune cells have also been implicated as causative factors of neurodegeneration and CNS disorders (Eikelenboom, Veerhuis et al. 2006, del Zoppo and Gorelick 2010). The term "inflammation," and subsequently the "inflammatory response," seek to combine many different processes and pathways into one unified theme when, in fact, they are distinct pathways that have different downstream consequences. Therefore, it is imperative to keep in mind that, while all of the aforementioned pathologies and pathologic states have an inflammation-related component to them, the specific inflammatory response could be, and most likely is, very different among the various diseases and injuries.

Susceptibility to stroke and subsequent prognosis are highly influenced by peripheral inflammatory cells. Numerous inflammatory cells, including neutrophils, macrophages, and T cells, are recruited to sites of ischemic injury (Jin, Yang et al. 2010). The mechanism by which these cells decrease neurogenesis following ischemic injury, and the way in which they affect NSCs, remains largely unknown. Post-ischemic inflammation is characterized by microglia activation followed by infiltration of circulating inflammatory cells (Schilling, Besselmann et al. 2003, Tanaka, Komine-Kobayashi et al.

2003, Kriz 2006, Amantea, Nappi et al. 2009, Jin, Yang et al. 2010). Acutely, reactive oxygen species and inflammatory mediators cause endothelial cell and leukocyte expression of adhesion molecules, promoting the adhesion and migration of circulating leukocytes that leads to a rapid inflammatory state at the site of injury. These leukocytes further release inflammatory cytokines that lead to tissue damage in the injury site and the ischemic penumbra (Figure 1).

Like any ischemia-reperfusion (I-R) injury, a large portion of the damage is due to the inflammatory cascade which follows reperfusion. This response results in an increase in toxic inflammatory mediators including, but not limited to, IL-1β, IL-6, IL-8, and TNF-α (Janardhan and Qureshi 2004). An increase in these molecules is sufficient to induce neuronal apoptosis within the infarcted tissue, ultimately causing irreversible brain damage. In addition to the presence of these classical inflammatory molecules, NO is dramatically increased following ischemia. While NO is neuroprotective at low levels (Fiscus, Yuen et al. 2002), high levels, such as those observed following I-R injury, have been shown to be pathologic as well as pro-apoptotic by further increasing ROS production (Fiscus, Yuen et al. 2002). These mechanisms are universal to all I-R type injuries and are not unique to cerebral ischemia. However, because neurons are especially sensitive to ischemia, it is critical to understand the neural response to inflammation following ischemia-reperfusion in order to begin contemplating therapies for such injuries.

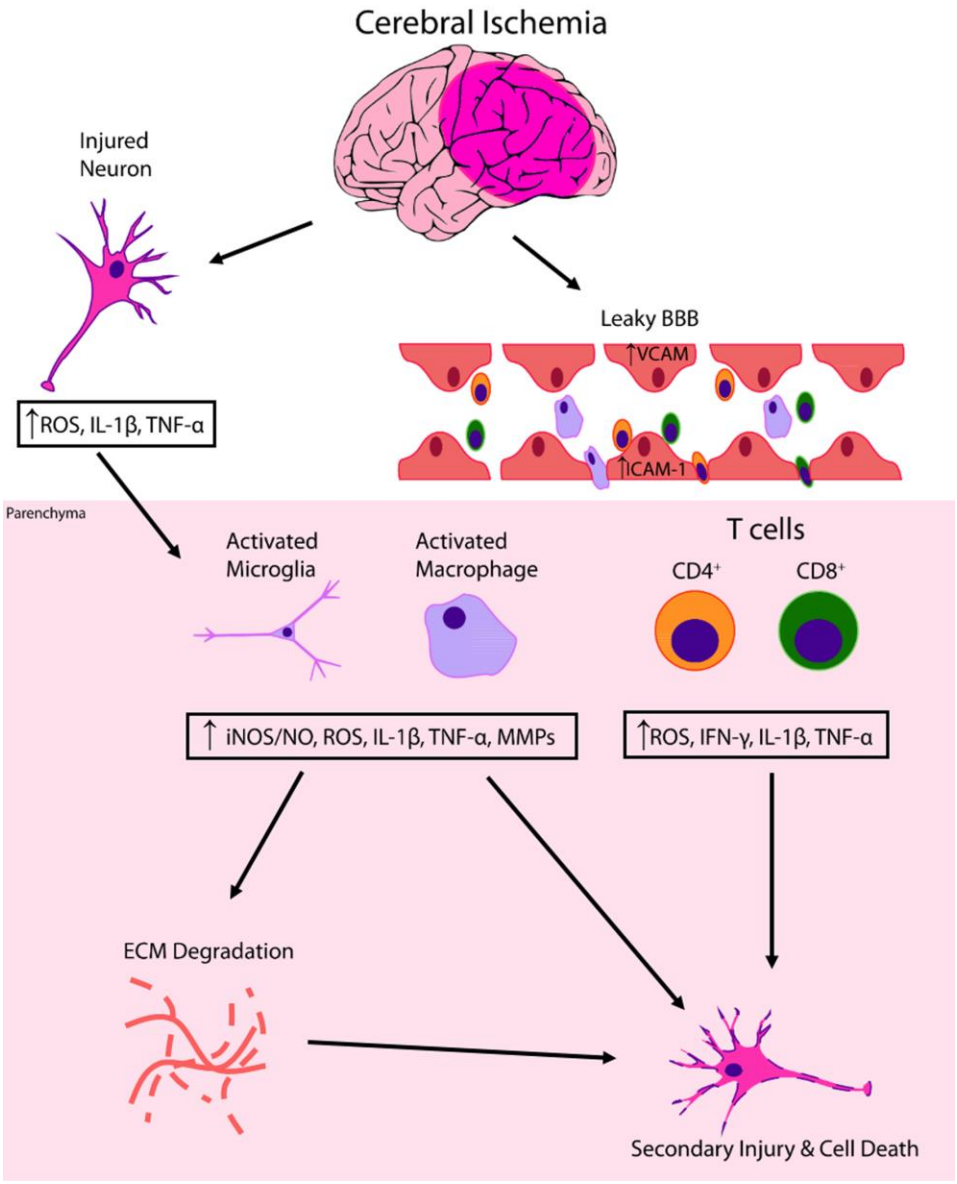

Figure 1. Inflammatory cascade leading to secondary brain inflammation and cell death following ischemic injury. Cerebral ischemia alone leads to both an initial cell necrosis and generation of ROS and proinflammatory molecules like IL-1β and TNF-α from injured neurons as well as inducing BBB dysfunction with loosening of cell-to-cell tight junctions between endothelial cells and upregulation of endothelial cell expression of various cell adhesion molecules (e.g. VCAM, ICAM-1). This increase causes adherence, migration, and extravasation of circulating leukocytes into the brain parenchyma. When in the brain, leukocytes and activated microglia generate a variety of proinflammatory molecules like iNOS, MMPs, IL-1β and TNF-α, and continue to generate ROS. These events lead to secondary brain injury, increased inflammation, and ultimately cell death. Abbreviations: VCAM – vascular cell adhesion molecule; ICAM-1 – intercellular cell adhesion molecule 1; ROS – reactive oxygen species; iNOS – inducible nitric oxide synthase; NO – nitric oxide; MMPs – matrix metalloproteinases; ECM – extracellular matrix. From Tobin et al (Tobin, Bonds et al. 2014).

2.2.2. Peripheral versus Resident Immune Response Following Ischemic Injury

It is well established that the brain, under normal physiological conditions, is "immune privileged," meaning peripheral immune cells do not have access to the brain (Rezai-Zadeh, Gate et al. 2009). This status is maintained by the BBB. Under such conditions, immune surveillance in the CNS is performed by resident microglia. When the BBB becomes dysfunctional, as occurs after injury, circulating immune cells can gain direct access to the brain. The relative contributions to the inflammatory response from peripheral immune cells and resident immune cells following injury, though, need to be further elucidated.

Acutely (4-24 hours) following ischemic injury, circulating immune cells begin to adhere to, and migrate along, the damaged endothelium lining the cerebral vasculature and start to infiltrate into brain parenchyma due to breakdown of the BBB (Stevens, Bao et al. 2002). Macrophages, which reside in the perivascular space in the glia limitans, are a large driving force behind infiltration of peripheral immune cells into the brain parenchyma (Konsman, Drukarch et al. 2007). Macrophages exist in multiple states which are phenotypically and functionally distinct. M1 type macrophages are proinflammatory and secrete numerous inflammatory mediators such as tumor necrosis factor (TNF)-α, interleukin (IL)-1β, IL-8, IL-12, and reactive oxygen species (ROS) (Mantovani, Sica et al. 2005, Iadecola and Anrather 2011). M2 type macrophages are anti-inflammatory in nature and secrete anti-inflammatory cytokines like IL-10, TGF-β, and arginase (Mantovani, Sica et al. 2005, Iadecola and Anrather 2011). Due to secretion of factors by macrophages, namely IL-8, and by binding to cell adhesion molecules on endothelial cells, neutrophils infiltrate the brain and release their secretory granules which include various

proinflammatory molecules such as nitric oxide (NO), myeloperoxidase, multiple matrix metalloproteinases, and elastase (Yilmaz and Granger 2010, Iadecola and Anrather 2011). Secretion of these factors by both macrophages and neutrophils initiates the acute phase of the innate immune response.

Following macrophage and neutrophil infiltration, lymphocytes begin to infiltrate the brain as well (Stevens, Bao et al. 2002). Under normal conditions, naïve T cells are not capable of migrating through the BBB to enter the brain. However, following injury, activated $CD4^+$ and $CD8^+$ T cells can enter the brain in an antigen- and Major Histocompatibility Complex (MHC)-independent fashion (Hickey, Hsu et al. 1991, Stenzel and Alber 2008). Additionally, there is evidence showing the presence of CNS-specific T cells located within the choroid plexus (CP) that promotes leukocyte trafficking into the CNS following injury (Kunis, Baruch et al. 2013, Schwartz, Kipnis et al. 2013). Approximately 15% of these CP T cells are $CD4^+$ T_H1 cells which secrete IFN-γ which is critical for the further recruitment of immune cells (Kunis, Baruch et al. 2013, Schwartz, Kipnis et al. 2013). These T_H1 cells further stimulate cytotoxic $CD8^+$ T cells, which secrete the membrane-permeabilizing molecule perforin and induce apoptosis via granzyme-induced caspase activation or via activation of the Fas ligand pathway. In addition to T_H1 cells, T_H2 cells secrete numerous interleukins (IL-4, 5, 9, 10, and 13) which are important for activation and recruitment of cells, namely B cells, involved in the humoral immune response. In the case of ischemic injury, the humoral immune response is less important; however, in infectious processes and degenerative diseases like multiple sclerosis, this response is crucial for development of pathology. In addition to helper T cells, a small population of γδ T cells has been implicated in both cytotoxicity and protective immune

modulation. It is unclear, however, what their role is in neuroinflammation (Iadecola and Anrather 2011).

While the peripheral immune response is an extremely important factor in neuroinflammation, the response of activated microglia is of equal, if not more, importance. Resting microglia are the resident immune cells of the brain and their job is to actively survey the brain. Like peripheral antigen-presenting cells, microglia are continuously extending and retracting their processes looking for any signs of damage. Similar to macrophages, microglia also exist in two different states, the M1 and M2 phenotypes (Aguzzi, Barres et al. 2013). Upon activation, as occurs in ischemic injury, microglia take on the M1 phenotype and secrete various proinflammatory molecules including IL-1β, TNF-α, and ROS. Additionally, microglia can take on the M2 phenotype and secrete the anti-inflammatory molecules IL-10 and TGF-β which govern the resolution of post-ischemic inflammation and as well as growth factors implicated in brain repair (IGF-1 and GDNF) (Iadecola and Anrather 2011, Schwartz, Kipnis et al. 2013). Table 1 summarizes many of the molecules that are known to be released during brain injury and their functions associated with the inflammatory cascade. This table is not exhaustive but highlights what are thought to be the most important signaling molecules associated with neuroinflammation.

Neuroinflammation following ischemic stroke is, for the most part, a self-limiting event. However, unlike systemic inflammation which subsides due largely in part to exhaustion of inflammatory mediators, resolution of inflammation in the brain seems to be an active process in which inflammatory mediators are suppressed by regulatory mechanisms (Iadecola and Anrather 2011). Among these suppressor molecules are

arachadonic acid derivatives such as lipoxins, resolvins, and protectins (Spite and Serhan 2010). Furthermore, resolution of inflammation in the brain, similar to systemic inflammation, involves clearing of dead and dying cells primarily via the phagocytic activity of activated microglia with help from infiltrating macrophages (Schilling, Besselmann et al. 2005, Denes, Vidyasagar et al. 2007) as well as production of anti-inflammatory, pro-regenerative signaling molecules like IL-10 and TGF-β which both suppress inflammation and exert neuroprotective effects on the surviving cells (Iadecola and Anrather 2011). In the chronic phase of stroke there is little contribution from either resident or peripheral immune cells; however, there is still an increase in the number of microglia that help in brain repair via clearing of dead and dying cells (Schilling, Besselmann et al. 2005, Denes, Vidyasagar et al. 2007, Thored, Heldmann et al. 2009).

Current research aimed at the inflammatory state following ischemia is targeted at reducing infarct size following ischemia (Schilling, Besselmann et al. 2003, Tanaka, Komine-Kobayashi et al. 2003, Kriz 2006, Amantea, Nappi et al. 2009, Jin, Yang et al. 2010). While this approach is important, it does not address a crucial aspect of repair: the neural stem cell. NSC numbers increase following ischemic stroke; however, they rapidly die (Palmer, Willhoite et al. 2000) thereby preventing successful brain repair. By understanding how inflammation increases the susceptibility toward premature NSC death, we can better design therapies to promote brain repair.

2.3. Neurogenesis in the Adult Brain

Traditionally, neurogenesis was thought to only occur during embryonic and perinatal development (Ming and Song 2011); however, over the last decade, it has

become clear that neurogenesis occurs throughout adulthood in distinct regions of the brain. These regions consist of the subventricular zone (SVZ), located adjacent to the lateral ventricle, and the subgranular layer (SGL) of the dentate gyrus (DG) in the hippocampus. Furthermore, these two regions of the brain maintain distinct populations of NSCs that exhibit multipotency and greater plasticity compared to other cellular components of the central nervous system (Lazarov, Mattson et al. 2010). The NSCs located in the SVZ, referred to as radial glia-like type B cells, are quiescent, glial fibrillary acidic protein (GFAP)-positive, and have characteristics in common with astrocytes (Suh, Deng et al. 2009, Lazarov, Mattson et al. 2010). These type B cells give rise to the so-called transit-amplifying type C cells, which are GFAP-negative. From there, type C cells become neural progenitor cells (NPCs) which give rise to doublecortin (DCX)-expressing neuroblasts. In rodents and non-human primates these neuroblasts travel through the rostral migratory stream (RMS) to the olfactory bulb where they ultimately become periglomerular neurons or granule cells (Figure 2) (Sanai, Tramontin et al. 2004, Lazarov, Mattson et al. 2010). However, while there is a comparable SVZ region in the human brain, there exists a unique hypocellular layer that lacks cellular bodies. This region is thought to be the site for the regulation of neuronal function, metabolic homeostasis, and/or NSC proliferation and differentiation (Quinones-Hinojosa, Sanai et al. 2007). Furthermore, the existence of an RMS or any pathway leading to the olfactory bulb is controversial with previous studies lacking demonstration of similar RMS track in humans (Sanai, Tramontin et al. 2004, Spalding, Bergmann et al. 2013). However, more recent studies (Curtis, Kam et al. 2007, Ernst, Alkass et al. 2014) describe the presence of NSCs in the human striatum (Ernst, Alkass et al. 2014) and also the presence of an RMS in

humans with neuroblast migration to the olfactory bulb (Figure 3) (Curtis, Kam et al. 2007, Wang, Liu et al. 2011). These studies illustrate the ongoing discussion in the scientific community about the presence or absence of an RMS in humans and demonstrate the need for further research to fully elucidate the extent of adult human neurogenesis.

NSCs in the DG give rise to new neurons, which reside within the granule cell layer (GCL). In both rodents and humans, two distinct subpopulations can be identified in the DG that are unique in their morphologies and molecular marker expression profiles. Similar to the type B cells of the SVZ, type I cells express GFAP and have a similar radial glia-like morphology. Type II cells are more similar to the type C cells of the SVZ and are also GFAP-negative. Type II cells can be further subdivided into two subpopulations: 1) type IIa cells which express Mash1 and continue to express the NSC marker Sox2, and 2) type IIb cells which are early-committed NPCs which express the transcription factors Prox1, NeuroD1, and DCX. Like in the SVZ, NSCs in the DG proceed through similar levels of differentiation from type I/II NSCs to NPCs to DCX-positive neuroblasts and ultimately into new, mature neurons in the GCL (Clarke and van der Kooy 2011). These newly-formed neurons project axons into the CA3 region of the DG and dendrites into the molecular layer much like neurons formed during embryogenesis (Zhao, Teng et al. 2006, Lazarov, Mattson et al. 2010). The rate at which this happens *in vivo* has been found to be comparable between adult mice and middle-aged humans, with a calculated annual turnover rate of 1.75 percent, suggesting that there is a sufficient amount of neurogenesis (approximately 700 new neurons per hippocampus per day) occurring in humans that could significantly contribute to functional repair (Spalding, Bergmann et al. 2013). The growing evidence supporting the occurrence of neurogenesis in humans, particularly in

areas highly sensitive to oxygen deprivation such as the hippocampus, suggests its potential role in neural repair after stroke. Additional studies are needed to understand this complex process, the mechanisms that affect it, and how it can be manipulated for the treatment of neurological diseases.

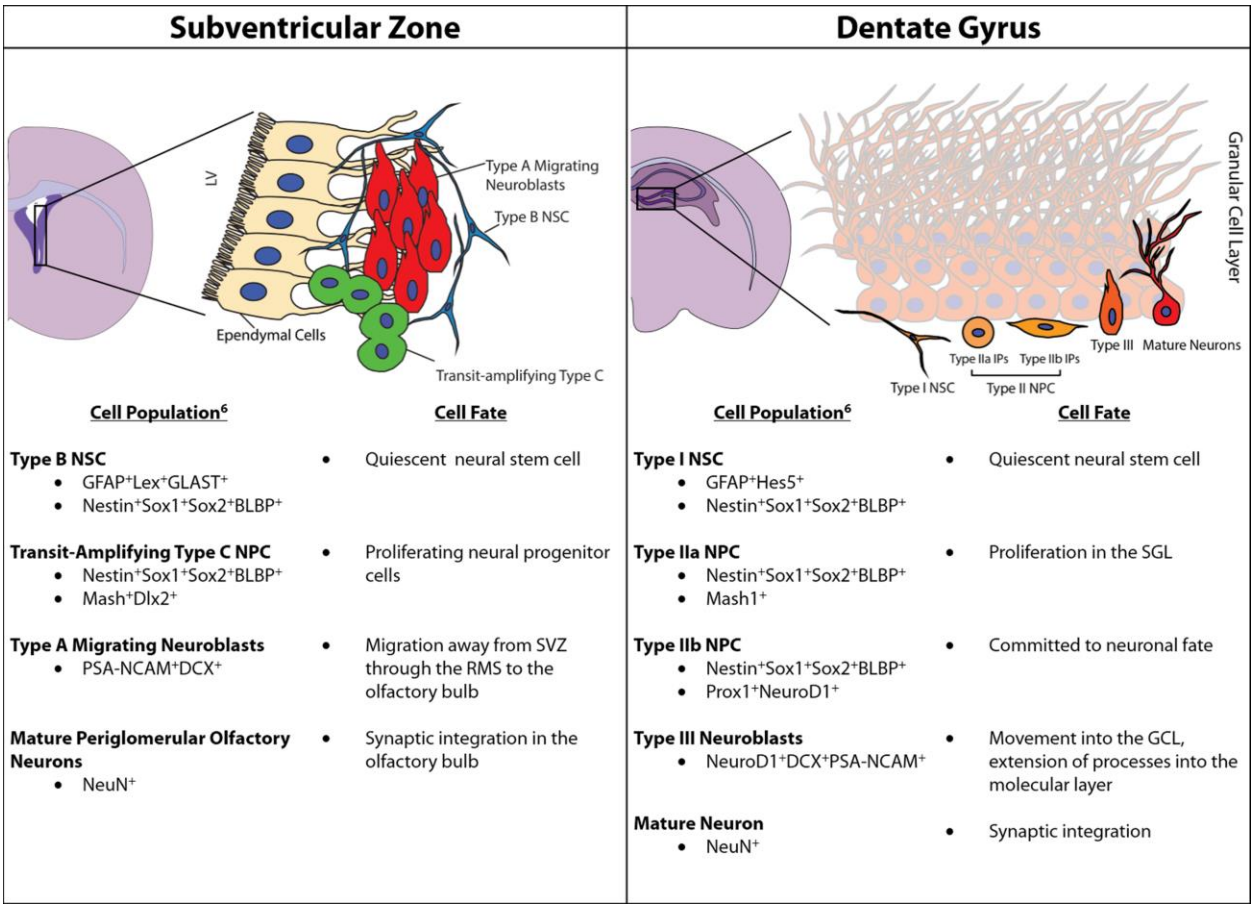

Figure 2. Adult neurogenesis in rodents. Coronal sections of the rodent show the neurogenic environments of the adult brain: the subventricular zone (SVZ; left) and the subgranular layer (SGL; right). The SVZ contains Type B NSCs which give rise to transit-amplifying Type C cells followed by Type A migrating neuroblasts. These cells migrate along the rostral migratory stream (RMS) towards the olfactory bulb before terminal differentiation. The SGL contains Type I NSCs which are similar to the Type B cells in the SVZ. Type I NSCs give rise to Type II NPCs (or intermediate progenitors; IP) which can be further classified as Type IIa and Type IIb. These Type IIb cells are early-committed neuronal progenitor cells which give rise to Type III neuroblasts which migrate into the granular cell layer where they exit the cell cycle and become mature neurons. All cell types described here can be identified based on a unique set of molecular and morphological markers, as described in the Cell Population column. From Tobin et al (Tobin, Bonds et al. 2014)

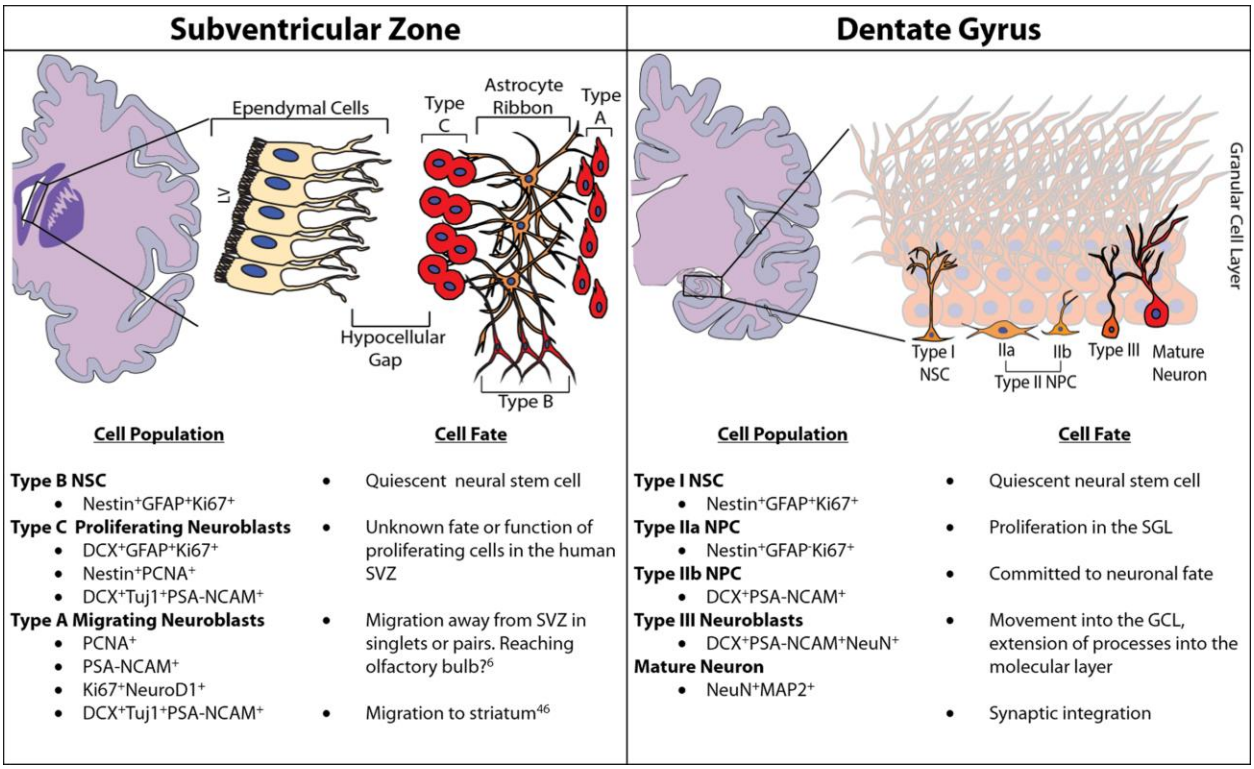

Figure 3. Adult neurogenesis in humans. Coronal sections of the human brain show the neurogenic environments of the adult brain: the subventricular zone (SVZ; left panel) and the dentate gyrus of the hippocampus (DG; right panel). Cell types unique to these regions as well as the fate of these cells are listed. Cell types described here can be identified based on a unique set of molecular and morphological markers, as noted in the Cell Population column. Abbreviations: LV – lateral ventricle; SGL – subgranular layer; GCL – granular cell layer. From Tobin et al (Tobin, Bonds et al. 2014)

2.3.1. Interaction between Inflammation and Neurogenesis

Thoughtful research has demonstrated the active role of neuroinflammation in both secondary brain injury and neuro-repair after stroke. The effect of the post-ischemic immune response on neurogenesis is not well understood. However, studies done in different models of disease demonstrated that an active crosstalk exists between inflammation and neurogenesis. Invertebrate models of brain injury and inflammation showed that inflammation is both sufficient and necessary to increase endogenous neurogenesis following injury (Kyritsis, Kizil et al. 2012).. Data obtained in vertebrate models of chronic neuroinflammation induced by stereotaxically-injected lipopolysaccharide (LPS) into the dentate gyrus, for example, demonstrated the functional integration of new, adult-born, highly plastic hippocampal neurons (Jakubs, Bonde et al. 2008). Also, the presence of chronic inflammation induced by electrical induction of status epilepticus was linked to a seven-fold increase in the number of mature neurons in the dentate granule cell layer formed during the first two weeks after seizure induction with the majority of these newborn cells replacing dead granule cells. Significantly, 6 months after seizure activity there was evidence of continued neuron formation in the hilus of the dentate gyrus supporting the long term effect of inflammation on neurogenesis (Morrens, Van Den Broeck et al. 2012). These reports are promising for utilization of endogenous neurogenesis as a repair mechanism following brain injury. However, the interplay of inflammation and neurogenesis is complex and there is substantial evidence obtained in vertebrate models of brain injury that show that inflammation impairs not only basal neurogenesis levels but also attenuates the increased neurogenesis seen following injury via increased activated $ED1^+$ microglia (Ekdahl, Claasen et al. 2003) and via secretion of

numerous proinflammatory cytokines including, IL-6, TNF-α, and IFN-γ (Vallieres, Campbell et al. 2002, Ben-Hur, Ben-Menachem et al. 2003, Ekdahl, Claasen et al. 2003, Wong, Goldshmit et al. 2004, Curtis, Kam et al. 2007, Bachstetter, Morganti et al. 2011). As an illustration, mice continuously infused with LPS have an 85% reduction in new neurons with no corresponding effect on already mature neurons and this phenomenon can be alleviated via anti-inflammatory treatment with minocycline (Ekdahl, Claasen et al. 2003). Mechanistically, hippocampal neurogenesis can be downregulated by proinflammatory cytokines, such as IL-6 (Vallieres, Campbell et al. 2002, Curtis, Kam et al. 2007) and NO(Packer, Stasiv et al. 2003) secreted by immune cells (Vallieres, Campbell et al. 2002, Packer, Stasiv et al. 2003, Curtis, Kam et al. 2007). Conversely, NPCs have been shown to promote neuroprotection via immunomodulation suggesting an innate and mutual interaction between NSCs and the immune system (Pluchino, Zanotti et al. 2005).

Both pro- and anti-inflammatory cytokines can influence the proliferation and migration of neural progenitors (Erlandsson, Lin et al. 2011, Bye, Turnley et al. 2012). The link between the immune response that occurs after ischemic stroke, neurogenesis, and subsequent functional recovery has not been well established; however, hypotheses regarding both the beneficial (Ziv, Ron et al. 2006) and detrimental (Iosif, Ekdahl et al. 2006, Iosif, Ahlenius et al. 2008) effects of inflammation have been proposed. Some of the beneficial effects have been attributed to the interaction of T cells with microglia which stimulates proliferation of SGL and SVZ progenitor cells (Ziv, Avidan et al. 2006) and directs both NPC migration and differentiation *in vitro* and *in vivo* (Ziv, Ron et al. 2006). Furthermore, hippocampal neurogenesis induced via enriched environment

demonstrates an increase in CNS T cell recruitment and activation of microglia in wild type mice with impaired neurogenesis in immune-deficient, SCID and nude mice (Ziv, Avidan et al. 2006). Some of the detrimental effects have been proposed to be caused by progenitor cell suppression via TNF-α secretion by activated microglia (Iosif, Ekdahl et al. 2006, Iosif, Ahlenius et al. 2008). Furthermore, LPS-activated microglia has been shown to compromise survival of newly formed neurons following brain injury (Ekdahl, Claasen et al. 2003, Monje, Toda et al. 2003). Additionally, in contrast to acute activation of microglia, chronic microglia activation seems to confer a neuroprotective effect supporting NSC survival. Newly born neurons that do not die following acute status epilepticus-induced microglia activation survive for at least six months following injury despite the presence of chronically activated microglia (Bonde, Ekdahl et al. 2006). Further *in vivo* studies have demonstrated unique proneurogenic phenotypes of microglia in the SVZ following stroke whereby activated microglia not only exhibited a ramified morphology, typical for resting microglia, but have increased production of IGF-1, a diffusible neurotrophic factor important for NPC proliferation (Thored, Heldmann et al. 2009, Morrens, Van Den Broeck et al. 2012). *In vitro* studies have also supported a beneficial role of microglia showing that NSCs co-cultured with microglia or grown in microglia-conditioned media have increased formation of neuroblasts which is otherwise lost following long-term culture (Aarum, Sandberg et al. 2003, Walton, Sutter et al. 2006). In contrast, NSCs co-cultured with increasing ratios of microglia in an acute setting demonstrated a dose-dependent reduction in NPC number (Gebara, Sultan et al. 2013). It is clear that there exists an intimate relationship between neurogenesis and the inflammatory response that plays a crucial role in the response following brain injury. The

dual role that microglia play following stroke is becoming increasingly more apparent and it would seem that the microglia response has both beneficial and negative consequences for neurogenesis (Ekdahl, Kokaia et al. 2009). By further understanding this interaction and the relationship between these two processes, our understanding of CNS injury and repair can be further advanced.

2.3.2. Effect of Ischemia on Neurogenesis

There are increasing amounts of evidence suggesting that ischemic injury drastically increases neurogenesis in the rodent SVZ and SGL(Liu, Solway et al. 1998, Arvidsson, Collin et al. 2002, Lichtenwalner and Parent 2006, Tsai, Yang et al. 2011) as well as in the primate SGL (Tonchev, Yamashima et al. 2003, Tonchev 2011). Furthermore, studies in mice (Takagi, Nozaki et al. 1999, Tureyen, Vemuganti et al. 2004) and rats (Jin, Minami et al. 2001, Kee, Preston et al. 2001, Yagita, Kitagawa et al. 2001, Takasawa, Kitagawa et al. 2002, Choi, Lee et al. 2003) demonstrate an increase in NPC proliferation in the dentate gyrus peaking around 7 days following ischemic injury (Yagita, Kitagawa et al. 2001, Tureyen, Vemuganti et al. 2004, Lichtenwalner and Parent 2006). However, the increased number of NSCs quickly returns to baseline with most of the NSCs dying shortly after proliferation. In fact, the number of NPCs that survive and become mature neurons are approximately equal in number in animals undergoing ischemia compared to animals without injury. The cells that do survive, however, migrate from the SGL into the GCL, have increasing dendritic length, and begin to both lose expression of immature neuronal markers and gain expression of mature neuronal markers with increasing time after ischemia following a similar time course to normal

neuronal maturation (Tanaka, Yamashiro et al. 2004). Despite the increase in NPC numbers after an ischemic injury, these cells prematurely die without the ability to repair dead tissue. The mechanisms by which these NPCs die early are as yet undetermined.

Similar to the SGL, NPCs in the SVZ have a short-lived proliferation again peaking around 7 days following ischemia (Lichtenwalner and Parent 2006, Liu, Chopp et al. 2013). Also like the cells in the SGL, those NPCs that do survive migrate out of the SVZ into the striatum and neocortex and mature into functional neurons (Arvidsson, Collin et al. 2002, Parent, Vexler et al. 2002, Jin, Sun et al. 2003, Thored, Wood et al. 2007, Zhang, Chopp et al. 2009, Li, Yu et al. 2010). Additionally, it has been demonstrated that transient angiogenesis following stroke allows neuroblasts to migrate along these newly formed blood vessels aiding in their migration out of the SVZ (Thored, Wood et al. 2007). While some of these newly generated neurons survive up to 5 weeks following ischemia, the majority seem to die with only approximately 0.2% of the cell surviving (Arvidsson, Collin et al. 2002). Furthermore, these surviving cells have been shown to be spiny neostriatal projection neurons (Arvidsson, Collin et al. 2002, Parent, Vexler et al. 2002) and small, calretinin^{+} interneurons (Liu, Xia et al. 2009). Despite these promising data demonstrating functional maturation of NPCs in both the SVZ and SGL following ischemic injury, much work still needs to be done to determine why the majority of these cells die, why the initial NPC proliferation fails to promote brain repair, and how neurogenesis can be manipulated for the support of functional recovery.

2.4. Prospective Therapies after Ischemic Stroke

Over the last decade, significant advances have been made in our understanding of the pathogenesis of brain injury from stroke. The knowledge gained, however, failed to translate into novel treatment strategies. Our current armamentarium to treat cerebral ischemia relies mainly on the use of pharmacological thrombolytics (t-PA) in acute cases and antithrombotic therapy along with correction of the modifiable vascular risk factors for recurrent stroke prevention. The time window for initiating the treatment with t-PA is limited to 3 hours after stroke symptom onset. The short therapeutic window, stroke severity, concern of the occurrence of major or fatal hemorrhage, severe hypertension and other variables greatly limit the number of patients that can benefit from this treatment. The development and implementation of hospital-based protocols with the goal of facilitating the identification of ischemic stroke patients and the early treatment with t-PA has increased the use of thrombolytics from 4% in the period 2003-2005 to 7% in 2010-2011 ($p<0.001$). These statistics and the known negative consequences of stroke highlight the desperate need for new safe and effective treatments for this condition. Because patients are often unaware of initial stroke symptoms, many do not seek care until well after the 3 hour window of t-PA has passed. Thus, identifying new strategies that can be used beyond the current time window and regulate post-ischemia inflammation or enhance neuro-repair are likely to revolutionize contemporary stroke care.

2.4.1. Antiinflammatory Treatment Strategies

As discussed previously, a large effector of stroke outcome is the post-ischemia inflammatory environment that exists. Therefore, large efforts are underway to target these inflammatory pathways in an attempt to reduce their effect on the brain following the initial ischemic injury. Various research studies as well as clinical trials have been conducted to examine the effect of various anti-inflammatory treatments following ischemic stroke (Table 2). While two of these studies report better outcomes with their anti-inflammatory treatment (Edaravone Acute Infarction Study 2003, Lampl, Boaz et al. 2007), the remaining studies report worse outcomes (Bath, Iddenden et al. 2001, Enlimomab Acute Stroke Trial 2001), no difference between treatment and placebo (Norris and Hachinski 1986, Krams, Lees et al. 2003, Shuaib, Lees et al. 2007, Liu, Xia et al. 2009), or were simply safety studies (Emsley, Smith et al. 2005, Pettigrew, Kasner et al. 2006, Lyden, Shuaib et al. 2007) with all of them failing to make it beyond clinical phase trials. Importantly, some of these studies were underpowered to detect a meaningful clinical effect. However, the dual effect of inflammation on stroke outcome and particularly on neurogenesis highlights that anti-inflammatory strategies might be a difficult avenue to pursue in ischemic stroke treatment. Further studies, however, need to be conducted to hone in on more specific targets in the inflammatory cascade that can hopefully be effective targets for future therapeutic trials. One such target is vascular adhesion protein-1 (VAP-1) which is expressed by endothelial cells and aides in neutrophil transmigration from the vasculature into the brain parenchyma. The pharmacologic agent LJP-1586, and its predecessor LJP-1207, are highly-selective VAP-1 inhibitors and prevent neutrophil transmigration into the brain parenchyma.

Furthermore, when these drugs are given to rodents subjected to transient forebrain ischemia (Xu, Salter-Cid et al. 2006) or transient MCAO(Watcharotayangul, Mao et al. 2012) 6 to 12 hours post-reperfusion, there is a profound anti-inflammatory action which is linked to neuroprotection (Xu, Salter-Cid et al. 2006, Watcharotayangul, Mao et al. 2012). These studies, and others currently in preclinical development may identify clinical targets for anti-inflammatory therapeutic options.

However, while these studies offer promising avenues for future research, the fact that blocking post-ischemia inflammation could also eliminate any beneficial effects of inflammation cannot be overlooked. While the consensus thus far is that inflammation is largely detrimental to neurogenesis following stroke there is evidence, as discussed above, showing that chronic neuroinflammation supports maturation of highly plastic hippocampal NSCs (Jakubs, Bonde et al. 2008, Morrens, Van Den Broeck et al. 2012). Therefore, investigators must weigh the advantages and disadvantages when considering these types of treatment approaches as they could potentially inhibit potent pro-regenerative effects.

2.4.2. Regenerative Strategies

Current therapies involving regenerative strategies have mostly involved two separate ideas: 1) the ability to repopulate infarcted tissue via transplantation of stem cells and 2) utilizing endogenous progenitor cells to repopulate the damaged brain. Transplantation of stem cells has been attempted in rodent models of disease (Hodges, Sowinski et al. 2000, Hodges, Veizovic et al. 2000, Qu, Brannen et al. 2001) with some degree of success, showing benefit to the animals receiving stem cell transplantation. In

both rodents and primates with damage to the hippocampus, functional recovery was seen following transplantation of both fetal and immortalized neuroepithelial stem cells (Hodges, Sowinski et al. 2000). Additionally, when compared to young animals, aged animals (which naturally experience decreased endogenous neurogenesis) demonstrated increased performance on hippocampus-based memory tasks following transplantation of immortalized neuroepithelial stem cells (Hodges, Veizovic et al. 2000). Furthermore, human NSCs injected into aged rat brains successfully integrated into brain parenchyma and increased performance on hippocampus-based memory tasks (Qu, Brannen et al. 2001). Stem cell transplantation seems to be beneficial; however, getting stem cells to engraft with a high degree of efficiency and to differentiate into mature cells is highly variable. Furthermore, the translation of these studies in animal models to humans poses significant technical hurdles that would make the use of cell transplantation difficult in clinical practice. Consequently, utilizing endogenous neurogenesis mechanisms provides an alternative approach to regenerative therapies following ischemic injury.

Not only has transplantation of stem cells been shown to be directly beneficial to injured brain, but it has also been shown to stimulate endogenous neurogenesis (Park, Eve et al. 2010). Endogenous neurogenesis, though, is not a one-step process. It is a series of events involving the proliferation of NSCs/NPCs, migration of these cells to the damaged area, survival of these cells, differentiation of progenitor cells into different lineages of neural cells, and functional integration of these mature cells. Therefore, therapies aimed at each of these steps could prove beneficial in successful brain repair following ischemic stroke. As discussed earlier, proliferation of NSCs does not seem to

be impaired following stroke. Rather, it is the survival of these progenitor cells that seems to be hindered with up to 80% of newborn neurons dying within 2 weeks after their birth (Ekdahl, Kokaia et al. 2009). It would therefore seem that therapies aimed at increasing the survival of NSCs and NPCs would be the most advantageous. These strategies, though, are not without complication. The existence of large numbers of NSCs is not seen in humans to the same extent as in rodents (Roy, Benraiss et al. 2000, Lichtenwalner and Parent 2006). Consequently, manipulation of endogenous NSCs alone may not be sufficient to adequately repopulate damaged brain tissue.

Furthermore, the pathological environment created following ischemic stroke pose numerous hurdles for newborn neurons that makes the utilization of endogenous repair mechanisms difficult. For instance, aged and injured brains have reduced neurogenic signaling making it even more difficult to direct the migration and differentiation of endogenous NSCs needed to repair infracted tissue (Hallbergson, Gnatenco et al. 2003, Lazarov, Mattson et al. 2010). Additionally, unlike other areas of the body, the brain is unique in its response to hypoxic cell death in that it ultimately leads to gliotic scar formation and liquefactive necrosis which will negatively impact all aspects of endogenous repair. Not only will NPCs and neuroblasts be unable to migrate but any surviving newborn neurons will have difficulty integrating into existing circuits and forming functional synaptic connections. Because of these issues, successful recruitment and differentiation of NSCs into cortical and subcortical structures may be difficult to attain, making the use of endogenous progenitor cells an unlikely source of independent brain repair.

Despite these obstacles, newborn neurons have several advantages compared to mature cells that can help overcome these barriers. The most obvious of these advantages is that, unlike the postmitotic mature neurons, NSCs and NPCs can undergo asymmetric cell division and not only produce mature daughter neurons but can maintain the stem and progenitor pools allowing for continued brain repair. Additionally, it has been shown that young, newborn neurons in the granule cell layer of the dentate gyrus are more active than old granule cells and that the young cells are necessary for enhanced pattern separation (Nakashiba, Cushman et al. 2012). Furthermore, immature and newborn neurons are more excitable than mature cells. Consequently, they fire more action potentials in a given time than their mature counterparts (Schmidt-Hieber, Jonas et al. 2004, Ge, Yang et al. 2007, Mongiat, Esposito et al. 2009). Thus, overall circuit excitation will be increased which could help ameliorate some of the loss of excitation following cell death after ischemia. Therefore, in combination with other strategies such as stem cell transplantation, the use of endogenous neurogenesis mechanisms could prove to be extremely beneficial for brain repair.

2.5. Mesenchymal Stem Cells in Ischemic Stroke

Mesenchymal stem cells (MSC) were first described in the 1970s by Friedenstein and colleagues (Friedenstein, Deriglasova et al. 1974, Friedenstein, Gorskaja et al. 1976) who isolated so called “clonogenic fibroblast precursor cells” from mouse hematopoietic organs (namely bone marrow). There, they described these as plastic-adherent cells which were inherently osteogenic. Since then, these cells have been isolated from numerous other sources including adipose tissue (Zuk, Zhu et al. 2001), umbilical cord

blood (Erices, Conget et al. 2000), dental pulp (Gronthos, Mankani et al. 2000), and amniotic fluid (In 't Anker, Scherjon et al. 2003) and are classically considered multipotent cells giving rise to mature osteocytes, chondrocytes, and adipocytes. More recently, MSCs have been shown to also give rise to cells of neuroectoderm origin (Kopen, Prockop et al. 1999, Zhao, Duan et al. 2002). However, it is not for their ability to differentiate into multiple lineages that these cells have gained popularity in the neuroscience community. It is more for their immunomodulatory and paracrine actions that researchers have started investigating the use of MSCs for the treatment of many different neurological disease.

Mesenchymal stem cells have very unique characteristics that make them an interesting tool to study brain repair after ischemic stroke. They have the ability to 1) reduce overall inflammation thereby eliminating the potentially toxic environment that could be leading to NSC death (Zhao, Wehner et al. 2010, Liu, Wang et al. 2011); 2) interconvert microglia from an inflammatory phenotype to a regenerative phenotype (Ohtaki, Ylostalo et al. 2008, Yang, Xie et al. 2013); and 3) help support NSC survival and function via secretion of various neurotrophic factors (Moradi, Haji Ghasem Kashani et al. 2012, Sadan, Melamed et al. 2012, Sadan, Shemesh et al. 2012). Furthermore, there is growing evidence demonstrating the non-immunogenic nature of MSCs (Ryan, Barry et al. 2005, McTaggart and Atkinson 2007, Jacobs, Pinxteren et al. 2013). A major obstacle to cell-based therapies is the need for a donor-recipient crossmatch. Because MSCs do not induce a recipient immune response, they can be administered without the need for this crossmatch. While these studies have demonstrated the seemingly immune-privileged nature of MSCs, there have been some recent studies showing the presence

of anti-donor immune responses following MSC treatment (Porcheray, Wong et al. 2009, Griffin, Ryan et al. 2013, Lohan, Treacy et al. 2017). Thus, it is clear that further research is needed to fully understand the immunogenicity of MSCs, however, the potential to utilize MSCs as an “off the shelf” therapy cannot be overlooked. To date, there have been many preclinical studies, as well as clinical trials, demonstrating the efficacy of MSC therapy in stroke preclinical studies, and safety of MSC treatment in clinical trials. What these studies, lack, however, is a clear mechanism by which MSC treatment conveys a functional benefit. Furthermore, most of the clinical trials to date using MSCs as a therapeutic for ischemic stroke patients have utilized this treatment in subacute (1 week to 1 month after the ischemic event)(Moniche, Gonzalez et al. 2012, Diez-Tejedor, Gutierrez-Fernandez et al. 2014, Moniche, Rosado-de-Castro et al. 2016) and chronic stroke patients (>30 days after the ischemic event) (Suarez-Monteagudo, Hernandez-Ramirez et al. 2009, Battistella, de Freitas et al. 2011, Bhasin, Srivastava et al. 2011, Honmou 2016, Steinberg, Kondziolka et al. 2016), with only 2 trials (Savitz, Misra et al. 2011, Friedrich, Martins et al. 2012) looking at the utility of MSCs in acute (<1 week) stroke patients. Therefore, whether these cells can be an effective therapy acutely is largely unknown.

Table 1. Signaling molecules associated with the inflammatory cascade

Released factor	*Function*	*Produced by*	*Role in stroke*	*Time to peak concentration*	*Species—method of stroke*
Proinflammatory					
TNF-α	Upregulation of caspases Upregulation of leukocyte adhesion molecule expression Increases endothelial cell dysfunction	Neurons, M1-type microglia, M1-type macrophages	Increases[113] or decreases[114] infarct volume	3–24 hours[114–117]	Mouse—pMCAO[114,115] Mouse—tMCAO[116] Rat—tMCAO[117]
IL-1α/β	Apoptosis	M1-type macrophages, microglia, endothelial cells	Increases infarct volume[118]	6–24 hours[115,117,119]	Mouse—tMCAO[115] Rat—tMCAO[117,119]
IL-6	Pyrogen	Macrophages, endothelial cells	Neuroprotective[120–122]	6–18 hours[117,119]	Rat—tMCAO[117,119]
IL-8	Neutrophil chemoattractant	Macrophages, endothelial cells	Increases infarct volume[123]	1–3 days[124]	Peripheral blood from human stroke patients[124]
IL-12	Promote T_H1 phenotype	Macrophages, T_H1 cells	Increases infarct volume[125]	Unknown	
IFN-γ	Macrophage activation	NK cells, T cells	Increases infarct volume[126]	10–14 days[127]	Rat—transient 4VO[127]
iNOS	Production of NO	Astrocytes, microglia, leukocytes, endothelial cells	Increases infarct volume[128]	12 hours[129]	Rat—tMCAO[129]
MMPs	Degradation of ECM proteins	Astrocytes, leukocytes	Increases infarct volume[130,131]	12–24 hours[132]	Blood plasma from human MCA stroke patients[132]
Elastase	Degradation of basal lamina and ECM proteins Recruitment of leukocytes	Neutrophils, macrophages	Increases infarct volume[133]	12 hours[134]	Mouse—tMCAO[134]
Antiinflammatory					
IL-10	Blocks conversion to T_H1 phenotype Inhibits synthesis of IFN-γ, IL-2, IL-3, TNF-α	Microglia, macrophages, T_{reg} cells, endothelial cells	Decreases infarct volume[135–137]	24 hours[127]	Rat—transient 4VO[127]
Arginase	Decreases production of NO	M2-type macrophages, microglia	Unknown	8–15 days[138]	Rat—photothrombotic cortical occlusion[138]
TGF-β	Inhibition of lymphocyte and monocyte-derived phagocyte activation	Microglia, M2-type macrophages	Decreases infarct volume[139–141]	2–4 days[142,143]	Rat—4VO[142] Rat—pMCAO[143]
Others					
ROS	Oxidation of cell signaling molecules	Neurons, microglia, astrocytes, leukocytes	Increased production after stroke[144,145] Early ROS burst increases infarct volume[146]	10 minutes–72 hours[146,147]	Rat—2VO[147] Mouse—tMCAO[146]
MPO	Generation of ROS	Neutrophils, macrophages	Decreases infarct volume[148]	3 days[149]	Mouse—tMCAO[149]

ECM, extracellular matrix; IFN-γ, interferon-gamma; IL, interleukin; iNOS, inducible nitric oxide synthase; MMP, matrix metalloproteinase; MPO, myeloperoxidase; pMCAO, permanent middle cerebral artery occlusion; ROS, reactive oxygen species; TGF-β, transforming growth factor-beta; tMCAO, transient middle cerebral artery occlusion; TNF-α, tumor necrosis factor-alpha; 2VO, 2-vessel occlusion (bilateral carotid artery occlusion); 4VO, 4-vessel occlusion (bilateral carotid artery and bilateral vertebral artery occlusion).

Table 1. Signaling molecules associated with the inflammatory cascade.
From Tobin et al (Tobin, Bonds et al. 2014)

Table 2. Clinical studies utilizing antiinflammatory agents in acute ischemic stroke

Antiinflammatory agent	*Mechanism of action*	*Outcome*	*Reference*
Dexamethasone	Immunosuppressant	No difference from placebo	98
Recombinant IL-1RA	IL-1 receptor antagonist	Safe No SAE	99
Enlimomab	Anti-ICAM-1 monoclonal antibody	Worse progression	93
Tirilazad	Lipid peroxidation inhibitor	Worse progression	94
UK-279,276	Neutrophil inhibitory factor	No difference from placebo No SAE Stopped for futility	95
Cerovive (NXY-059)	Nitrone-based free radical trapping agent	Safe No SAE	96,100
Acetaminophen	Anti-pyretic effect	Results not reported	150
Minocycline	Antiinflammatory	Significant improvement over placebo	91
Ginsenoside	Ca^{2+} channel antagonist	No difference from placebo	97
Edaravone (MCI-186)	Free radical scavenger	Significant improvement over placebo	92
ONO-2506 (arundic acid)	Astrocyte modulator	Safe No SAE	101

ICAM, intracellular adhesions molecule; SAE, serious adverse events. Adapted from Lakhan, *et al.*[4]

Table 2. Clincal studies utilizing anti-inflammatory agents in acute ischemic stroke.
From Tobin et al (Tobin, Bonds et al. 2014)

3. MATERIALS AND METHODS

3.1. Materials

3.1.1. Chemicals and Reagents

Chemicals and reagents used are listed below with vendors listed in parenthesis. Primers used for qRT-PCR are listed in Appendix 1 and antibodies are listed in Appendix 2.

3.1.2. Animals

All animal experiments were approved by the University of Illinois at Chicago Institutional Animal Care and Use Committee. For surgical experiments, female Sprague-Dawley rats (age 14 to 16 weeks, weight 225-275 grams) were purchased from Envigo (Huntingdon, Cambridgeshire, UK) and were group housed and maintained in standard housing conditions (14/10 hour light/dark cycle) with access to food and water *ad libitum*. Post-operatively, animals were singly housed. For neonatal mixed glial cell isolations, breeding pairs of Sprague-Dawley rats (age 8 weeks) were purchased from Charles River Laboratories and were maintained as above. Female breeders were used for up to 3 litters before being replaced as breeders. Animals used for mesenchymal stem cell and subventricular neural stem cell isolation were obtained from an in-house breeding pair.

3.2. Methods

3.2.1. Mixed glial cell culture and microglia isolation

Rat pups (P0-5, mixed gender) were decapitated and the brains were dissected into ice cold HBSS. Meninges were removed and neocortex was dissected out into ice

cold HBSS. Tissue was then combined and incubated in 0.25% trypsin plus 50 µg DNase I for 7 minutes at room temperature and then washed with DMEM plus 10% FBS. Tissue was then washed twice with HBSS and then passed 5 times each through decreasing size serological pipet (10 mL, 5 mL, glass Pasteur pipet) to dissociate the tissue. Tissue suspension was filtered through a 70 µm cell strainer, spun at 300g for 10 minutes and plated in DMEM plus 10% FBS plus 1% antibiotic-antimycotic (3 brains per T-75 cm^2 flask) and cultured at 37°C plus 5% CO_2. Media is changed the next day and every 3 days afterwards until confluent. Once confluent, microglia are isolated from mixed glial population by sealing flasks and shaking at 280 rpm for 30 minutes at 37°C. Microglia-containing media is collected and utilized for downstream applications.

3.2.2. Subventricular zone neural stem cell isolation

4-6-week-old female rats were euthanized via isoflurane overdose and decapitation and the brains were dissected into ice cold HBSS. Brains were cut at the level of the optic chiasm and the subventricular zone was dissected out. Tissue was minced using a scalpel and was transferred to 3 mL of warm media (DMEM/F-12, 20% B27 supplement, 10% N2 supplement, 1% penicillin-streptomycin, 1 mM glutamine, 20 mM KCl, 2 µg/mL heparin) and allowed to settle. Media was aspirated and tissue was resuspended in 1.25 mL 0.1% trypsin-EDTA plus 50 µg DNase I and incubated with agitation for 7 minutes at 37°C. Following incubation, 3 mL of trypsin inhibitor (Sigma-Aldrich #T6522; 139 µg/mL plus 10 µg/mL DNase I in HBSS) and spun at 300g for 5 minutes. Tissue pellet is resuspended in 1 mL of warm media and pipetted 25X with a P1000 pipet set to 800 µL. Media is added to 5 mL and tissue suspension is filtered

through a 70 µm cell strainer and spun at 300g for 5 minutes. Cell pellet is resuspended in warm media plus 20 ng/mL EGF + 10 ng/mL bFGF. Growth factors are added every 2 days and media is changed once a week. Neurospheres were passaged using Accumax (Innovative Cell Technologies #AM105) by incubating cells in 1 mL of Accumax for 10 minutes at room temperature on an orbital rotator. Cells were then pipetted 25X with a P1000 pipet set to 900 µL and added to 9 mL of growth media. Cells were then passed through a 70 µm cell strainer, spun at 300g for 5 minutes, and plated for either culture maintenance or for individual experiments.

3.2.3. Oxygen-glucose deprivation

For oxygen-glucose deprivation, cells were dissociated into single cell suspensions, resuspended in 1X HBSS + 1% antibiotic, and plated at appropriate densities. Cells were cultured in 1% oxygen for 4 hours and then transferred back to normal growth conditions.

3.2.4. Bone marrow isolation and culture

Female rats less than 4 weeks of age were euthanized via isoflurane overdose and decapitation. Femurs and tibias were dissected out into ice cold dissection media (50:50 MEMα/F-12, 10% FBS) and washed three times in cold dissection media. The ends of the bones were cut off and bone marrow plugs were flushed out with 10 mL of cold dissection media. Bone marrow plugs were pipetted 10X with a 10 mL serological pipet and were passed through a 70 µm cell strainer. Using the plunger from a 10 mL syringe, bone marrow plugs were pushed through the cell strainer which was then wash

twice with 10 mL ice cold dissection media. The cell suspension was spun at 300g for 10 minutes and the pellets were resuspended in warm growth media (50:50 MEMα/F-12, 10% FBS, 1% antibiotic-antimycotic) and plated at 37°C plus 5% CO_2. After 24 hours, and then every 3 days thereafter, the media was replaced until the cells reached confluency. At that point, cells were trypsinized and underwent magnetic bead purification.

3.2.5. Magnetic bead purification of mesenchymal stem cells

Trypsinized cells were counted and 200,000 cells were set aside to use as a "pre-purification" sample. The remaining cells were spun at 300g for 5 minutes and were resuspended in 50µL flow buffer (1X DPBS without calcium and magnesium, 2% BSA, 25 mM HEPES, 5 mM EDTA) per 10^6 cells containing 10 µg/mL each of biotin anti-rat CD45 and biotin anti-rat CD11b/c (Table A3) and were incubated for 30 minutes at 4°C. Cells were washed with 10X volume of flow buffer and spun at 500g for 10 minutes. The cell pellet was resuspended in 80 µL flow buffer plus 10 µL anti-biotin microbeads (Miltenyi Biotec #130-090-485) per 10^7 cells and incubated for 15 minutes at 4°C. Cells were washed with 10X volume of flow buffer and spun at 500g for 10 minutes. While spinning, an LS column (Miltenyi Biotec #120-000-475) was washed with 3 mL of flow buffer. The cell pellet was resuspended in 3 mL flow buffer and added to the LS column attached to a QuadroMACS separator (Miltenyi Biotec #130-090-976) and allowed to flow through into a 15 mL conical tube. The column was washed three times with 3 mL flow buffer and collected into the same conical tube, which contains purified mesenchymal stem cells. 5 mL of flow buffer was added to the LS column and the supplied plunger was

used to plunge the bound cells (macrophages) into a new 15 mL conical tube. The purified MSCs were counted and 10^5 cells/per tube were taken for phenotype analysis by flow cytometry and the remainder of the cells were put back into culture for continued use.

3.2.6. Mesenchymal stem cell flow cytometry

Pre-purification cells, bead-bound macrophages, and purified MSCs were stained and analyzed by flow cytometry to determine the purity of the MSC population. Cells were stained for CD11b, MHC-II (RT1D), CD29, CD45, CD90 or isotype controls (Table 1). Cell events were analyzed on a Fortessa cell analyzer (Becton Dickinson, Franklin Lakes, NJ, USA) and analyzed using FlowJo Software (FlowJo, LLC, Ashland, OR, USA).

3.2.7. Interferon-γ activation of mesenchymal stem cells

Mesenchymal stem cells were plated at a density of 3,000 cells/cm^2 and supplemented with 500 U/mL recombinant rat IFN-γ on days 0 and 3 of plating. Cells were used on day 6 after plating.

3.2.8. Collection of MSC conditioned media

Mesenchymal stem cells were plated at a density of 3,000 cells/cm^2 and were cultured normally or treated with IFN-γ as above. On day 6 after plating, media was removed, cells were washed three times with 1X DPBS and neurosphere media containing 20 ng/mL EGF and 10 ng/mL bFGF was added. After 24 hours, media was collected, spun at 300g for 10 minutes to remove cell debris and filtered through a 0.22

µm syringe filter. Media was either used immediately or frozen at -80°C for use at a later time.

3.2.9. MSC cell labeling

MSCs were fluorescently labeled either with CFSE (Thermo Fisher #C34554; intrastriatal transplantation) or using DiIC$_{18}$(5)-DS (Thermo Fisher #D12730; intravenous administration) according to manufacturer's recommended protocols. CFSE was used at a working concentration of 5 µM and DiIC$_{18}$(5)-DS was used at a working concentration of 1 µM.

3.2.10. Quantitative reverse transcription polymerase chain reaction

RNA was extracted from cultured cells using the ISOLATE II RNA Mini Kit (Bioline USA, Inc, Taunton, MA, USA) according to manufacturer's instructions and was quantified using a Nanodrop and stored at -80°C until used. cDNA synthesis was performed using the SuperScript™ III First-Strand Synthesis SuperMix (ThermoFisher Scientific) according to manufacturer's instructions starting with 1 µg total RNA per sample and using oligo(dT) priming and stored at -20°C until used. qPCR was performed using SensiFAST™ SYBR® & Fluorescein Kit (Bioline USA, Inc, Taunton, MA, USA). Each reaction was done using 1 µL of starting cDNA. Relative expression was calculated using the ΔΔCt method using RPLP0 as the housekeeping gene. Primer sequences are listed in Table A2.

3.2.11. Western blot analysis

Cells were collected and spun at 300g for 5 minutes. The cell pellet was resuspended in RIPA buffer containing protease inhibitor cocktail (1:100, Sigma-Aldrich #P8340) and was sonicated once for 15 seconds at 40% amplitude and then spun at 14,000g for 10 minutes. Supernatants were collected, quantified via the BCA method, and diluted to 1 µg/µL with lysis buffer and 2X Laemmli sample buffer and boiled for 10 minutes at 95°C with leftover protein being stored at -80°C. 15 µg of each sample was loaded into a 10% Mini-PROTEAN TGX precast gel, run in 1X Tris/Glycine/SDS buffer for 30 minutes at 200V at room temperature and then transferred to nitrocellulose membrane at 100V for 1 hour at 4°C. The membrane was stained with Ponceau S for 5 minutes to confirm protein transfer, destained with 0.1N NaOH and was then washed three times in PBST to remove any trace stain or NaOH. The membrane was then blocked in 5% nonfat milk in 1X PBS plus 0.01% Tween 20 (PBST) for 1 hour at room temperature and incubated for 1 hour at room temperature in primary antibody (Table 1) diluted in PBST. The membrane was then washed three times in PBST and then incubated for 1 hour at room temperature in appropriate secondary antibody (Table 1) diluted in 5% BSA in PBST plus 0.1% NaN_3. The membrane was then washed three times in PBST followed by once in PBS and imaged using an Odyssey CLx (700 nm or 800 nm channel set to Auto) and protein expression levels were quantified using Image Studio Lite (version 5.2.5; Li-Cor). All protein levels were normalized to levels of actin.

For Western blot analysis of tissue extract, rat brain hemispheres were lysed using the Bio-Plex Cell Lysis Kit (Bio-Rad, Inc) according to manufacturer's instructions, quantified using the BCA method, and diluted to 3 µg/µL with lysis buffer and 2X Laemmli

sample buffer and boiled for 10 minutes at 95°C with leftover protein being stored at -80°C. SDS-PAGE and Western blot was performed as above using 30 µg of total protein per sample.

3.2.12. BrdU Flow Cytometry

Cell cycle analysis was done utilizing a FITC BrdU Flow Kit (BD Biosciences) according to manufacturer's instructions. Briefly, neural stem cells were singly dissociated and plated in either normal growth media, nMSC conditioned media, or aMSCγ conditioned media and allowed to grow for 24, 48, or 72 hours. 4 hours prior to fixation, BrdU (10 µM final concentration) was added to each well to label dividing cells. At appropriate time points, cells were fixed and permeabilized, and treated with DNase I to expose the incorporated BrdU. Cells were then incubated with a FITC-conjugated anti-BrdU antibody and labled with 7-AAD. Cell events were analyzed on a Fortessa cell analyzer (Becton Dickinson, Franklin Lakes, NJ, USA) and analyzed using FlowJo Software (FlowJo, LLC, Ashland, OR, USA).

3.2.13. Middle cerebral artery occlusion

Anesthesia was induced and maintained in isoflurane in 100% oxygen for the duration of the procedure and body temperature was maintained at 37 ± 0.4°C via rectal probe-monitored heating pad. The ventral neck was shaved and remaining hair was removed with depilatory cream. The skin was prepped with 3 alternating wipes of isopropanol wipes and povidone-iodine swabs and an approximately 3.5 cm incision was made. Glandular tissue and fascia was dissected using a combination of blunt and sharp

dissection until the underlying muscles on the right side were visualized. The right omohyoid muscle was resected to expose the common carotid artery (CCA) and the carotid bifurcation. A 0.5 cm section of the proximal common carotid artery was dissected free from surrounding adventitia taking care to not disturb the adjacent vagus nerve. Following CCA dissection, the carotid bifurcation, external carotid artery (ECA), superior thyroid artery, occipital artery, and the internal carotid artery (ICA) were dissected free from surrounding adventitia. The superior thyroid artery and occipital artery were both coagulated and divided to allow for free movement of the ECA. The ECA was then dissected as distally as possible, coagulated, and divided and a loosely tied 5-0 silk suture was tied around the proximal ECA stump. The remaining ICA was dissected distally to expose the bifurcation of the ICA and the pterygopalatine artery. Temporary vessel clips were placed first on the previously dissected 0.5 cm segment of the CCA and then on the ICA as distally as possible. A small arteriotomy was made in the ECA stump and a silicone-coated 4-0 nylon filament (Doccol #404156PK10Re) was inserted through the arteriotomy into the ICA. The 5-0 silk tie was tightened to secure the filament, the ICA vessel clip was removed and the filament was inserted into the ICA until resistance was felt. At this time, the animal received a single BrdU injection (100 mg/kg IP) and the filament was left in place to occlude the middle cerebral artery for 90 minutes. After 90 minutes, the filament was withdrawn, a temporary vessel clip was placed on the ICA, the ECA stump was coagulated to close the arteriotomy, the two vessel clips were removed and the skin was closed. The animal was then placed into a recovery chamber maintained at 30°C and received 2.0 mL of warm saline intraperitoneally. Following a 3-hour recovery

period, the animal was re-anesthestized and was administered either vehicle (1X PBS) treatment, 5.0 X 10^6 nMSC/kg, or 5.0 X 10^6 aMSCγ/kg intravenously.

3.2.14. Intravenous administration of MSCs

Three hours following onset of reperfusion after MCAO, animals were re-anesthetized with isoflurane and MSCs were administered intravenously (IV) via the retro-orbital sinus. Cells were given at a dose of 5 X 10^6 cells/kg.

3.2.15. Stereotactic intracranial injections

Anesthesia was induced and maintained in isoflurane in 100% oxygen for the duration of the procedure and body temperature was maintained at 37 ± 0.4°C via rectal probe-monitored heating pad. Animals are then secured in a prone position into a stereotactic frame. An approximately 1.5 cm midline scalp incision is made. Musculature and periosteum are cleared via cotton tip applicator and the skull is washed with 3% hydrogen peroxide using a cotton tip applicator to demarcate the cranial sutures. Bregma is marked and the stereotactic coordinates are recorded. The injection needle is then positioned in the stereotactic frame at the appropriate stereotactic coordinates for a striatal injection (AP -1.0 mm, ML -3.3 mm from bregma). The skull is then marked with a sterile marker and using a high speed drill a burr hole is drilled over the marked skull position. Using a 27G needle, a small incision is made in the dura and the injection needle is lowered into position (DV -6.0 mm from dura) and left in place for 1 minute. The automatic injector is then initialized to deliver syringe contents (500,000 CFSE-labeled aMSCγ, 3 µL at a rate of 0.2 µL/minute over 15 minutes). Following the injection, the

needle is left in place for 5 minutes at which point it is slowly retracted and the skin is closed.

3.2.16. Magnetic resonance imaging

A. Image Acquisition

48 hours after surgery, animals were anesthetized using isoflurane and magnetic resonance imaging was performed using an Agilent 9.4T MR system (Agilent Technologies, Santa Clara, CA), with a 600 mT/m gradient insert, a 72 mm ID active decoupling birdcage RF coil for transmission, and a 4-channel phase array coil as the receiver (Rapid Biomed, Ripmar, Germany). In each animal, T1-, T2-, and diffusion-weighted MR images were acquired, using spin echo multi slice (SEMS) sequences. For the T1 sequence, imaging settings were as follows: TR/TE = 555/13 ms, FOV = 40X40 mm, Averages = 6, matrix = 256X256, slice thickness = 1.0 mm, gap = 0 mm. For the T2 sequence, imaging settings were as follows: TR/TE = 2000/45 ms, FOV = 40X40 mm, Averages = 4, matrix = 256X256, slice thickness = 1.0 mm, gap = 0 mm. For the diffusion weighted imaging (DWI) sequence, imaging settings were as follows: TR/TE = 2000/45 ms, FOV = 40X40 mm, Averages = 2, matrix = 128X128, slice thickness = 1.0 mm, gap = 0 mm, two *b*-values of 0 and 650 s/mm^2, diffusion separation Δ = 25 ms, diffusion gradient duration δ = 5 ms.

B. Infarct Volume calculation

Infarct volume and percent infarction were calculated using the DWI MRI sequences. Correcting for edema, these were calculated as follows:

$$Infarct\ Volume\ (mm^3) = \sum_{1}^{n} InV_n - (IpV_n - CoV_n)$$

$$Percent\ Infarction\ (\%) = 100 * \frac{\sum_1^n InV_n}{\sum_1^n (IpV_n + CoV_n)}$$

Where the individual slice infarct volume is InV, the individual slice ipsilateral hemisphere volume is IpV, individual slice contralateral hemisphere volume is CoV, and n is the slice number.

3.2.17. Functional testing after MCAO

A. Modified Neurological Severity Score

Animals were scored using the modified neurological severity score (mNSS) outlined in Appendix 3. Scores were obtained at baseline before surgery and on postoperative days 1-7, 14, and 21. The mNSS is a cumulative scoring system that combines motor, sensory, balance, and reflex deficits. One point is given for an inability to perform a motor or sensory task and one point is given for the absence of one of the reflexes. The section scores are summed for a maximum score of 18, with higher scores indicating a more impaired animal.

B. Open Field Testing

Animals were tested in an open field apparatus (Med Associates, Inc) for 15 minutes 24 hours and 7 days after surgery. Center/periphery analysis and rotational analysis were done using predetermined configurations in the corresponding Activity Monitor Software package (Med Associates, Inc).

3.2.18. Brain processing

At appropriate time points, rats were euthanized via isoflurane overdose followed by transcardial perfusion with ice cold heparinized saline (10 U/mL) for 12 minutes and with ice cold 4% paraformaldehyde for 15 minutes. Brains were then removed and post-fixed in PFA for 16 hours at 4°C, washed once in 1X PBS, and transferred to 30% sucrose until they sunk. Brains were then sectioned at 50 µm and stored in cryoprotectant (47.6% 1X PBS, 28.6% ethylene glycol, 23.8% glycerol) at -20°C.

3.2.19. Immunofluorescence staining

Tissue sections were washed three times at room temperature in 1X TBS for 5 minutes each. Tissue was then blocked in blocking buffer (1X TBS, 0.3M glycine, 5% normal donkey serum, 0.25% Triton X-100) for 2 hours at room temperature and then incubated in primary antibody (Table A3), diluted in blocking buffer, for 72 hours at 4°C. Tissue was then washed three times at room temperature in 1X TBS for 5 minutes each and incubated in secondary antibody (Table A3), diluted in blocking buffer, for 2 hours at room temperature. Tissue was then washed three times at room temperature in 1X TBS for 5 minutes each and incubated in DAPI (0.5 µg/mL; ThermoFisher Scientific #D1306) or TO-PRO-3 Iodide (1 µM; ThermoFisher Scientific #T3605) for 5 minutes at room temperature and then mounted and stored at 4°C. For sections that were stained for BrdU, tissue was washed three times at room temperature in 1X TBS for 5 minutes each then incubated in 2N HCl at 37°C for 30 minutes. Afterwards, tissue was incubated in 0.1M borate buffer for 10 minutes at room temperature, washed six times at room temperature in 1X TBS for 5 minutes each, and stained as above.

3.2.20. Stereological quantification

Cell counts were performed using design-based stereology (StereoInvestigator, MBF Biosciences). For the analysis, every sixth section of brain tissue was quantified using the optical fractionator workflow of StereoInvestigator. Regions of interest were traced under 5X magnification with counting performed under 63X magnification with a counting frame of 225 µm x 145 µm and sampling grid of 100 µm x 100 µm with 12.5 µm top and bottom guard zones.

3.2.21. Quantification of CD68 staining

To quantify level of microglia activity, tissue sections were stained for CD68 and were imaged using a Zeiss AxioImager with a 10X objective and were tiled in AxioVision (Carl Zeiss). Intensity analysis was performed in ImageJ. On each section, the intensity of the region of interest was measured as well as three background regions. CD68 staining was background corrected and normalized to measured area according to the following formula:

$$CD68\ Intensity = \frac{\sum_1^n (Int_{ROI})_n - (\bar{x}_{BackInt})_n}{\sum_1^n Area_n}$$

Where Int_{ROI} is the intensity of the defined region of interest, $\bar{x}_{BackInt}$ is the average of the background intensity, Area is the measured area of the region of interest, and n is the section number.

3.2.22. Quantification of CNPase and PDGFRα in the striatum

For each animal, 3 to 4 randomly selected fields (280 x 280 µm) from the striatum in 4 sections with 300 µm separating each section were acquired using a Zeiss LSM 880 confocal microscope with Airyscan detector. Forty-eight micron maximum projection z-stacks were reconstructed and the number of CNPase-positive and PDGFRα-positive cells per mm^2 were determined using the ImageJ Cell Counter plugin analysis tool.

3.2.23. *In vitro* and *In vivo* cytokine analysis

A. In vitro cytokine analysis

100,000 primary rat microglia were plated in triplicate per well of a 96 well plate and grown in oxygn-glucose deprivation or normal growth conditions for 4 hours. After 4 hours, media was replaced with the normal growth media, nMSC conditioned media, or aMSCγ conditioned media. Supernatants were collected 24 hours, 48 hours, 4 days, or 7 days later and stored at -80°C until analyzed. Cytokines levels were determined using the Rat Proinflammatory Panel 2 V-PLEX Assay (Meso Scale Discovery) according to manufacturer's instructions.

B. In vivo cytokine analysis

1 week after surgery, animals were euthanized and perfused with ice cold heparinized saline (10 U/mL) for 12 minutes and brains were extracted and snap frozen using liquid nitrogen and stored at -80°C until analyzed. Rat brain hemispheres were homogenized using the Bio-Plex Cell Lysis Kit (Bio-Rad, Inc) according to manufacturer's instructions and quantified using the BCA method. Cytokines were analyzed using the

Bio-Plex Pro™ Rat Cytokine 23-Plex Assay (Bio-Rad, Inc) according to manufacturer's directions. The kit was run using recommended starting amount of protein and was analyzed using a Luminex FLEXMAP 3D®.

3.2.24. Mass spectrometry

A. Sample preparation, TMT labeling, and fractionation

15 mL of conditioned media was collected as above and concentrated using an Amicon Ultra-15 centrifugal filter unit with a 3 kDa molecular weight cutoff (Millipore, Burlington, MA, USA). Concentrated protein was quantified using a BCA protein assay kit (ThermoFisher Scientific, Waltham, MA, USA) and 100 µg of total protein from each sample was processed by filter aided sample preparation. Proteins were diluted in 8 M urea, reduced in 5 mM DTT in 8 M urea for 20 minutes at 55°C and then alkylated in 10 mM iodoacetamide for 20 minutes at room temperature in the dark. The samples were then urea exchanged with 50 mM triethylammonium bicarbonate (TEAB) and trypsin (2 µg per sample) was added and samples were incubated overnight at 37°C. Peptides were eluted with 80 µL of 50 mM TEAB and then digested peptides were labeled using 2 tandem mass tag (TMT) kits (ThermoFisher Scientific) according to manufacturer's instructions where samples were labeled using 126-131 tags (one replicate per mass tag). Subsequently, the individual samples where combined, lyophilized, and resuspended in 10 mM ammonium hydroxide and fractionated (20 fractions) via high pH reverse phase chromatography. Each fraction was then lyophilized and resuspended in 20 µL 0.1% formic acid prior to nano-LC-MS/MS

B. Nano-LC-MS/MS analysis and data analysis

Mass detection occurred with an Orbitrap Velos Pro (ThermoFisher Scientific) equipped with an Agilent HPLC system. Chromatographic separation of peptides was accomplished using a Zorbax 300SB-C18 column (3.5 µm ID x 150 mm, particle size 5 µm, pore size 100 Å, Agilent Technologies). The peptides were loaded onto a Zorbax 300SB-C18 trap cartridge at a flow rate of 3 µL/minute for 10 minutes. After washing with 0.1% formic acid, the peptides were eluted using a 5-40% B gradient for 60 minutes at a flow rate of 250 nL/minute acid (mobile phase A = 0.1% formic acid; mobile phase B = 0.1% formic acid in acetonitrile). The flow-through was analyzed using DDA settings to select the top 10 most abundant ions for HCD fragmentation. Proteins were identified by searching MS/MS spectra against the Human SwissProt database using the Mascot search engine employing a reversed decoy database to calculate the false discovery rate (FDR). Trypsin was set as the protease with two missed cleavages and searches were performed with precursor and fragment mass error tolerances were set at 15 ppm and 0.4 Da, respectively. Peptide precursors of +2, +3, and +4 were considered. Peptide variable modifications allowed during the search were: oxidation (M) and deamination (NQ), whereas carbamidomethyl (C) and TMT6plex (K and N-term) were set as fixed modifications. To calculate the FDR, the search was performed using the “decoy” option in Mascot. Scaffold Q+ was used to quantitate TMT-labeled peptides from the samples. Peptide identifications were accepted if they could be established at a greater than 95.0% probability by the Scaffold Local FDR algorithm. Protein identifications were accepted if they could be established at a greater than 99.0% probability and contained at least 2 identified peptides. Protein probabilities were assigned by the Protein Prophet algorithm.

Proteins that contained similar peptides and could not be differentiated based on MS/MS analysis alone were grouped to satisfy the principles of parsimony. Proteins sharing significant peptide evidence were grouped into clusters. Normalization was performed iteratively (across samples and spectra) on intensities. Medians were used for averaging. Spectra data were log-transformed, pruned of those matched to multiple proteins, and weighted by an adaptive intensity weighting algorithm. Differentially expressed proteins were determined by applying the Scaffold permutation test with unadjusted significance level $p<0.05$. Pathway analyses were conducted using the PANTHER database (www.pantherdb.org) and the DAVID Gene Functional Classification Tool (https://david.ncifcrf.gov).

3.2.25. Statistical analyses

All statistical analyses were done in GraphPad Prism (Version 7.03; GraphPad Software Inc). All data shown represent mean ± SEM and a probability of less than 0.05 was considered statistically significant. Individual statistical analyses are described in the appropriate text and figure legends.

4. RESULTS

4.1. Hypoxia induces a proinflammatory microglia phenotype

A large portion of damage done following stroke is a result of inflammatory mediators released by immune cells, especially activated microglia. This response results in an increase in toxic inflammatory mediators including, but not limited to, IL-1β, IL-6, and TNF-α (Janardhan and Qureshi 2004). The increase in these molecules is sufficient to induce neuronal apoptosis within the infarcted tissue ultimately causing irreversible brain damage. How these mediators affect NSCs and NPCs is still largely unknown; however, hypotheses demonstrating the detrimental effects of inflammation have been proposed (Iosif, Ekdahl et al. 2006, Iosif, Ahlenius et al. 2008). These effects have been proposed to be caused by progenitor cell suppression via TNF-α secretion by activated microglia (Iosif, Ekdahl et al. 2006, Iosif, Ahlenius et al. 2008). Furthermore, LPS-activated microglia have been shown to compromise survival of newly formed neurons following brain injury (Ekdahl, Claasen et al. 2003, Monje, Toda et al. 2003). While there is a clear interaction between neurogenesis and microglial function, the details of this interaction are still largely unknown. Numerous peripheral inflammatory cells, including neutrophils, macrophages, and T cells, are recruited to sites of ischemic injury (Jin, Yang et al. 2010). The mechanism by which these cells contribute to decreased neurogenesis following ischemic injury, and the way in which they affect NSCs remains largely unknown. Post-ischemia inflammation is characterized by microglial activation followed by infiltration of circulating inflammatory cells (Schilling, Besselmann et al. 2003, Tanaka, Komine-Kobayashi et al. 2003, Kriz 2006, Amantea, Nappi et al. 2009, Jin, Yang et al. 2010)

4.1.1. *In vitro* oxygen-glucose deprivation increases proinflammatory cytokine production by microglia

To examine the effect that an *in vitro* model of stroke has on primary microglia, microglia were subjected to oxygen-glucose deprivation and then proinflammatory cytokines in the supernatants were measured using a multiplex kit (Rat Proinflammatory Panel 2 V-PLEX Assay; Meso Scale Discovery). Proinflammatory cytokines IL-6 (Figure 4A) and TNF-α (Figure 4B) were significantly increased 48 hours after OGD compared to the levels at 24 hours.

4.1.2. Conditioned media from hypoxia-primed microglia decreases neural stem cell proliferation

It is not well established how microglia, especially microglia under hypoxic conditions, affected neural stem cell behavior. To try to understand this interaction better, proliferation of neural stem cells was examined after growth in normal media, conditioned media from normoxia-primed microglia, and conditioned media from hypoxia-primed microglia. Interestingly, proliferation of neural stem cells 24 hours after being put into the different media types have significantly increased proliferation in both normoxia- and hypoxia-primed microglia media (Figure 5A). However, by 48 hours and 72 hours, neural stem cells have significantly decreased proliferation when grown in hypoxia-primed microglia media (Figures 5B,C) suggesting that the proinflammatory mediators in the hypoxia-primed microglia media are detrimental to neural stem cell proliferation.

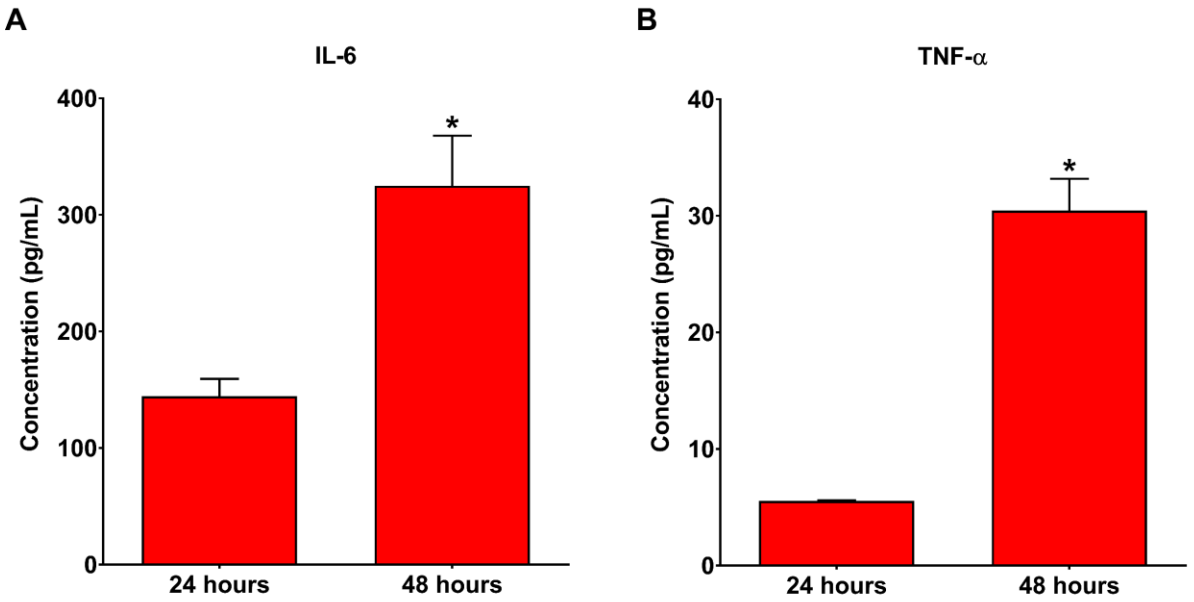

Figure 4. Oxygen-glucose deprivation increases microglia secretion of proinflammatory cytokines. Primary rat cortical microglia were subjected to oxygen-glucose deprivation for 4 hours before being transferred back to normal growth conditions. IL-6 (A) and TNF-α (B) were measured in cell culture supernatants 24 and 48 hours after cells were transferred back to normal growth conditions. Cells had secreted significantly more IL-6 and TNF-α 48 hours afterwards compared to 24 hours. Data were analyzed using a two-tail, unpaired t-test. *p≤0.05.

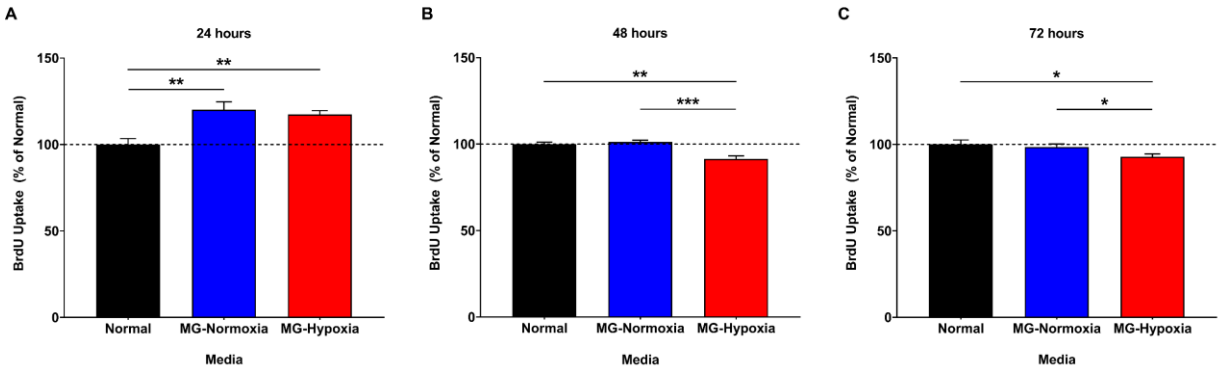

Figure 5. Hypoxia-primed microglia decrease neural stem cell proliferation. Neural stem cells were cultured in normal media, media from normoxia-primed microglia, or media from hypoxia-primed microglia in the presence of BrdU. Cells were analyzed at 24 hours, 48 hours, and 72 hours for rates of proliferation expressed as BrdU uptake. **A.** At 24 hours, neural stem cells grown in media from normoxia- and hypoxia-primed microglia exhibited significantly increased proliferation. **B,C.** After 48 hours (B) and 72 hours (C), neural stem cells had significantly reduced proliferation when grown in media from hypoxia-primed microglia. Data were analyzed using a one-way ANOVA with Holm-Sidak multiple comparison testing. *p≤0.05, **p<0.01, ***p<0.001.

4.2. Hypoxia reduces normal growth capacity of neural stem cells

Utilization of endogenous neurogenesis following ischemic injury is critical in aiding in functional recovery. Endogenous neurogenesis is a series of events involving the proliferation, migration, differentiation, and integration of NSCs/NPCs into damaged brain areas. NSC numbers have been shown to increase following ischemic stroke; however, they rapidly die (Palmer, Willhoite et al. 2000) thereby preventing successful brain repair. Proliferation of NSCs following ischemic stroke does not seem to be impaired. Rather, it is the survival of these progenitor cells that seems to be hindered with an estimated 10% of newborn cells surviving (Ohab, Fleming et al. 2006). Furthermore, aged and injured brains have reduced neurogenic signaling making it even more difficult to direct the migration and differentiation of endogenous NSCs needed to repair infracted tissue (Hallbergson, Gnatenco et al. 2003, Lazarov, Mattson et al. 2010)

4.2.1. Hypoxia causes a transient increase in neural stem cell proliferation

To try to understand what was occurring with neural stem cells following stroke, we wanted to see how their proliferation was affected *in vitro* when exposed to oxygen-glucose deprivation. To do this, primary SVZ-derived neural stem cells were grown in OGD for 4 hours before being transferred back to normal growth conditions in the presence of BrdU. Cells were then examined for rates of proliferation, measured by BrdU uptake, 24, 48, and 72 hours later. Interestingly, at 24 hours, neural stem cells had significantly increased proliferation after OGD compared to cells grown under normal growth conditions the entire time (Figure 6). This increased proliferation, however, declined back to normal levels at 48 and 72 hours (Figures 6).

4.2.2. Hypoxia causes a transient increase in neurotrophic factor mRNA in neural stem cells

To help elucidate what is occurring in the neural stem cells after OGD that could account for the changes in proliferation, we next examined mRNA levels of different neurotrophic factors including GDNF, BDNF, IGF-1, NT3, and NGF. Neural stem cells were grown as above and RNA was then collected 24 hours and 48 hours later to measure mRNA expression of these neurotrophic factors. Remarkably, after 24 hours, mRNA levels of all of these factors was drastically increased (Figure 7). However, at 48 hours, while NGF and NT3 remained increased, mRNA levels of GDNF, BDNF, and IGF-1 were significantly decreased to below normal levels (Figure 7). This suggests that the rapid increase in neurotrophic factor levels is responsible for the acute increase in proliferation while loss of GDNF, BDNF, and IGF-1 in combination is sufficient enough to have deleterious effects on proliferation of neural stem cells.

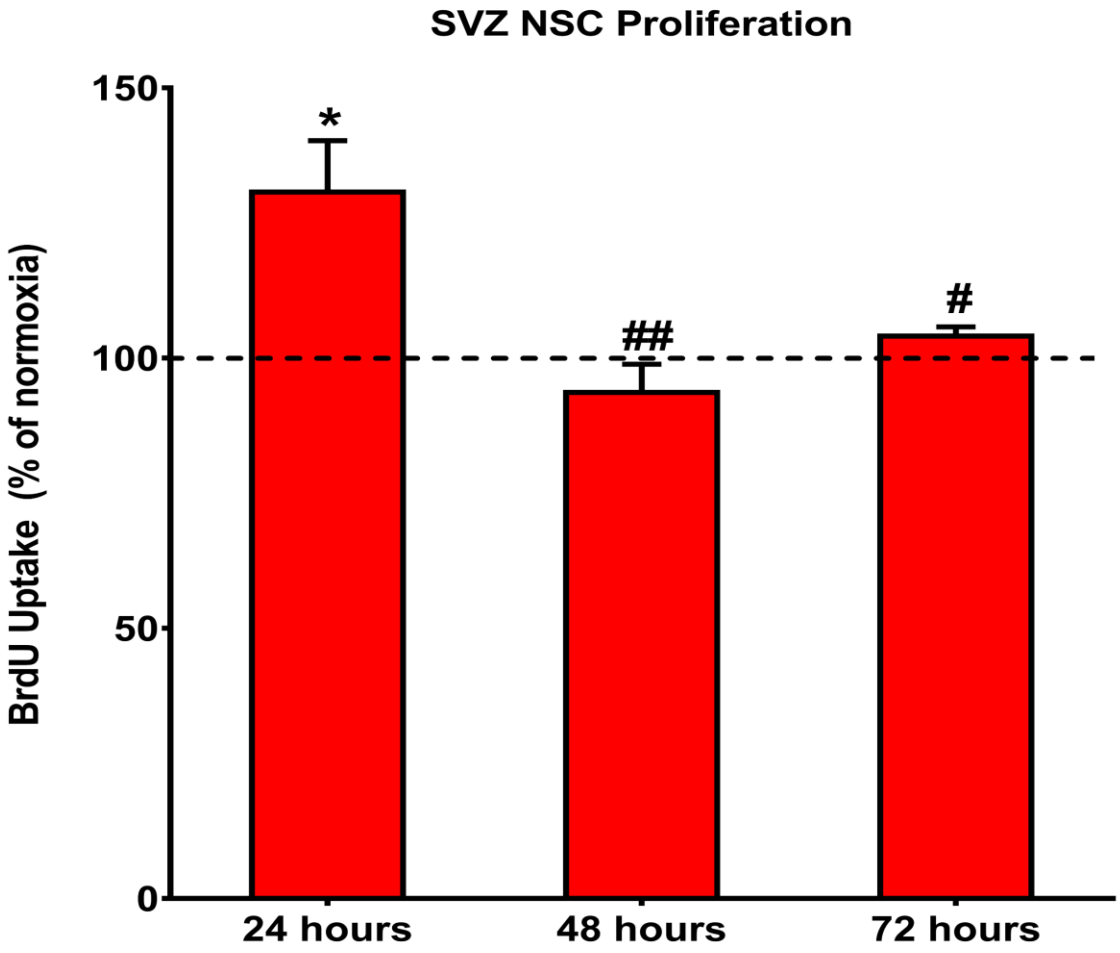

Figure 6. Oxygen-glucose deprivation causes a transient increase in NSC proliferation. Neural stem cell were primed in normal growth conditions or in OGD for 4 hours before having the media replaced with BrdU-containing media and transferred back to normal growth conditions for 24, 28, or 72 hours. After 24 hours, cells primed in OGD exhibited significantly increased proliferation compared to cells grown normally. This increase was lost at 48 and 72 hours. Normoxia vs OGD data were analyzed using two-tail, unpaired t-test. Data across time was compared using one-way ANOVA with Holm-Sidak multiple comparison testing. *Compared to normoxia. $^{\#}$Compared to 24 hours. *$p \leq 0.05$, $^{\#}p \leq 0.05$, $^{\#\#}p < 0.01$.

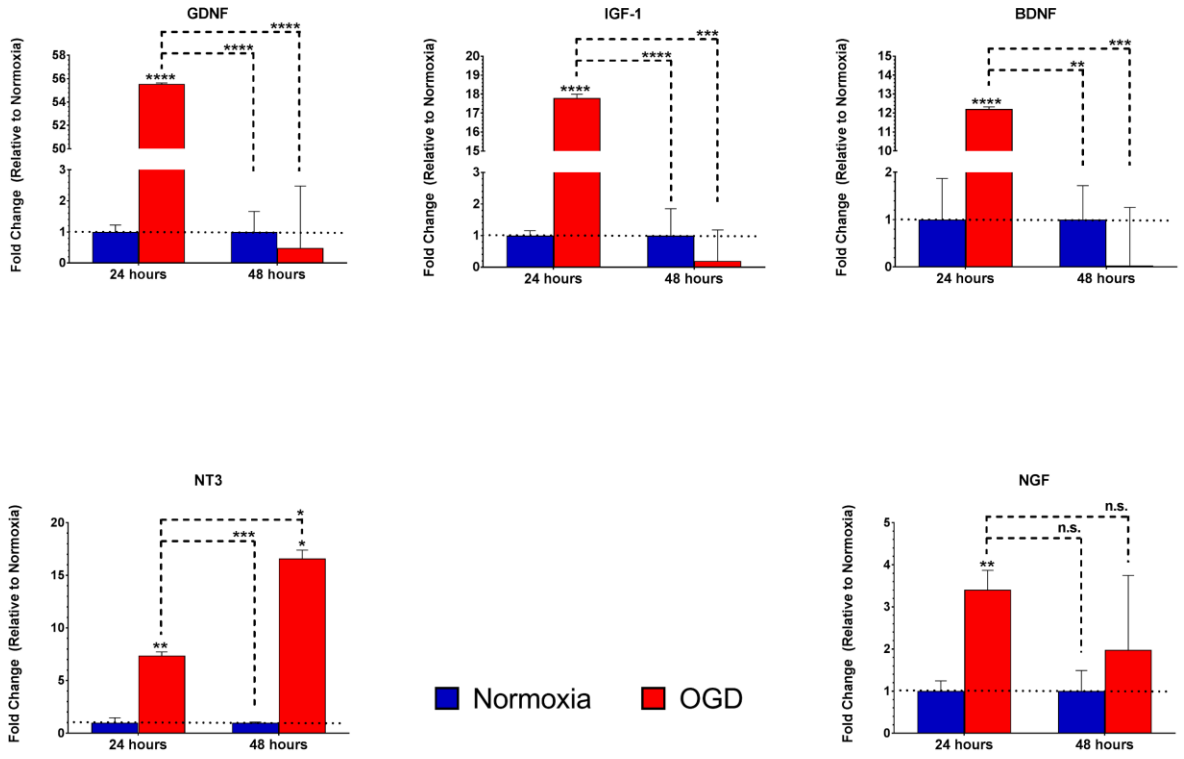

Figure 7. Oxygen-glucose deprivation causes an acute increase in neurotrophic factor mRNA expression. SVZ-derived neural stem cells were primed in OGD for 4 hours and then transferred to normal growth conditions. After 24 hours of OGD, mRNA levels of GDNF, IGF-1, BDNF, NT3, and NGF were all significantly elevated. After 48 hours, the levels of GDNF, IGF-1, and BDNF were significantly decreased with NT3 and NGF remaining elevated. Data were analyzed using a two-way ANOVA with Holm-Sidak multiple comparison testing. *p≤0.05, **p<0.01, ***p<0.001, ****p<0.0001.

4.3. Mesenchymal stem cells improve functional recovery following middle cerebral artery occlusion

Numerous preclinical rodent students have demonstrated the efficacy of MSCs following ischemic stroke (Li, Chen et al. 2002, Nomura, Honmou et al. 2005, Honma, Honmou et al. 2006, Chen, Cheng et al. 2008, Koh, Kim et al. 2008, Lim, Jeong et al. 2011, Liu, Zhang et al. 2011, Wei, Fraser et al. 2012, Xin, Li et al. 2013, Yang, Liu et al. 2014, Gutierrez-Fernandez, Rodriguez-Frutos et al. 2015, Lowrance, Fink et al. 2015, Quittet, Touzani et al. 2015, Toyoshima, Yasuhara et al. 2015, Yamauchi, Kuroda et al. 2015). However, the mechanism by which MSCs effect these beneficial responses is largely unknown. Additionally, previous literature has demonstrated that when activated by interferon-γ ex vivo, the effect of MSCs is greatly enhanced and similar effect sizes can be seen using substantially fewer cells (Polchert, Sobinsky et al. 2008, Lee, Szilagyi et al. 2013). Based on these previously published studies we set out to determine whether interferon-γ-activated MSCS (aMSCγ) could be more beneficial in treating ischemic stroke compared to naïve, non-activated MSCs (nMSC). The mesenchymal stem cells used were bone marrow derived stem cells obtained from P5 rat pups and cell type was confirmed by phenotypic analysis of cell surface markers by flow cytometry. Mesenchymal stem cells were confirmed by positive expression of CD29 and CD90 and absence of CD11b, MHC-II (RT1D), and CD45 (Figure 8).

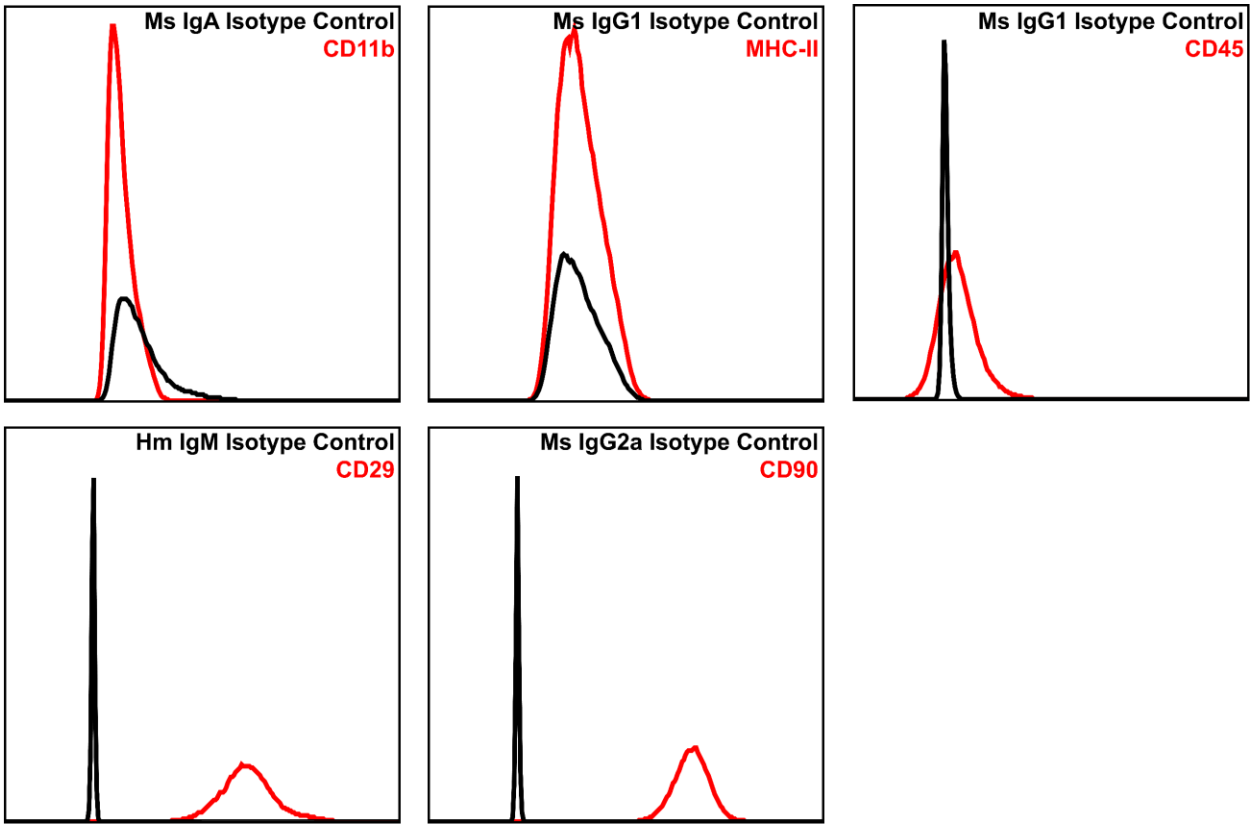

Figure 8. Phenotype of isolated MSCs. To confirm purity and identify of isolated bone marrow MSCs, flow cytometry was performed to analyze surface expression of CD11b, MHC-II, CD45, CD29, and CD90. Isolated cells were positive for CD29 and CD90 (bottom panels) and did not express the monocyte markers CD11b, MHC-II, or CD45 (top panel), indicating a pure population of MSCs.

4.3.1. Intravenously delivered MSCs traffic to the brain after stroke

To determine whether MSCs traffic to the brain following stroke, rats were subjected to 90 minutes of middle cerebral artery occlusion (MCAO) and were then administered nMSC or aMSCγ intravenously 3 hours after reperfusion. Brains were then harvested for whole organ fluorescence imaging. Five minutes after delivery of MSCs, they were detectable in the rat brains (Figure 9) demonstrating that rapid uptake of MSCs into the brain.

4.3.2. MSC treatment causes a more rapid and sustained sensorimotor improvement after ischemic stroke

Using the MCAO model of ischemic stroke, adult (age 14-16-week-old) female Sprague-Dawley rats were subjected to a transient 90-minute MCAO followed by vehicle, nMSC ($5.0x10^6$ cells/kg), or aMSCγ ($5.0x10^6$ cells/kg) treatment 3 hours after MCAO. Animals were then scored using the modified neurological severity score (mNSS) each day for the first 7 days and then again on days 14 and 21. Animals treated with both nMSC and aMSCγ exhibited a more rapid recovery with animals returning to near baseline functional status by day 21 (Figure 10). While vehicle treated animals did improve significantly from Day 1 to Day 21, they still remained significantly more impaired compared to MSC treated animals and there were no differences between nMSC and aMSCγ treated animals.

4.3.3. MSC treatment significantly improves open field activity after MCAO

In addition to the mNSS, animals were tested in an open field apparatus to examine strictly their motor impairments following MCAO with or without MSC treatment. Animals were treated as above and then underwent open field testing at 24 hours and 7 days following MCAO. Animals were allowed to explore the open field for 15 minutes and the total distance traveled, ambulatory episodes, ambulatory time, average velocity, clockwise rotations (an indicator of ipsilateral motor deficits), and time in the center versus periphery (with increased time in the center being a correlate for reduced anxiety levels) were examined. 24 hours after stroke, vehicle treated animals traveled significantly shorter distances (Figure 11B), ambulated fewer times (Figure 11C), spent significantly less time ambulating (Figure 11D), had increased numbers of clockwise rotations (Figure 11F), and spent significantly more time in the center of the open field (Figure 11G) compared to sham animals. With MSC treatment, these deficits were reversed (Figures 11B-G). With the exception of clockwise rotations and time spent in the center of the open field. These differences are maintained 7 days after MCAO (Figure 12).

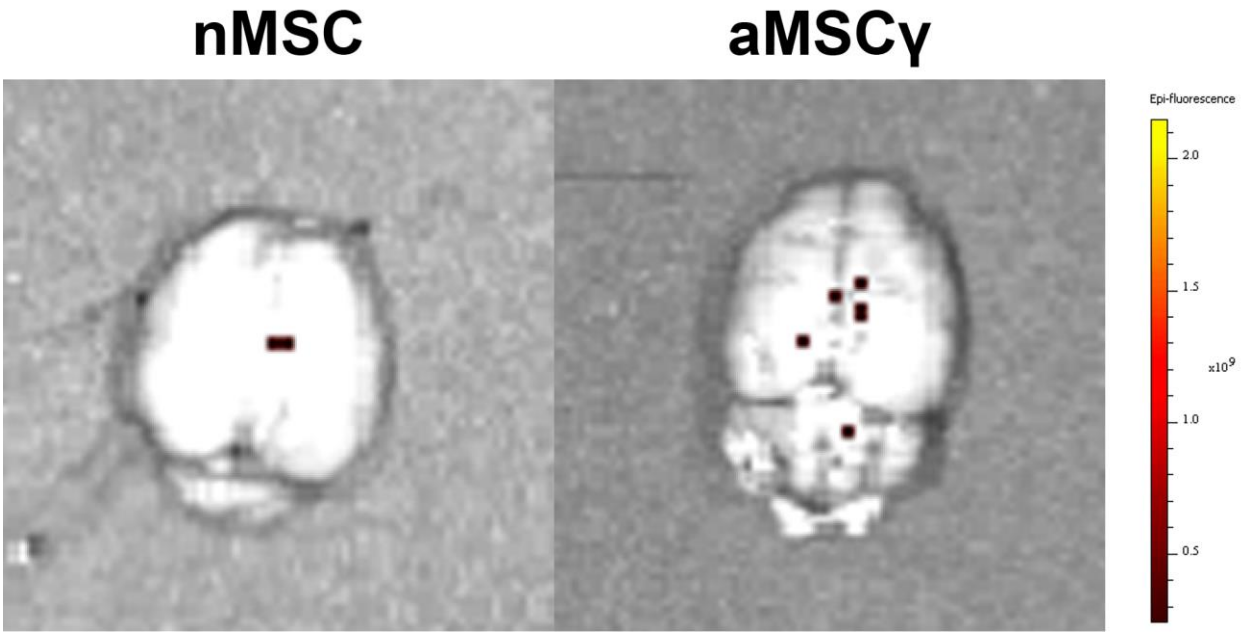

Figure 9. MSCs rapidly accumulate in the brain following MCAO. Rats underwent 90-minute MCAO. Three hours after, rats were administered either nMSC ($5.0X10^6$ cells/kg), or aMSCγ ($5.0X10^6$ cells/kg) intravenously and were sacrificed 5 minutes later to harvest brains for IVIS imaging. Following MCAO, nMSC and, to a larger extent, aMSCγ are rapidly detected in brain tissue.

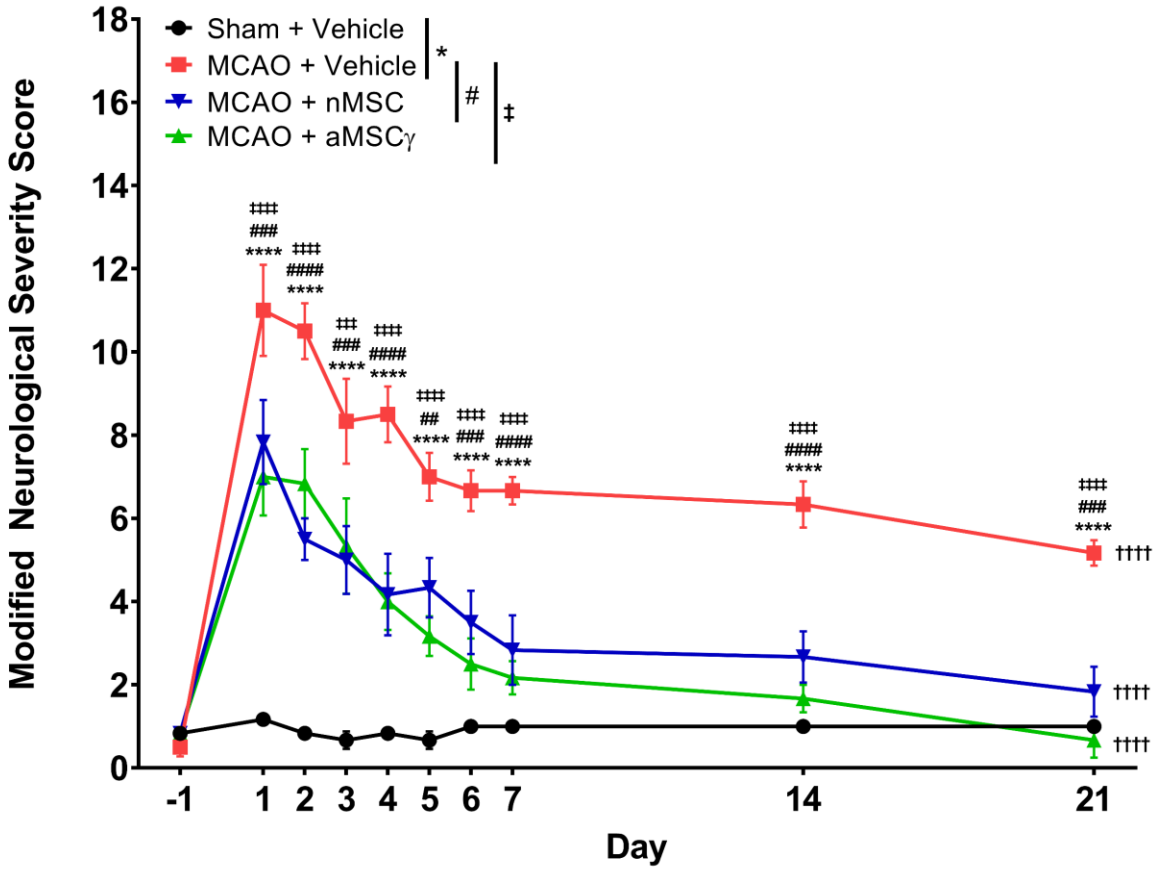

Figure 10. MSC treatment improves functional recovery following MCAO. Rats underwent either sham surgery or 90-minute MCAO (N = 6 per group). Three hours after, rats were administered either vehicle, nMSC ($5.0X10^6$ cells/kg), or aMSCγ ($5.0X10^6$ cells/kg) intravenously and assessed via the modified neurological severity score (mNSS) daily for the first seven days and then again on days 14 and 21. Following MCAO, vehicle-treated rats have significantly higher mNSS scores than sham rats at all time points. Animals treated with MSCs recover more rapidly compared to vehicle-treated rats and demonstrate sustained improvement up to 21 days following MCAO with no difference between nMSC and aMSCγ. Data were compared using repeated measures, two-way ANOVA with Holm-Sidak multiple comparison testing. *Sham + Vehicle vs MCAO + Vehicle; #MCAO + Vehicle vs MCAO + nMSC; ‡MCAO + Vehicle vs MCAO + aMSCγ; †Day 1 vs Day 21. **p<0.01, ***p<0.001, ****p<0.0001, ##p<0.01, ###p<0.001, ####p<0.0001, ††††p<0.0001, ‡‡‡p<0.001, ‡‡‡‡p<0.0001.

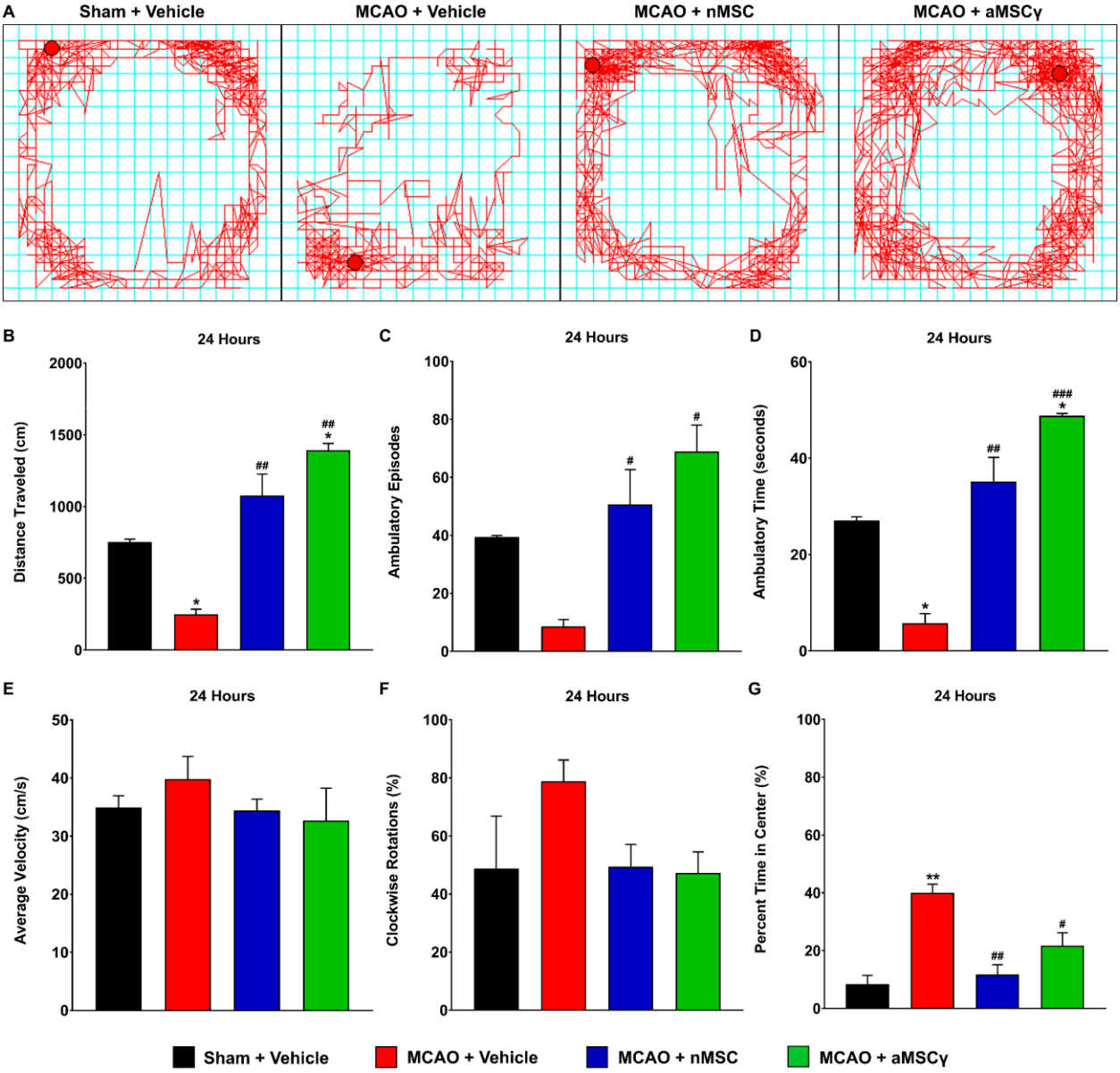

Figure 11. MSC treatment improves motor function 24 hours after MCAO. Rats underwent either sham surgery or 90-minute MCAO (N = 3 per group). Three hours after, rats were administered either vehicle, nMSC ($5.0X10^6$ cells/kg), or aMSCγ ($5.0X10^6$ cells/kg) intravenously and assessed via open field testing. **A.** Representative open field tracking. Vehicle treated animals traveled less (B), fewer times (C), and for a shorter period of time (D) with MSC treatment causing recovery in these deficits. Average velocity was not different between groups (E) and vehicle treated animals had increased clockwise rotations (F) and spent more time in the center of the field (G). Data were compared using one-way ANOVA with Holm-Sidak multiple comparison testing. *Compared to Sham + Vehicle. #Compared to MCAO + Vehicle. *p≤0.05, **p<0.01, #p≤0.05, ##p<0.01, ###p<0.001.

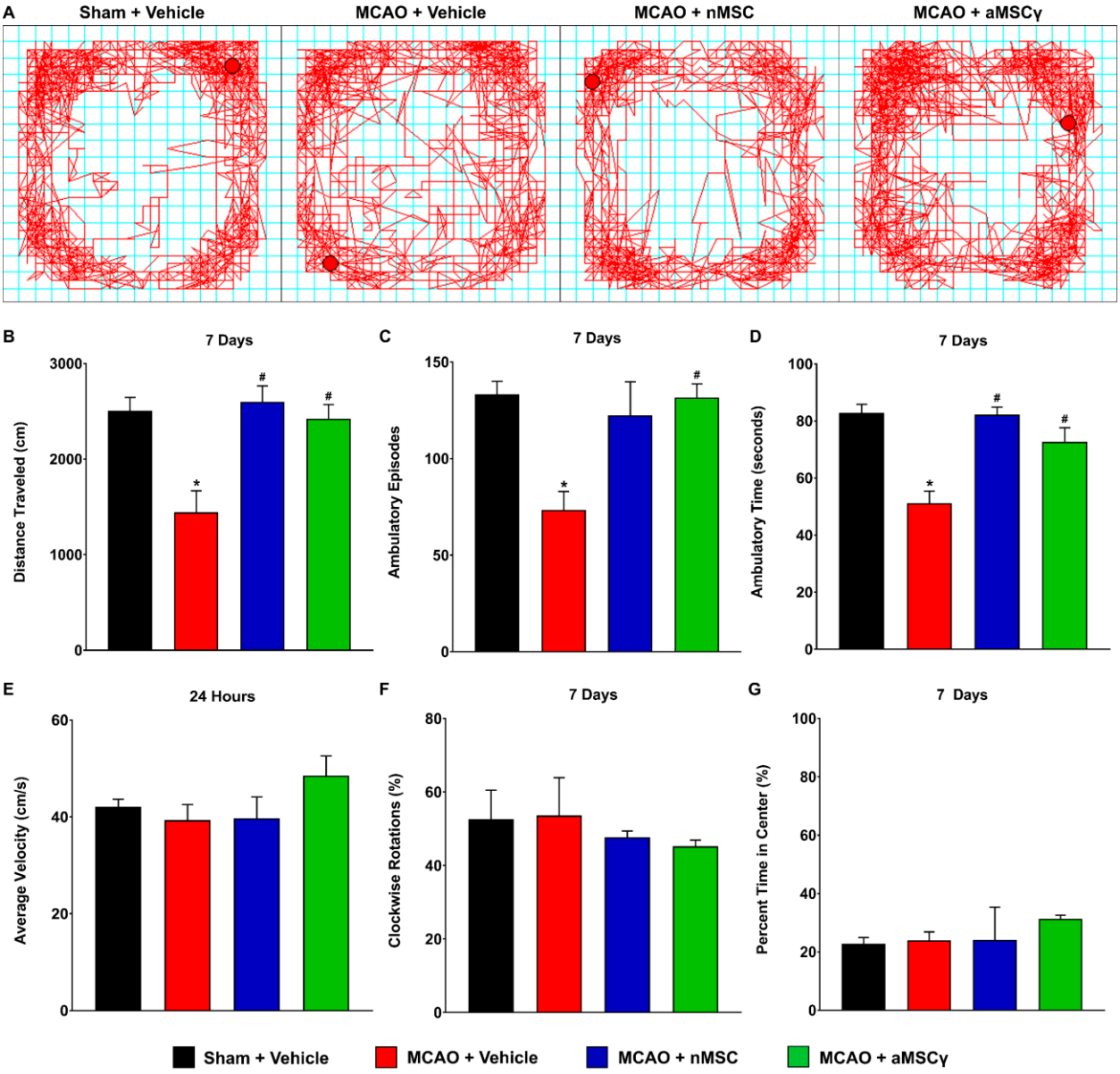

Figure 12. Motor recovery is sustained 7 days after MCAO. Rats underwent either sham surgery or 90-minute MCAO (N = 3 per group). Three hours after, rats were administered either vehicle, nMSC ($5.0X10^6$ cells/kg), or aMSCγ ($5.0X10^6$ cells/kg) intravenously and assessed via open field testing. **A.** Representative open field tracking. Vehicle treated animals traveled less (B), fewer times (C), and for a shorter period of time (D) with MSC treatment causing recovery in these deficits. Average velocity was not different between groups (E) and there were no changes in clockwise rotations (F) or time spent n the center of the field (G). Data were compared using one-way ANOVA with Holm-Sidak multiple comparison testing. *Compared to Sham + Vehicle. #Compared to MCAO + Vehicle. *p≤0.05, **p<0.01, #p≤0.05.

4.3.4. MSC treatment decreases infarct volume and percent infarction

To test the effect of MSC treatment on infarct volume and percent infarction, animals underwent MCAO with or without MSC treatment as previously described. After 48 hours, animals were then imaged using a 9.4T MRI (Appendix 6) to obtain T1, T2, and DWI imaging to assess the extent of infarction in sham animals, vehicle treated animals, and MSC treated animals. Sham animals did not have any infarct detectable on MRI (data not shown), while both nMSC and aMSCγ treated animals had significantly reduced infarct volume (Figure 13B) and percent infarction (Figure 13C).

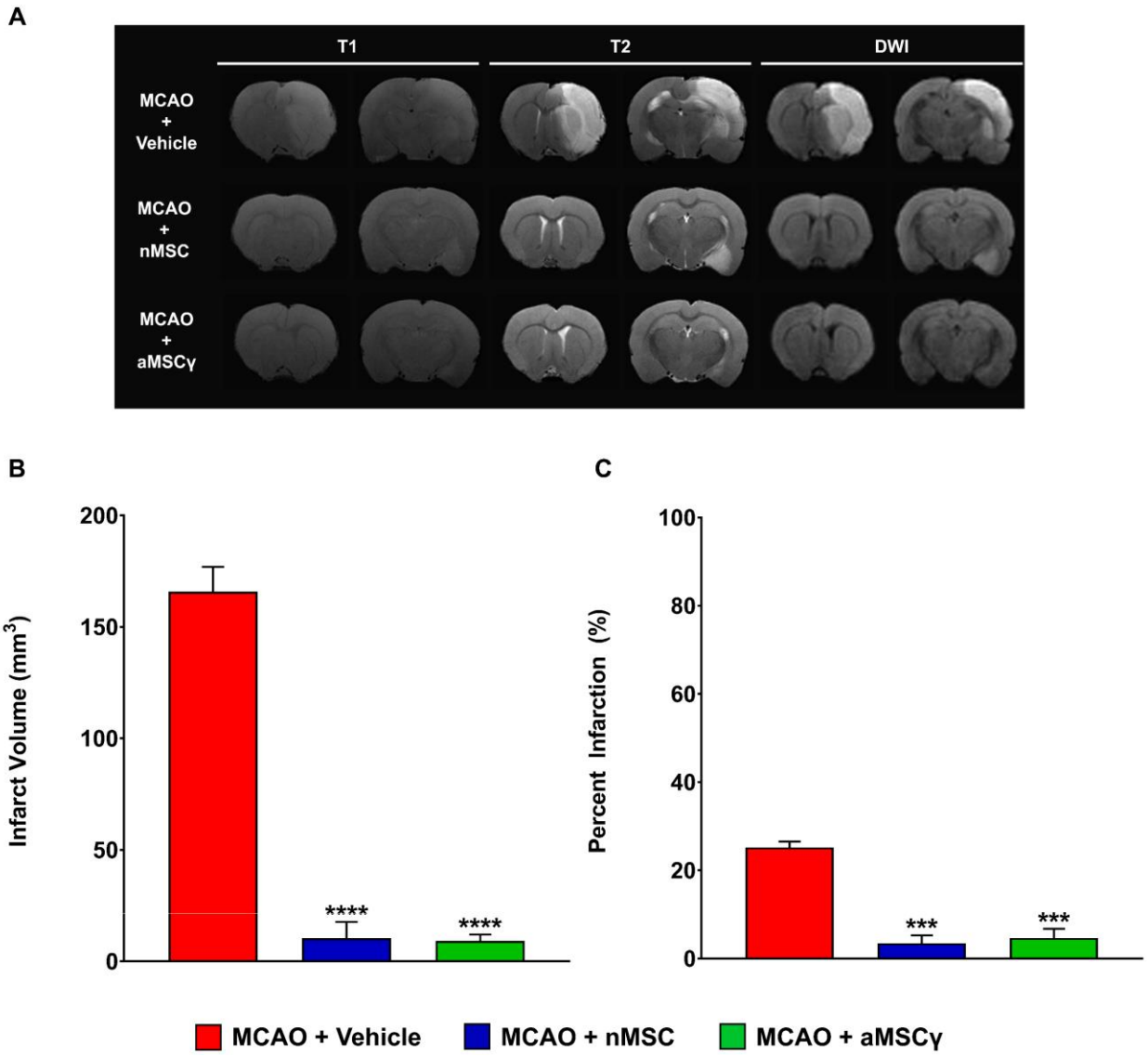

Figure 13. MSC treatment reduces infarct size. Rats underwent 90-minute MCAO and, after three hours, were administered either vehicle, nMSC ($5.0X10^6$ cells/kg), or aMSCγ ($5.0X10^6$ cells/kg) intravenously and MRI imaging was performed 48 hours later. A. Representative T1, T2, and DWI images. MSC treatment significantly reduced both infarct volume (B) and percent infarction (C). Data were compared using one-way ANOVA with Holm-Sidak multiple comparison testing. ***p<0.001, ****p<0.0001.

4.4. Mesenchymal stem cells convert microglia to a pro-regenerative phenotype

MSCs have the unique ability to reduce inflammation, produce neurotrophic factors, and to produce extracellular matrix components. They are therefore a novel tool that could be greatly beneficial for brain repair following stroke. Additionally, when co-cultured with bone marrow derived macrophages, MSCs have been demonstrated to preferentially polarize macrophages to an M2-like pro-regenerative phenotype as well as reduce secreted levels of IL-12 and TNF-α and increase secretion of the pro-regenerative IL-10 (Kim and Hematti 2009). Furthermore, it has been shown that in a mouse model of wound healing, both nMSC and, to a greater extent, aMSCγ, MSCs enhance regeneration and wound healing demonstrated by increased wound tensile strength with this effect being abrogated by depletion of macrophages (Lee, Szilagyi et al. 2013). As microglia are specialized cells originating from a hematopoietic lineage, similar to macrophages, we hypothesized that these interactions between macrophages and MSCs would hold. However, after an extensive literature search, it seems the vast majority of published work looking at the interaction between MSCs and microglia have been performed using immortalized microglia cell lines with nothing being done using primary microglia. There are established differences in the phenotypes and cytokine profiles between primary microglia and these cell lines (Horvath, Nutile-McMenemy et al. 2008, Stansley, Post et al. 2012). Consequently, we wanted to establish how MSCs effect primary microglia specifically.

To investigate the effect that MSCs have on primary microglia cytokine production, microglia were primed in oxygen-glucose deprivation for 4 hours before being transferred back to normoxia conditions and grown in either normal growth media, nMSC conditioned

media, or aMSCγ conditioned media for 24 hours, 48 hours, 4 days, or 7 days. Cell culture supernatants were collected and cytokines were measured using a multiplex kit (Rat Proinflammatory Panel 2 V-PLEX Assay; Meso Scale Discovery). Proinflammatory cytokines IL-6 (Figure 14A) and TNF-α (Figure 14B) were significantly decreased when microglia were grown in MSC conditioned media. Additionally, the pro-regenerative IL-4 (Figure 14C) and IL-10 (Figure 14D) were detected 7 days later only in cells grown in aMSCγ conditioned media.

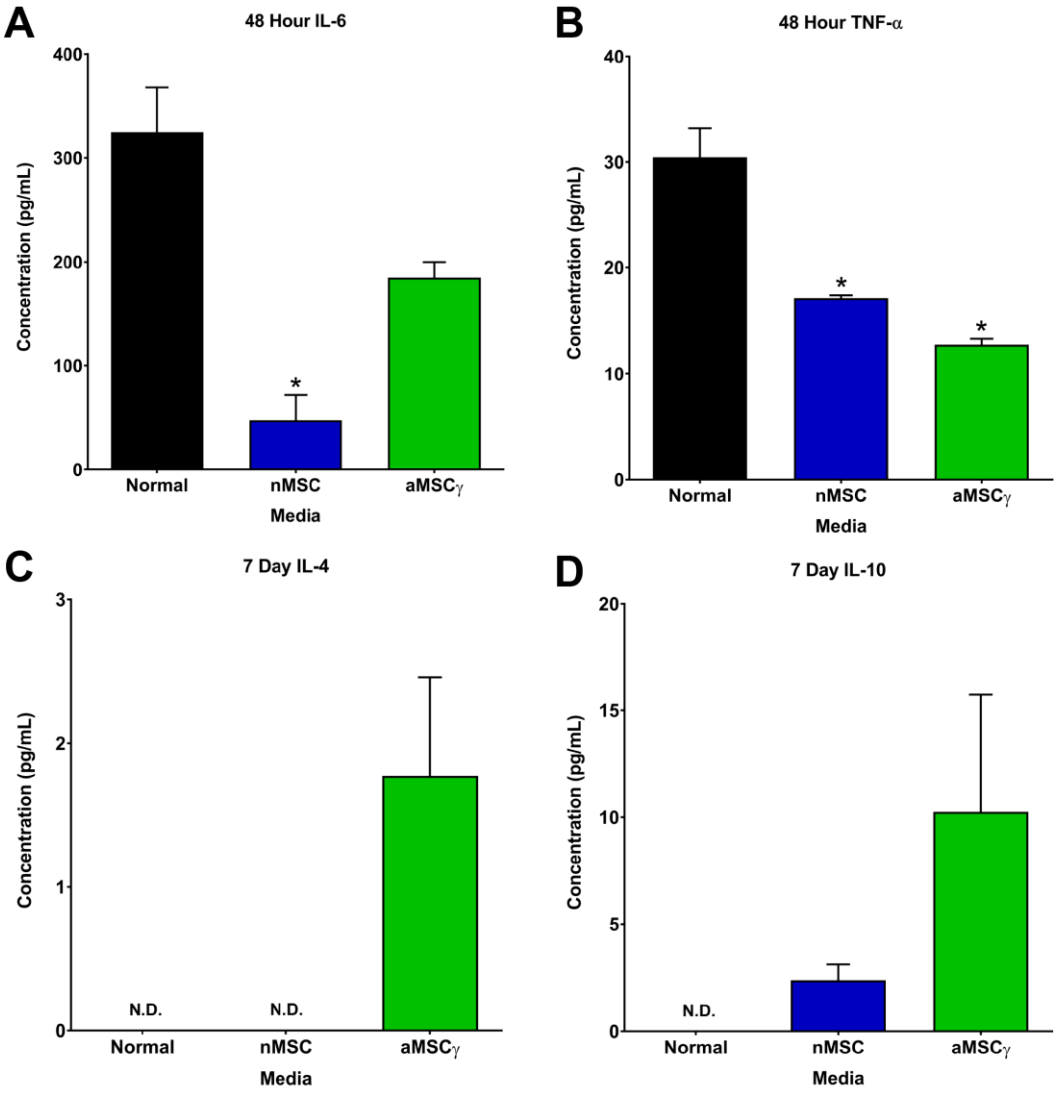

Figure 14. MSC conditioned media converts microglia to a pro-regenerative phenotype. Primary rat cortical microglia were subjected to oxygen-glucose deprivation for 4 hours before being transferred back to normoxia and growth in normal media, nMSC conditioned media, or aMSCγ conditioned media. IL-6, TNF-α, IL-4, and IL-10 were measured in cell culture supernatants 48 hours and 7 days after cells were transferred back to normoxia. **A.** When cultured in nMSC levels of IL-6 were significantly reduced with a trending reduction when grown in aMSCγ conditioned media 48 hours later. **B.** When cultured in nMSC and aMSCγ conditioned media, levels of TNF-δ were significantly reduced 48 hours later. **C.** At 7 days, levels of IL-4 are only detectable when cells are grown in aMSCγ conditioned media. **D.** At 7 days, levels of IL-10 are only detectable when cells are grown in MSC conditioned media with this level being further increased in cells grown in aMSCγ conditioned media. Data were analyzed using a one-way ANOVA with Holm-Sidak multiple comparison testing. *p≤0.05.

4.5. Mesenchymal stem cell treatment reduces microglia activation following MCAO

It is well established that mesenchymal stem cells can cause a phenotypic switch in peripheral macrophages under many different circumstances and, in fact, when co-cultured with bone marrow-derived macrophages they cause macrophages to adopt a pro-regenerative phenotype (Kim and Hematti 2009). Furthermore, MSCs have been demonstrated to suppress proinflammatory microglia in a fractalkine-dependent fashion while inducing microglia to secrete the neuroprotective molecules, CX3CR1, nuclear receptor 4 family, CD200R, and IGF-1 (Giunti, Parodi et al. 2012). It has also been shown that MSCs can reduce microglia activation via TGF-β signaling which reduces proinflammatory signaling of microglia via reduction in NF-κB signaling and induces a pro-regenerative microglia phenotype with upregulation of the fractalkine receptor, CD200R, and mannose receptor (Noh, Lim et al. 2016). Additionally, MSC conditioned media increases the phagocytic activity of microglia (Noh, Lim et al. 2016). To determine what was occurring in the context of ischemic stroke, microglia activation was assessed following MCAO with or without MSC treatment.

4.5.1. MSC treatment following MCAO reduces CD68 expression in the ipsilateral hemisphere

To address levels of microglia activation following MCAO, rat brains were stained for CD68 which is a lysosomal associated protein and is a marker for specifically activated microglia (Graeber, Streit et al. 1990, Slepko and Levi 1996, Kingham, Cuzner et al. 1999). Animals underwent MCAO with or without MSC treatment and were sacrificed at

24 hours, 1 week, or 3 weeks following surgery. Animals from the 24 hour time point did not exhibit significant CD68 positivity (data not shown) as this is likely too early of a time frame to demonstrate substantial, localized microglia activation. Vehicle treated animals from the 1 week time point, however, demonstrated significant microglia activation in the ipsilateral hemisphere. Animals treated with both nMSC and aMSCγ had significantly reduced microglia activation as demonstrated by a reduction CD68 staining intensity (Figure 15). This reduction was maintained in the animals from the 3 week time point as well. At this time point, however, in the vehicle treated animals, tissue had undergone liquefactive necrosis and there was a large cavitary lesion in what was the ischemic area (Figure 16A, dashed line indicates the approximate location of where the lateral border of the tissue would be without the cavity). MSC treated animals did not demonstrate this same cavitary lesion and had sustained reduction in microglia activation (Figure 16B,C).

4.5.2. MSC treatment following MCAO causes microglia to maintain a resting-like morphology

In addition to extent of microglia activation, we wanted to determine what morphology microglia adopted following MCAO with or without MSC treatment. Normally, resting microglia have a morphology that is highly ramified, with small cell bodies and numerous branching processes (Figure 17A, arrows). Activated microglia, typically have a morphology that is described as more amoeboid, with larger cell bodies and fewer processes (Figure 17B, arrowheads). One week after surgery, microglia from vehicle treated animals exhibit morphological changes consistent with microglia activation (Figures 18A,A') as well as express CD68. Interestingly, microglia from both nMSC and

aMSCγ treated animals exhibit morphology more similar to resting state microglia (Figures 18B-C,B'-C'); however, they also stain for CD68 suggesting that while these cells would be considered activated based upon CD68 expression, they are not actively phagocytosing cellular debris.

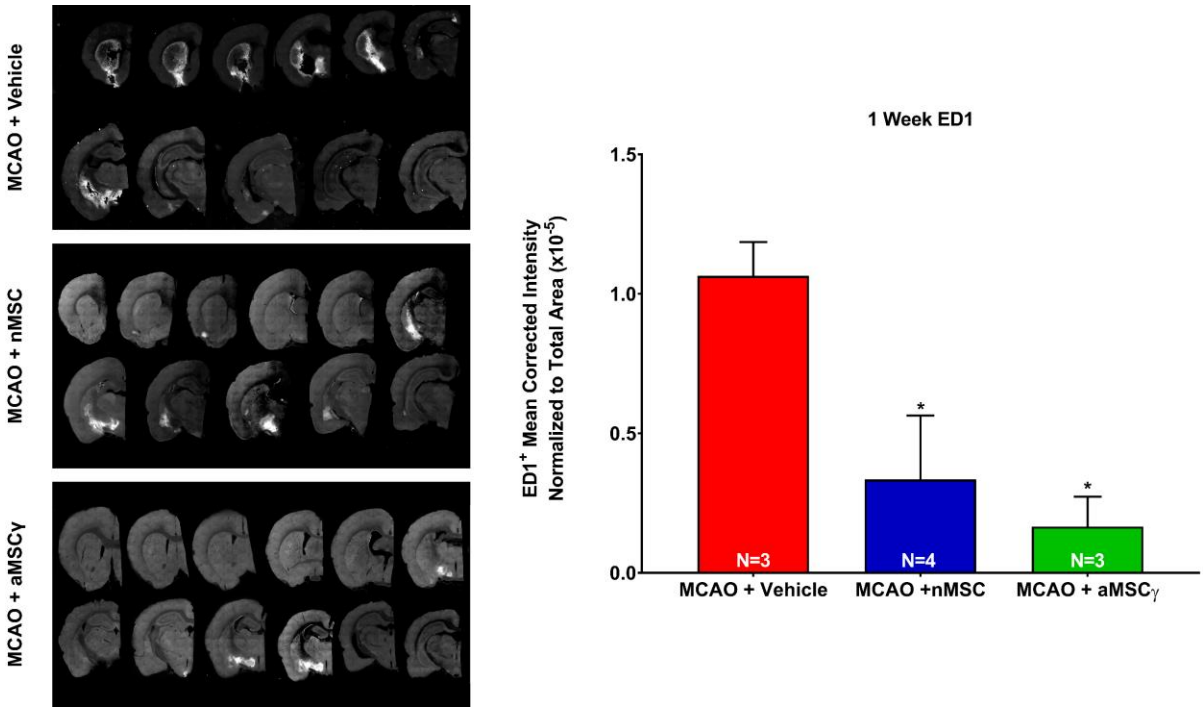

Figure 15. MSC treatment reduces microglia activation after MCAO. Rats underwent either sham surgery or 90-minute MCAO (N = 3 per group). Three hours after, rats were administered either vehicle, nMSC ($5.0X10^6$ cells/kg), or aMSCγ ($5.0X10^6$ cells/kg) intravenously and were sacrificed 1 week later. When treated with nMSC or aMSCγ, rats had significantly reduced microglia activation demonstrated here by reduction in CD68 staining intensity. Fluorescence images are representative of all animals per group and represent every 6^{th} section through the entire brain. Data were analyzed using one-way ANOVA with Holm-Sidak multiple comparison testing. *p≤0.05.

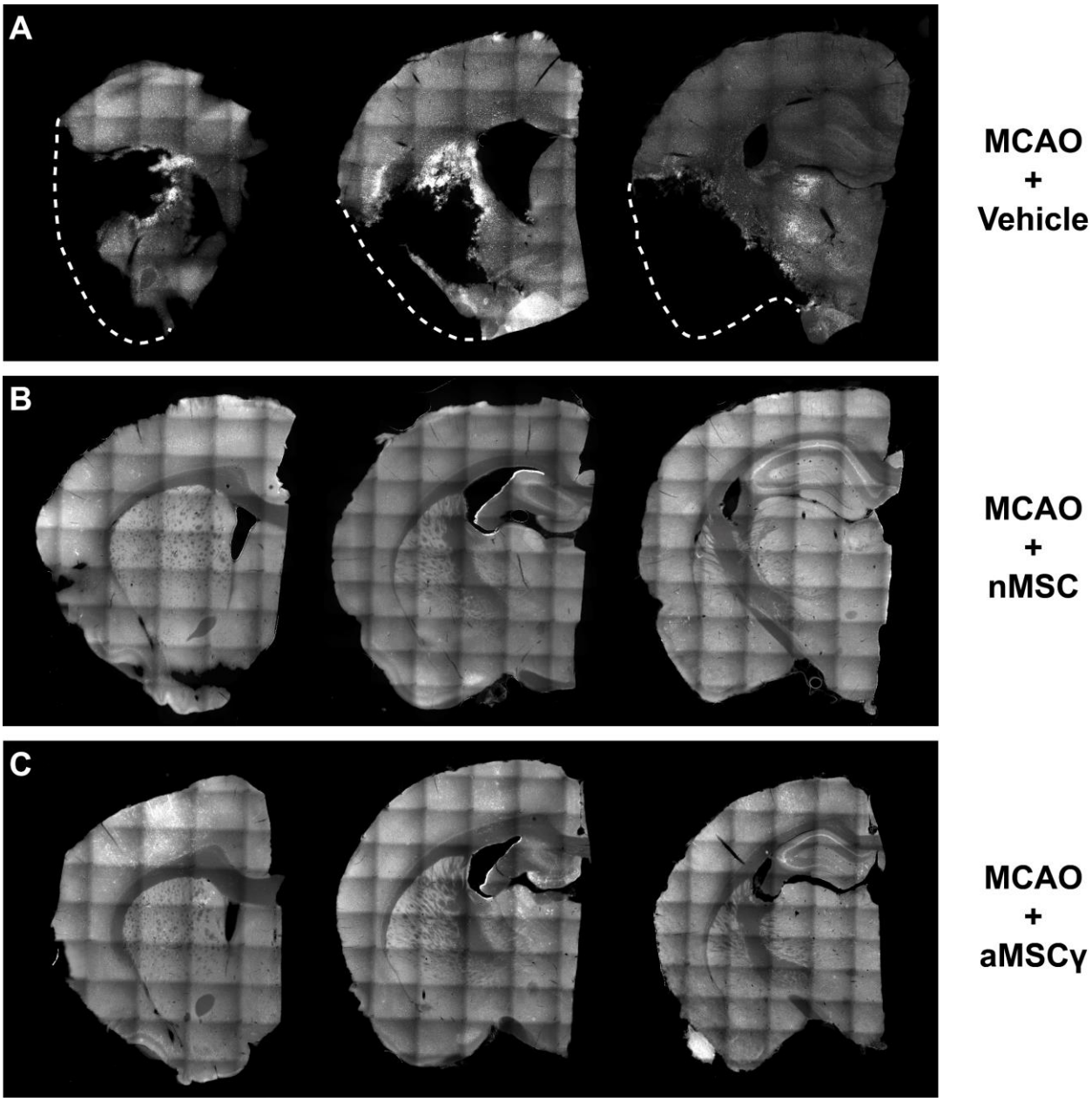

Figure 16. MSC-induced reduction in microglia activation is sustained 3 weeks after MCAO. Rats underwent either sham surgery or 90-minute MCAO (N = 3 per group). Three hours after, rats were administered either vehicle, nMSC ($5.0X10^6$ cells/kg), or aMSCγ ($5.0X10^6$ cells/kg) intravenously and were sacrificed 3 weeks later. Tissue in vehicle treated animals underwent liquefactive necrosis to form a cavitary lesion by 3 weeks after MCAO (dashed lines approximate the location of the lateral border of the tissue in a normal brain). Animals treated with nMSC or aMSCγ did not form cavitary lesions and had sustained reduction of microglia activation. Sections represent all sections through the entire cranial-caudal axis of the rat brain.

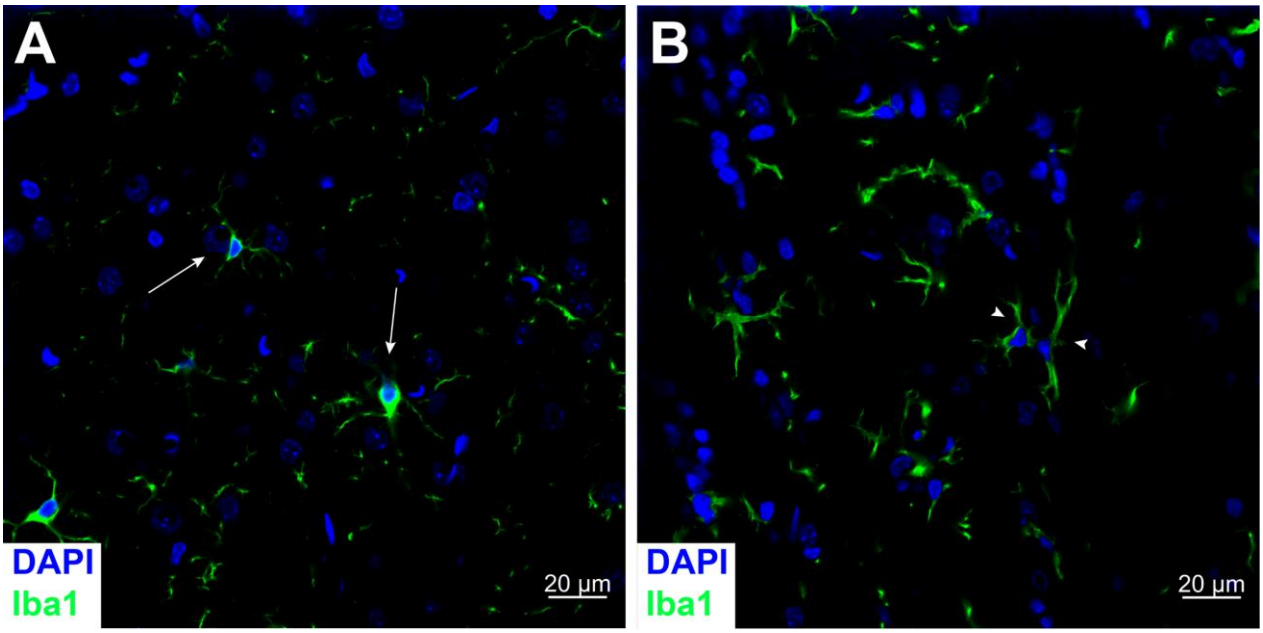

Figure 17. Morphological characteristics of microglia. A. Resting microglia are depicted next to the arrows. Resting microglia exhibit a so-called ramified morphology with small cell bodies and numerous branching processes. **B.** Activated microglia demonstrate a morphology described as amoeboid with larger small bodies and substantially fewer, if any, processes (arrowheads).

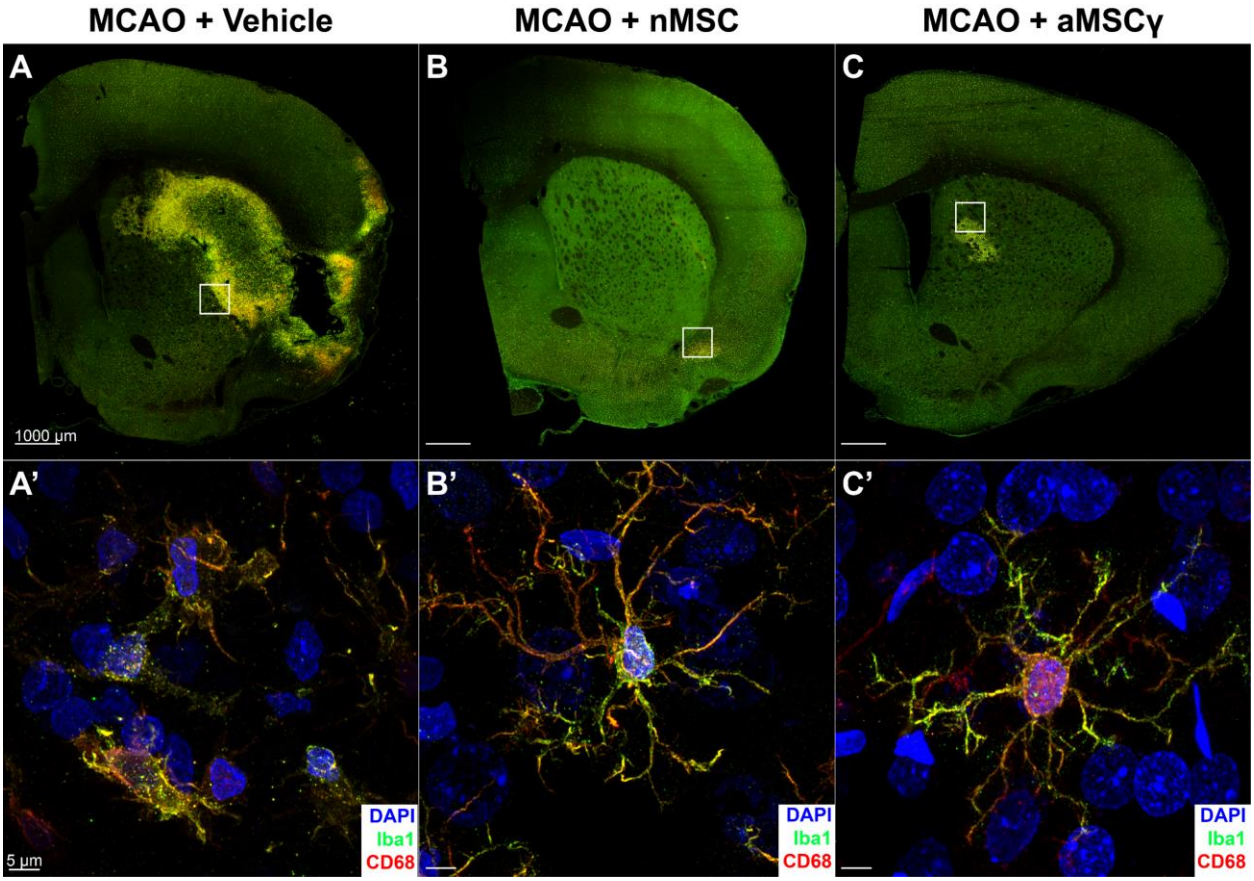

Figure 18. MSC treatment induces a resting state-like morphology of microglia. A-C. Representative slices of rat brains from the animal group sacrificed 1 week after surgery. Sections are stained with Iba1 (green), CD68 (red), and DAPI (blue). White boxes indicate locations of high magnification imagines in A'-C'. **A'.** Microglia from the vehicle treated animals demonstrate morphology consistent with activated microglia having large cell bodies with few processes. **B',C'.** Microglia from nMSC (B') and aMSCγ (C') exhibit morphological features consistent with resting microglia with small cell bodies and numerous process formations. These cells still express CD68.

4.6. Mesenchymal stem cells promote neural stem cell function

Activation of neurogenic mechanisms is a natural process that occurs acutely following ischemic stroke. Therapies aimed at improving functional neurological recovery are currently being investigated to aide in brain repair following ischemic stroke (Liu, Solway et al. 1998, Crain, Nikodemova et al. 2013, Yang, Xie et al. 2013). Replacement of mature cells following ischemic injury is critical in aiding functional recovery. Endogenous neurogenesis, though, is not a one-step process. It is a series of events involving the proliferation of NSCs/NPCs, migration of these cells to the damaged area, survival of these cells, differentiation of progenitor cells into different lineages of neural cells, and functional integration of these mature cells. Therefore, therapies aimed at each of these steps could prove beneficial in successful brain repair following ischemic stroke.

4.6.1. Mesenchymal stem cells express neurotrophic factors

To investigate whether MSCs could be beneficial in supporting the trophic factor loss seen from the neural stem cells, we wanted to determine which, if any, of these factors are made by MSCs. To do, this mesenchymal stem cells were grown under normal growth conditions or were activated with interferon-γ. After the 6 day activation protocol, RNA was extracted from both the nMSC and the aMSCγ to look for mRNA levels of BDNF, NT3, NGF, GDNF, and IGF-1. All of these factors were detected in nMSC while GDNF and IGF-1 were significantly increased in aMSCγ with a trending decrease in NGF (Figure 19). These data suggest that by growing neural stem cells with MSCs present, neurotrophic factor expression by neural stem cells could be replaced or even enhanced.

4.6.2. Mesenchymal stem cells enhance neurotrophic factor expression from neural stem cells

To test whether MSCs can, in fact, enhance neurotrophic factor mRNA levels from neural stem cells, a co-culture system was utilized. First, neural stem cells were primed in OGD for 4 hours. Next, cells were transferred back to normal growth conditions or normoxia with the addition of aMSCγ in a transwell insert at a ratio of 10:1 NSC:aMSCγ. Cells were then grown for 24 or 48 hours in normoxia before RNA was isolated from the neural stem cells. qRT-PCR was then performed to look at mRNA levels of GDNF, BDNF, and IGF-1. Interestingly, with the addition of aMSCγ, mRNA levels of all three factors was increased both at 24 and 48 hours (Figure 20).

4.6.3. Mesenchymal stem cells induce morphological changes in neural stem cells suggestive of differentiation

Originally, we hypothesized that growing neural stem cells either in conditioned media from MSCs or in a co-culture system would causes changes in neural stem cell proliferation. However, an interesting phenotype was apparent in neural stem cells grown in conditioned media from MSCs. Normally, neural stem cells grow as 3D spheres in suspension (Figure 21A). However, when grown in nMSC or aMSCγ conditioned media, they no longer grow in suspension as spheres but grow as adherent single cells that form processes (Figures 21B,C). Process formation begins as early as 30 minutes after plating and continues as long as the cells are in culture with cells eventually becoming confluent.

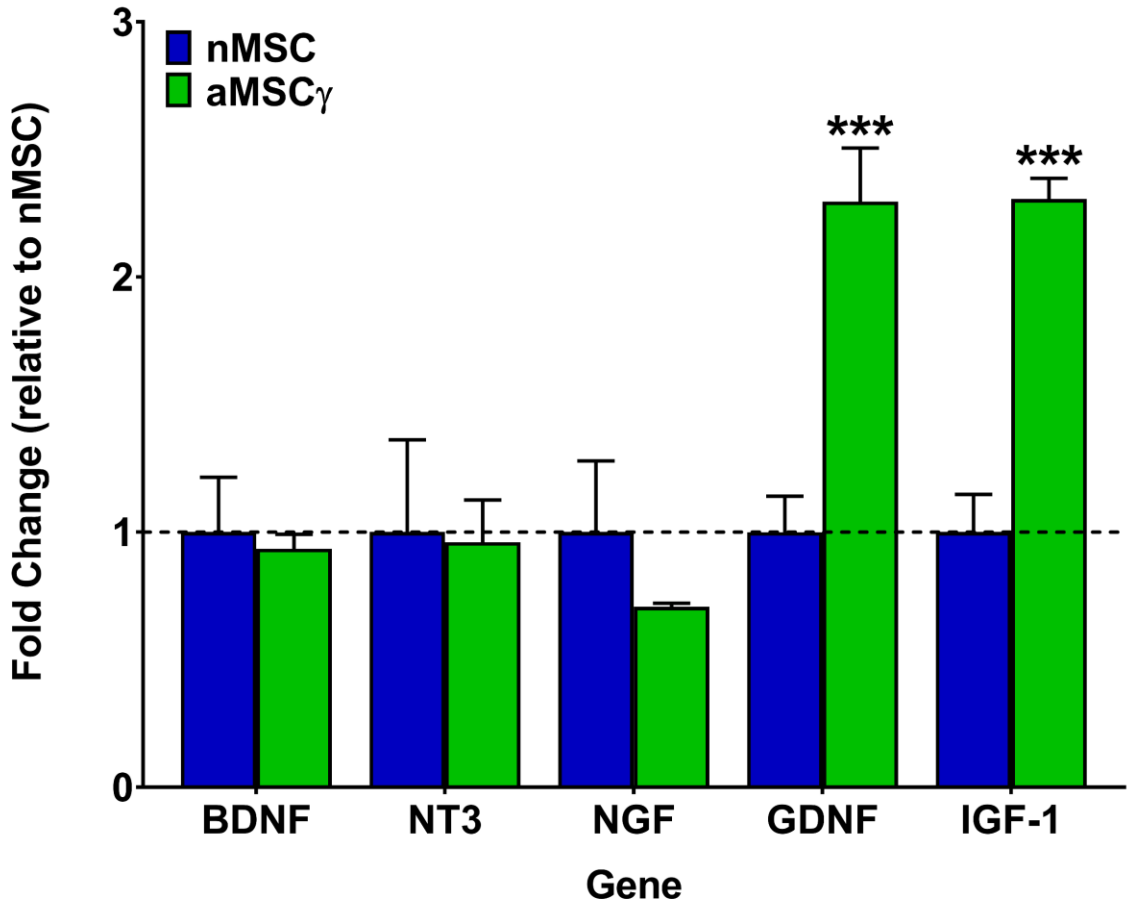

Figure 19. MSC expression of neurotrophic factor mRNA. MSCs were plated under normal growth conditions or were activated with interferon-γ for 6 days. RNA was then isolated from these cells for qRT-PCR analysis of BDNF, NT3, NGF, GDNF, and IGF-1. All of the neurotrophic factors were detectable in nMSC while aMSCγ had significantly elevated levels of GDNF and IGF-1 with a trending decrease in NGF. Data were analyzed using two-tail, unpaired t-tests. ***$p<0.001$.

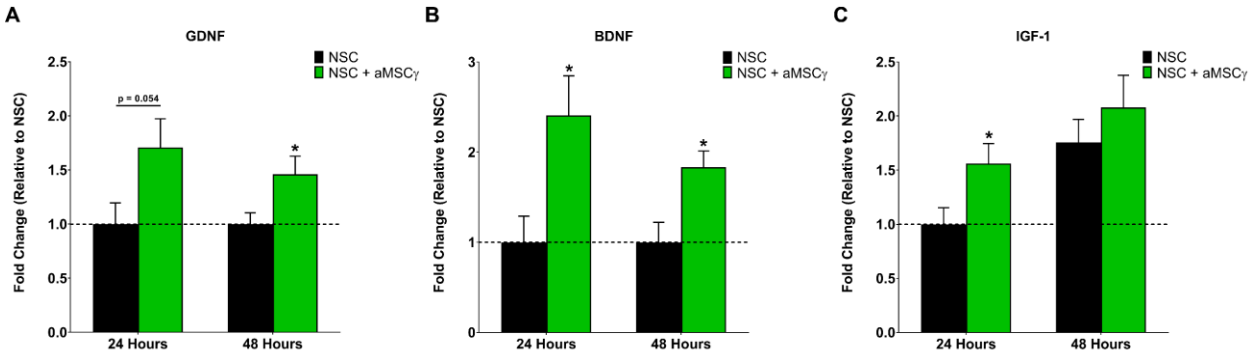

Figure 20. aMSCγ increases neurotrophic factor mRNA expression from neural stem cells after OGD. Neural stem cells were primed in OGD for 4 hours before being transferred back to normal growth conditions. aMSCγ were added in a transwell at a ratio of 10:1 NSC:aMSCγ. **A.** Levels of GDNF with aMSCγ had a trending increase at 24 hours and were significantly elevated at 48 hours. **B.** BDNF was significantly elevated both at 24 and 48 hours with addition of aMSCγ. **C.** IGF-1 was significantly elevated after 24 hours with aMSCγ. Data were analyzed using two-tail, unpaired t-tests. NSC+aMSCγ is compared to NSC alone within each time point. *p≤0.05.

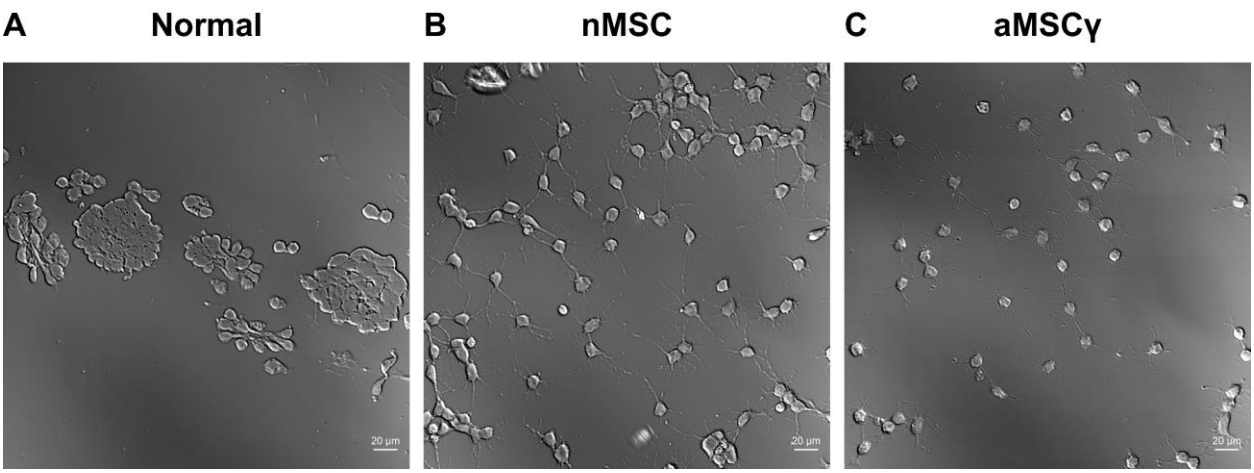

Figure 21. MSC conditioned media causes morphological changes in neural stem cells. 24 hours after plating, neural stem cells grown in MSC conditioned media exhibit morphological features consistent with cells undergoing differentiation compared to cells grown in normal growth media. **A.** Cells grown in normal growth media grow as spheres, in suspension. **B,C.** Cells grown in nMSC and aMSCγ conditioned media no longer grow as spheres in suspension but grow as singly adherent cells that form processes.

4.6.4. Mesenchymal stem cell conditioned media decreases neural stem cell proliferation

Based on the morphological changes observed in the neural stem cells grown in MSC conditioned media we next sought to determine what was happening with these cells. The morphological changes seen are suggestive of cells undergoing differentiation rather than proliferation. Therefore, we wanted to determine how MSC conditioned affected neural stem cell proliferation. To do this, neural stem cells were first singly dissociated and plated either in normal growth media, nMSC conditioned media, or aMSCγ conditioned media for 24, 48, or 72 hours. Four hours prior to the respective time points, cells were pulsed with BrdU (Figure 22A). After the 4-hour pulse period, cells were fixed and stained for cell cycle analysis using a FITC BrdU flow kit (BD Biosciences). When neural stem cells were grown in nMSC or aMSCγ conditioned media, significantly fewer cells were in the S stage of the cell cycle at all three time points while there significantly more cells in the G0/1 stage of the cell cycle (Figure 22B-G). Interestingly, when cells were grown in aMSCγ conditioned media, this effect was enhanced compared to cells grown in nMSC conditioned media suggesting either a difference in nMSC and aMSCγ media composition or a change in relative abundance of secreted signaling molecules between the two types of conditioned media.

4.6.5. Mesenchymal stem cells induce *in vitro* oligodendrocyte differentiation of neural stem cells

Given the morphological changes and the cell cycle changes exhibited by neural stem cells grown in MSC conditioned media, it is apparent that the neural stem cells are, in fact, differentiating. To determine what cell types they are becoming, neural stem cells

were singly dissociated and grown in normal growth media, nMSC conditioned media, or aMSCγ conditioned media. After 6 days, whole cell protein extracts were collected for Western blot analysis of lineage specific markers. When grown in MSC conditioned media, neural stem cells had significant reductions in expression of the astrocyte marker GFAP (Figure 23B), the neuron marker Neurofilament-L (Figure 23E), and the stem cell marker Sox2 (Figure 23F), with a significant increase in the oligodendrocyte marker PDGFRα (Figure 23C). These data demonstrate that neural stem cells grown in MSC conditioned media are, in fact, differentiating and are differentiating into oligodendrocytes.

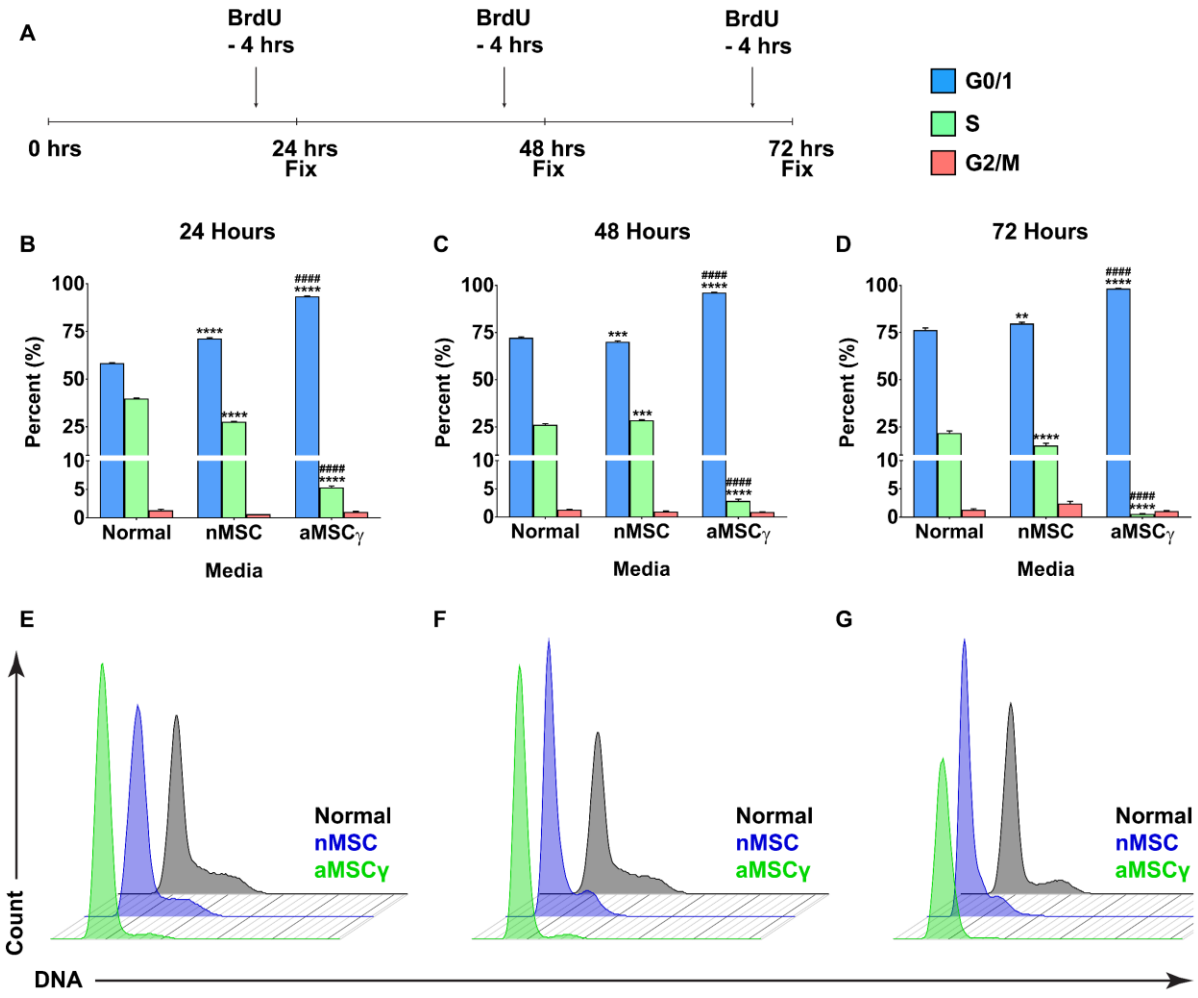

Figure 22. MSC conditioned media decreases neural stem cell proliferation. To determine how MSCs affect neural stem cell proliferation, neural stem cells were singly dissociated and plated in conditioned media from nMSC and aMSCγ. **A.** Time course for experiment. Cells were fixed at 24, 48, or 72 hours, and were pulsed with 10 µM BrdU for 4 hours prior to fixation. **B-D.** Percentage of cells in each stage of the cell cycle at 24 hours (B), 48 hours (C), and 72 hours (D). Cells grown in MSC conditioned media had a significantly larger percentage of cells in the G0/1 stage of the cell cycle and significantly fewer cells in the S stage of the cell cycle at all three time points. **E-G.** DNA histogram plots for each condition at 24 hours (E), 48 hours (F), and 72 hours (G). Data were analyzed using two-way ANOVA with Holm-Sidak multiple comparison testing. *Compared to Normal. #Compared to nMSC. **p<0.01, ***p<0.001, ****p<0.0001, ####p<0.0001.

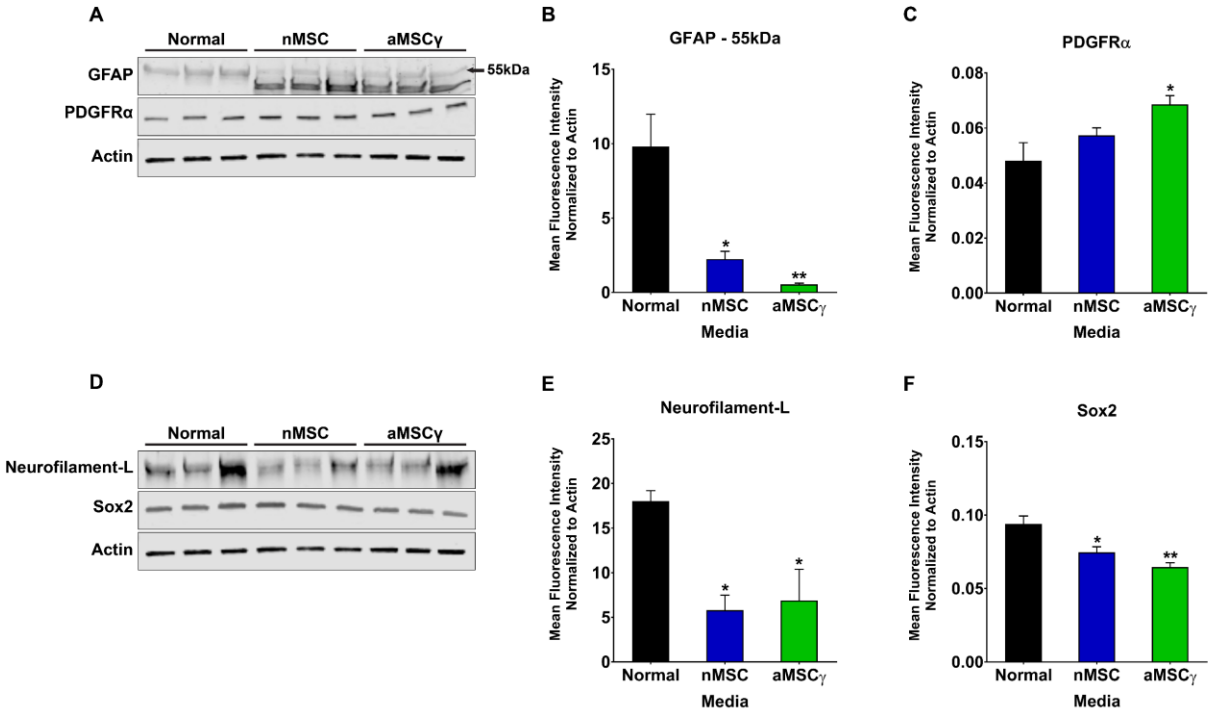

Figure 23. MSC conditioned media induces oligodendrocyte differentiation of neural stem cells. 6 days after culture in MSC conditioned media, neural stem cells were fixed and protein was extracted for Western blot analysis. **A,D.** Representative Western blots of the lineage specific markers GFAP, PDGFRα, Neurofilament-L, and the stem cell marker Sox2. **B.** Cells grown in MSC conditioned media had significantly reduced expression of the astrocyte marker GFAP. **C.** Cells grown in MSC conditioned media had significantly increased expression of the oligodendrocyte marker PDGFRα. **E.** Cells grown in MSC conditioned media had significantly reduced expression of the neuron marker Neurofilament-L. **F.** Cells grown in MSC conditioned media had significantly reduced expression of the stem cell marker Sox2. *Compared to Normal. *p≤0.05, **p<0.01.

4.7. aMSCγ induces oligodendrogenesis following MCAO

4.7.1. MCAO does not cause an increase in SVZ-derived neurogenesis

Previous literature has demonstrated an acute enhancement of neurogenic mechanisms from the SVZ following MCAO. To determine the extent of neurogenesis in our model, rats underwent sham surgery or MCAO surgery with or without MSC treatment. Animals were then sacrificed 24 hours or 1 week after surgery. The 24 hour time point is relevant to determine numbers of proliferating cells while the 1 week time point will provide information regarding differentiation and maturation of different cell lineages. Interestingly, against previous literature, after 24 hours vehicle treated animals had a significant reduction in the number of proliferating cells in the SVZ (Figure 24B) compared to sham animals. Furthermore, there were no changes in the number of neuroblasts/immature neurons (Figure 24C) expressing DCX or oligodendrocyte progenitor cells (OPC) expressing PDGFRα (Figure 24D) in vehicle treated animals compared to sham animals. Additionally, the reduction in immature neurons seems to be in the more ventral aspects of the SVZ while the dorsal aspects seem to be more densely populated with DCX-expressing cells suggesting that perhaps these cells are migrating out of the SVZ.

4.7.2. MSC treatment increases proliferation in the SVZ after MCAO

To determine how MSC treatment affects SVZ proliferation after MCAO, rats underwent sham surgery or MCAO with or without MSC treatment as above. Animals were sacrificed at 24 and 1 week following surgery. Interestingly, despite our earlier data demonstrating that MSCs reduce proliferation of neural stem cells *in vitro*, animals treated

with both nMSC and aMSCγ have increased cell proliferation (Figure 24B) in the SVZ 24 hours after MCAO. Furthermore, in a small cohort of animals without stroke, intrastriatal transplantation of aMSCγ increases the amount of cell proliferation in the SVZ and adjacent areas of the brain 48 hours after transplantation (Figure 25). These data, however, do not necessarily dispute the *in vitro* data, as there were not changes in the populations of cells co-labeled for BrdU and DCX or BrdU and PDGFRα (data not shown) suggesting that the increase in cell proliferation seen with MSC treatment arises from proliferation changes in astrocytes and microglia, both cell types not previously studied *in vitro*.

4.7.3. aMSCγ increases oligodendrocyte progenitor cells in the SVZ following MCAO

Because MSC conditioned media induces oligodendrocyte differentiation of neural stem cells *in vitro*, we next wanted to determine if this happens *in vivo* as well after stroke. Interestingly, and matching with the *in vitro* data, animals treated with aMSCγ have reduced numbers of neuroblasts/immature neurons in the SVZ 24 hours after surgery (Figure 24c) and have significantly increased numbers of oligodendrocyte progenitor cells in the SVZ 24 hours after surgery (Figure 24D). These changes do not persist and are no longer present in animals sacrificed 1 week after surgery (Figure 26B,C). However, these cell counts are limited to the SVZ alone and do not address whether these cells are becoming more fully differentiated or are moving out of the SVZ. To address this, SVZ counts of BrdU, DCX, and CNPase, a marker for more mature oligodendrocytes, were completed in animals that were sacrifice 3 weeks after surgery. Interestingly, there was a significant decrease in the proliferation in animals treated with nMSCs (Figure 27A) and

a trending decrease in CNPase$^+$ cells in animals treated with nMSC and aMSCγ (Figure 27C). A possible explanation for this is that the oligodendrocytes are moving out of the SVZ towards the lesion site thereby depleting the numbers of oligodendrocytes in the SVZ. To determine if this was the case, numbers of both CNPase$^+$ cells and PDGFRα$^+$ cells were quantified in the striatum. Vehicle treated stroke animals had significantly fewer CNPase$^+$ cells (Figure 28A,B) and fewer PDGFRα$^+$ cells (Figure 28A,C) in the striatum compared to sham animals while animals treated with both nMSC and aMSCγ had significantly more CNPase$^+$ cells and PDGFRα$^+$ cells compared to vehicle treated animals.

4.7.4. aMSCγ increases myelination in the ipsilateral hemisphere following MCAO.

To address the question of whether there were more myelinating oligodendrocytes in the ipsilateral hemisphere after MCAO, rats underwent sham surgery or MCAO with or without MSC treatment as above and were sacrificed 1 week after surgery. Ipsilateral hemispheres were homogenized and whole homogenate samples were run for Western blot analysis of PDGFRα and myelin basic protein (MBP). Remarkably, animals treated with aMSCγ had significant increases in protein expression of both PDGFRα and MBP (Figures 29B,C). further supporting the hypothesis that the increase in oligodendrocyte progenitor cells in the SVZ after 24 hours is contributing to a large population of cells that ultimately migrates out of the SVZ towards the infarct to fully differentiate into mature, myelinating oligodendrocytes. It is possible, though, that the increases of PDGFRα and MBP are not the result of specifically remyelination but could be due to preservation of existing myelin.

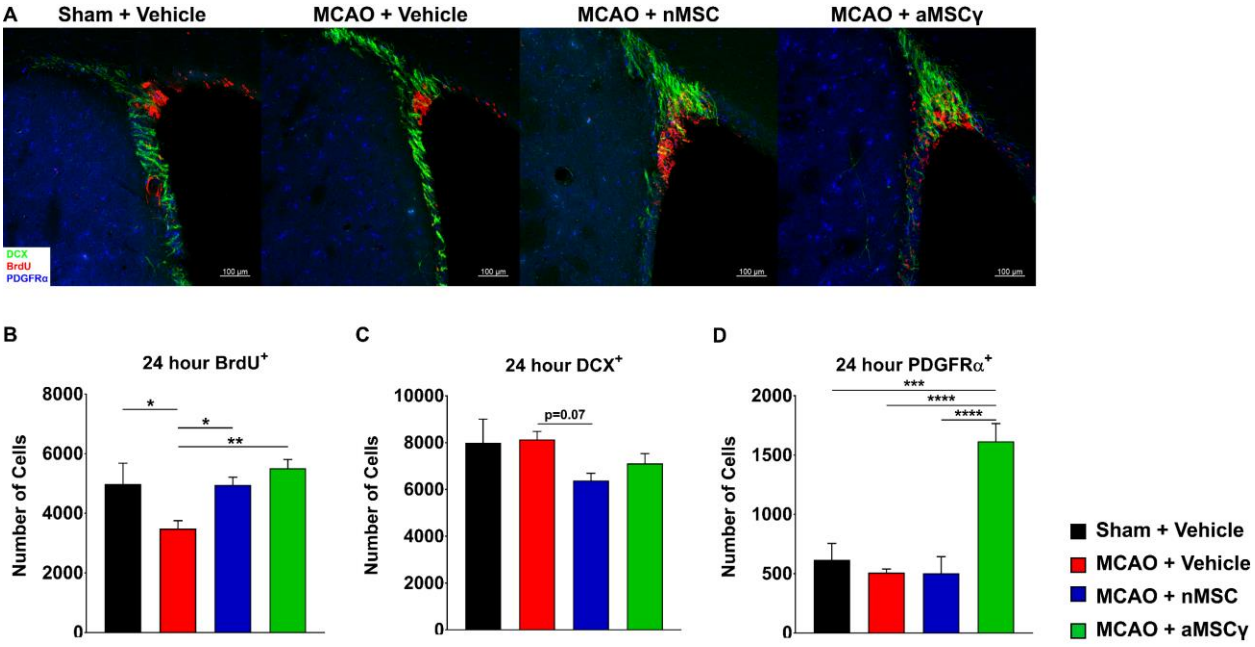

Figure 24. MSC treatment enhances proliferation and oligodendrocyte progenitors 24 hours after MCAO. Rats underwent either sham surgery or 90-minute MCAO (Sham, N = 3; Remaining groups, N = 5-6). Three hours after, rats were administered either vehicle, nMSC ($5.0X10^6$ cells/kg), or aMSCγ ($5.0X10^6$ cells/kg) intravenously and were sacrificed 24 hours later. **A.** Representative images of the SVZ stained for DCX (green), BrdU (red), and PDGFRα (blue). **B.** Proliferation was assessed by counts of $BrdU^+$ cells. Vehicle treated animals had significantly fewer proliferating cells than sham animals and both nMSC and aMSCγ treated animals had significantly increased numbers of proliferating cells compared to vehicle treated animals, with numbers rising to equivalent numbers to the sham animals. **C.** Neuroblasts/immatures neurons were quantified using DCX. There were no changes in the vehicle treated animals compared to sham animals but MSC treated animals had a trending reduction in DCX-expressing cells. **D.** Oligodendrocyte progenitor cells were quantified using PDGFRα. Animals treated with aMSCγ had significantly more oligodendrocyte progenitor cells compared to sham animals, vehicle treated animals, and nMSC treated animals. Data were analyzed using a one-way ANOVA with Holm-Sidak multiple comparison testing. *p≤0.05, **p<0.01, ***p<0.001, ****p<0.0001.

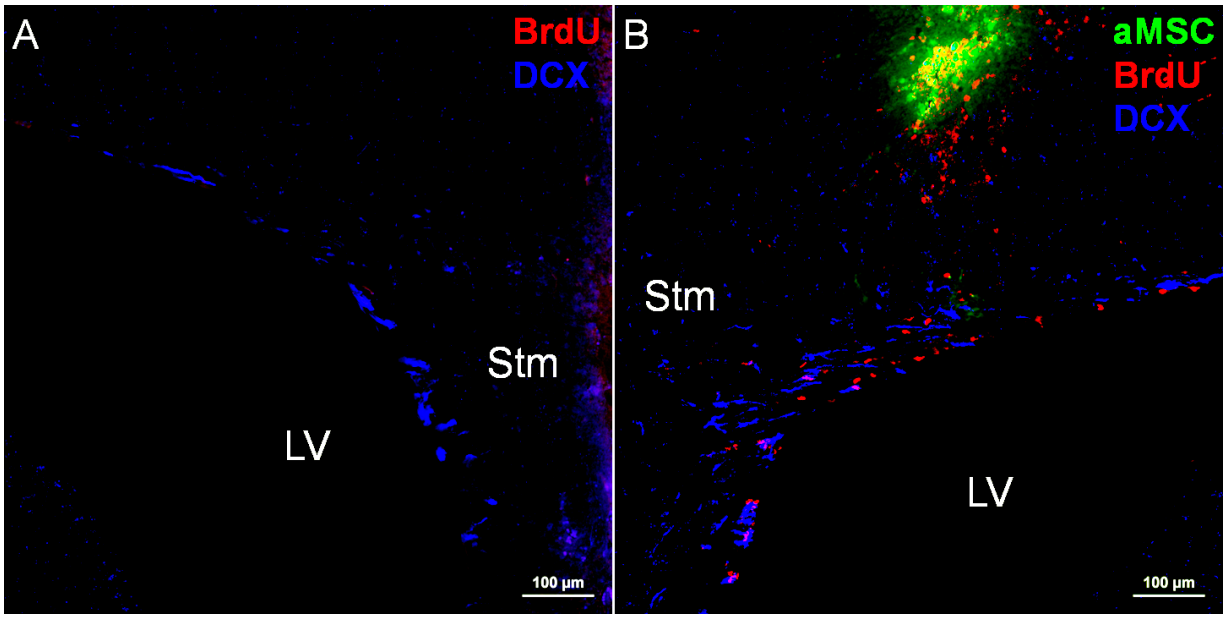

Figure 25. Intrastriatal transplantation of aMSCγ enhances proliferation 48 hours after transplantation. Rats underwent stereotactic surgery for intrastriatal transplantation of aMSCγ (500,000 cells per rat) and were sacrificed 48 hours later. Brains were collected and stained for BrdU (red), DCX (blue), and aMSCγ were prelabeled with CFSE. **A.** aCSF transplanted animals exhibited little to no proliferation demonstrated by the low numbers of $BrdU^+$ cells. **B.** aMSCγ transplanted animals had increased proliferation with a substantial number of $BrdU^+$ cells.

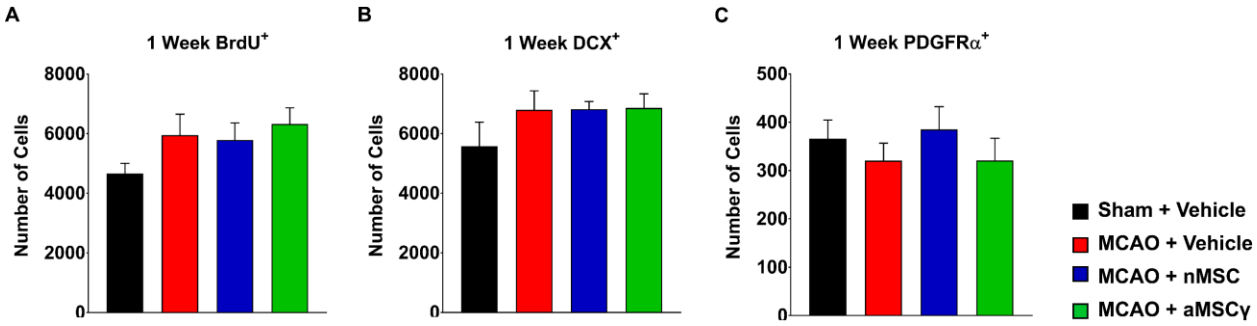

Figure 26 Changes in SVZ composition do not persist 1 week after surgery. Rats underwent either sham surgery or 90-minute MCAO (Sham, N = 3; Remaining groups, N = 5-6). Three hours after, rats were administered either vehicle, nMSC ($5.0X10^6$ cells/kg), or aMSCγ ($5.0X10^6$ cells/kg) intravenously and were sacrificed 1 week later. There were no significant differences detected in proliferating cells (A), neuroblasts/immature neurons (B), or oligodendrocyte progenitor cells (C) 1 week after surgery. Data were analyzed using a one-way ANOVA with Holm-Sidak multiple comparison testing.

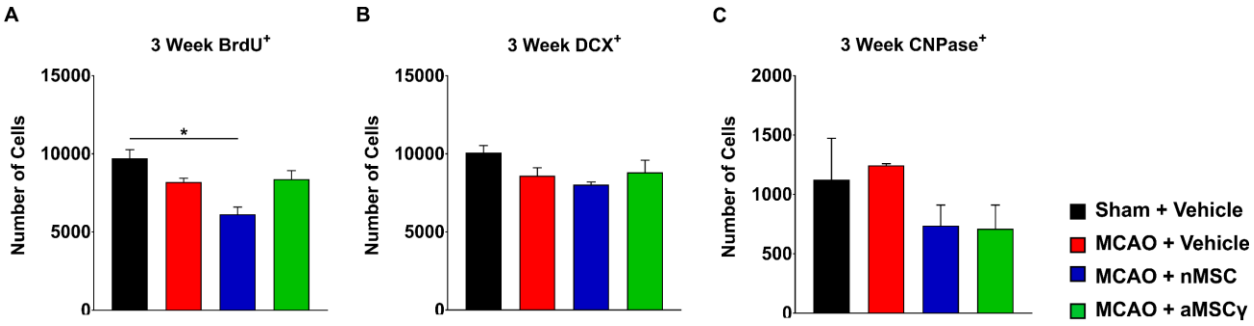

Figure 27. Long-term SVZ proliferation and mature oligodendrocyte numbers are decreased with MSC treatment. Rats underwent either sham surgery or 90-minute MCAO (N = 2 per group). Three hours after, rats were administered either vehicle, nMSC ($5.0X10^6$ cells/kg), or aMSCγ ($5.0X10^6$ cells/kg) intravenously and were sacrificed 3 weeks later. **A.** Proliferation was assessed by counts of $BrdU^+$ cells. nMSC treated animals had significantly fewer proliferating cells than sham animals with no significant changes between the remaining groups. **B.** There were no changes detected in numbers of neuroblasts or immature neurons between any of the groups. **C.** Though not significant, animals treated with nMSC or aMSCγ had a trending decrease in the number of $CNPase^+$ cells in the SVZ. Data were analyzed using a one-way ANOVA with Holm-Sidak multiple comparison testing. *p≤0.05.

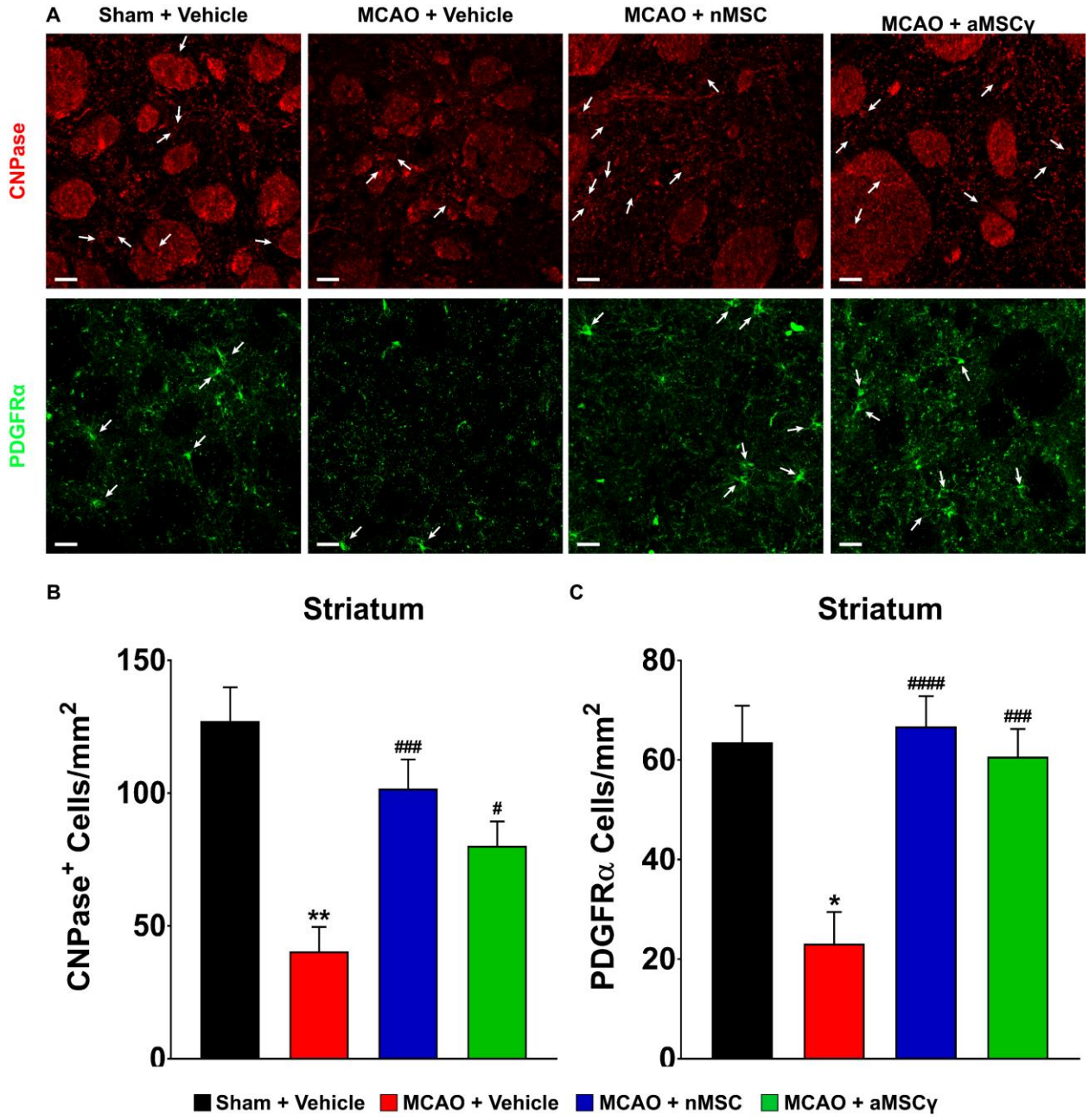

Figure 28. MSC treatment increases the number of OPCs and mature oligodendrocytes in the striatum after 3 weeks. A. Representative images of CNPase and PDGFRα expression in the striatum. Cell bodies are marked by arrows. Scale bar represents 20 µm. **B.** Vehicle treated animals had significantly fewer CNPase$^+$ cells than sham animals and both nMSC and aMSCγ treated animals had significantly increased numbers of these cells compared to vehicle treated animals. **C.** Vehicle treated animals had significantly fewer PDGFRα$^+$ cells than sham animals and both nMSC and aMSCγ treated animals had significantly increased numbers of these cells compared to vehicle treated animals. Data were analyzed using a one-way ANOVA with Holm-Sidak multiple comparison testing (N = 2 per group). *Compared to Sham + Vehicle. $^{\#}$Compared to MCAO + Vehicle. *p≤0.05, **p<0.01, $^{\#}$p≤0.05, $^{\#\#\#}$p<0.001, $^{\#\#\#\#}$p<0.0001.

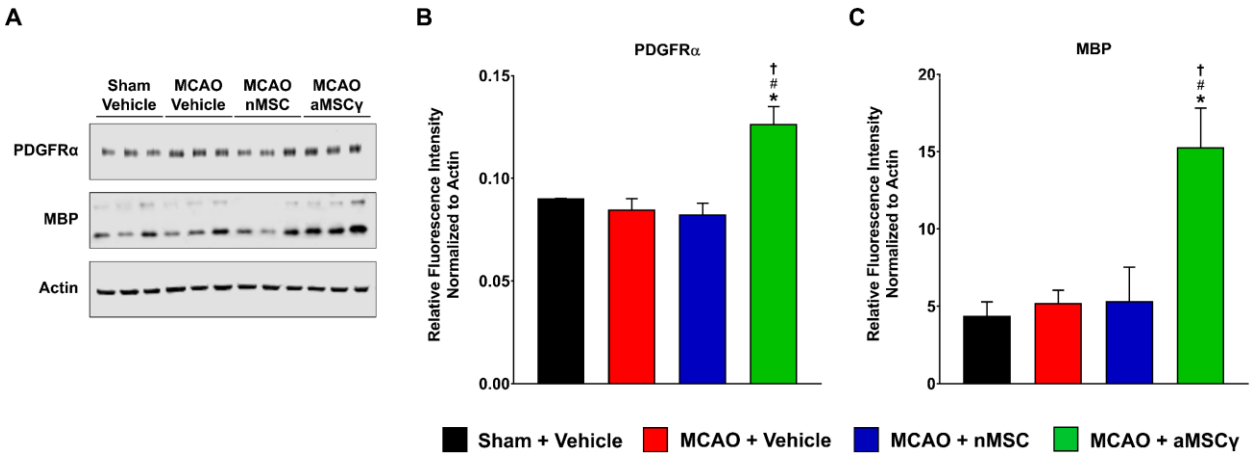

Figure 29. aMSCγ increases expression of PDGFRα and MBP following MCAO. Rats underwent either sham surgery or 90-minute MCAO (N = 3 per group). Three hours after, rats were administered either vehicle, nMSC ($5.0X10^6$ cells/kg), or aMSCγ ($5.0X10^6$ cells/kg) intravenously and were sacrificed 1 week later. **A.** Western blots for PDGFRα, MBP, and actin from the ipsilateral hemisphere. **B.** Quantitation of PDGFRα demonstrating that animals treated with aMSCγ had significantly increased levels of PDGFRα. **C.** Quantitation of MBP demonstrating that animals treated with aMSCγ have significantly increased levels of myelination. Data were analyzed using one-way ANOVA with Holm-Sidak multiple comparison testing. *Compared to Sham + Vehicle. $^{\#}$Compared to MCAO + Vehicle. †Compared to MCAO + nMSC. *$p \leq 0.05$, $^{\#}p \leq 0.05$, $^{\dagger}p \leq 0.05$.

4.8. MSC treatment reduces reactive gliosis following MCAO

One of the hallmark pathologies in brain injury, including stroke, is the presence of reactive gliosis finally leading to the formation of a glial scar (Morioka, Kalehua et al. 1993, Nowicka, Rogozinska et al. 2008, Lively, Moxon-Emre et al. 2011, Huang, Wu et al. 2014). This process is characterized by primarily an increase in reactive astrocytes but also involves a microglia response and deposition of ECM proteins. It is a widely accepted phenomenon in CNS injury but the effects of gliosis and eventually scar formation are poorly understood. More recently reactive gliosis has been described as being beneficial in the acute stage of disease as it closes off the injury site and helps to regulate local immune responses (Rolls, Shechter et al. 2009). Long-term, however, glial scar formation is ultimately detrimental to brain repair as it acts as local physical barrier to axon growth and regeneration.

To investigate how reactive gliosis is affected by stroke and MSC treatment, rats underwent sham surgery or MCAO with or without MSC treatment and were sacrificed one week after surgery. Ipsilateral hemispheres were homogenized and whole homogenate samples were run for Western blot analysis of GFAP. Not surprisingly, compared to sham animals, vehicle treated animals had significantly increased GFAP expression in the ipsilateral hemisphere (Figure 30). Animals treated with both nMSC and aMSCγ had significant reductions in GFAP expression compared to vehicle treated stroke animals demonstrating that MSC treatment also reduces reactive gliosis after stroke.

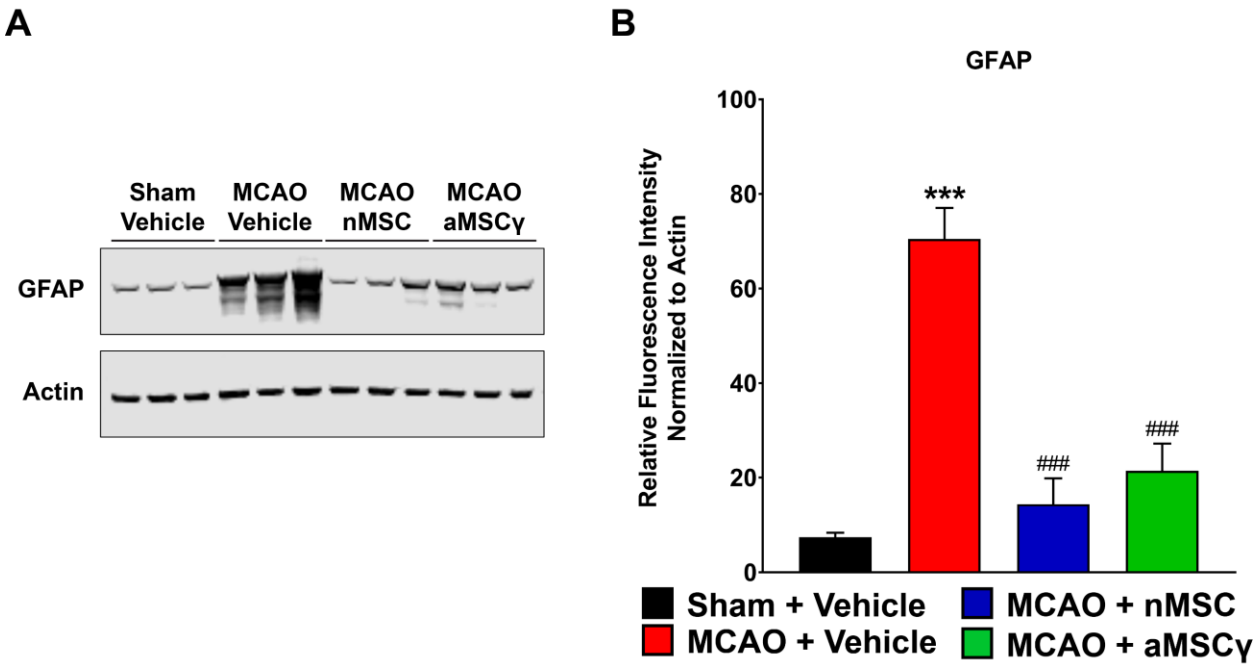

Figure 30. MSCs decrease reactive gliosis following MCAO. Rats underwent either sham surgery or 90-minute MCAO (N = 3 per group). Three hours after, rats were administered either vehicle, nMSC ($5.0X10^6$ cells/kg), or aMSCγ ($5.0X10^6$ cells/kg) intravenously and were sacrificed 1 week later. **A.** Western blots for GFAP, and actin from the ipsilateral hemisphere. **B.** Quantitation of GFAP demonstrating vehicle treated animals have significantly increased GFAP expression compared to sham animals while animals treated with both nMSC and aMSCγ have significantly reduced GFAP levels. Data were analyzed using one-way ANOVA with Holm-Sidak multiple comparison testing. *Compared to Sham + Vehicle. #Compared to MCAO + Vehicle. ***$p<0.001$, #$p<0.001$.

4.9. Identification of MSC-secreted proteins

The protein secretome from MSCs is fairly well described (Silva, Moreira et al. 2013, Rocha, Calamia et al. 2014, Xiao, Rao et al. 2016, Maffioli, Nonnis et al. 2017, Wang, Chen et al. 2017), however, the differences in secreted proteins between nMSC and aMSCγ has never been described before. Therefore, in order to determine what potential protein factors secreted by the MSCs were responsible for the changes we observed *in vitro* and *in vivo*, proteomics analysis of the MSC secretome was performed via mass spectrometry (Figure 32,32). From this approach, 244 proteins were identified (Appendix 4), with 16 proteins being unique to nMSC, 27 proteins being unique to aMSCγ, and the remaining 201 proteins being secreted by both MSC types (Figure 31A). Additionally, secreted proteins belong to many different biologic processes and protein classes with almost a quarter of proteins (21.6%) belonging to the signaling molecule or extracellular matrix classes (Figure 31B). Further, the secretome between both experimental and biological replicates remains consistent with very little variability between replicates both in the number of secreted proteins and the amount of those proteins (Figure 32A). Furthermore, with *ex vivo* IFN-γ activation, there are 35 proteins that are significantly upregulated (>2-fold increase) and 34 proteins that are significantly downregulated (>2-fold decrease) compared to nMSC (Figure 32B).

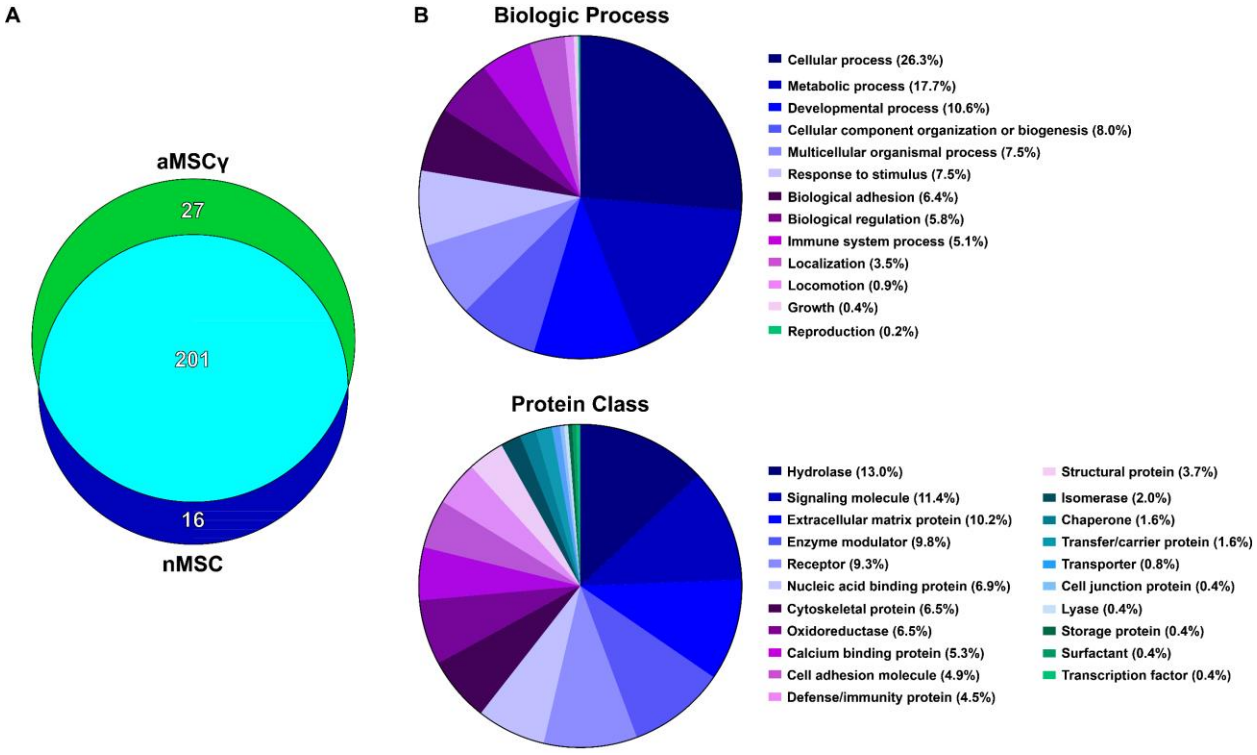

Figure 31. Qualitative analysis of MSC protein secretome. Mass spectrometry analysis of conditioned media from both nMSC and aMSCγ was performed to determine the protein composition of the media **A.** Venn diagram illustrating the number of proteins identified each media type. There were 244 unique proteins identified with 201 shared between nMSC and aMSCγ, 16 proteins unique to nMSC and 27 proteins unique to aMSCγ. **B.** Biologic Process (top chart) and Protein Class (bottom chart) breakdowns of identified proteins.

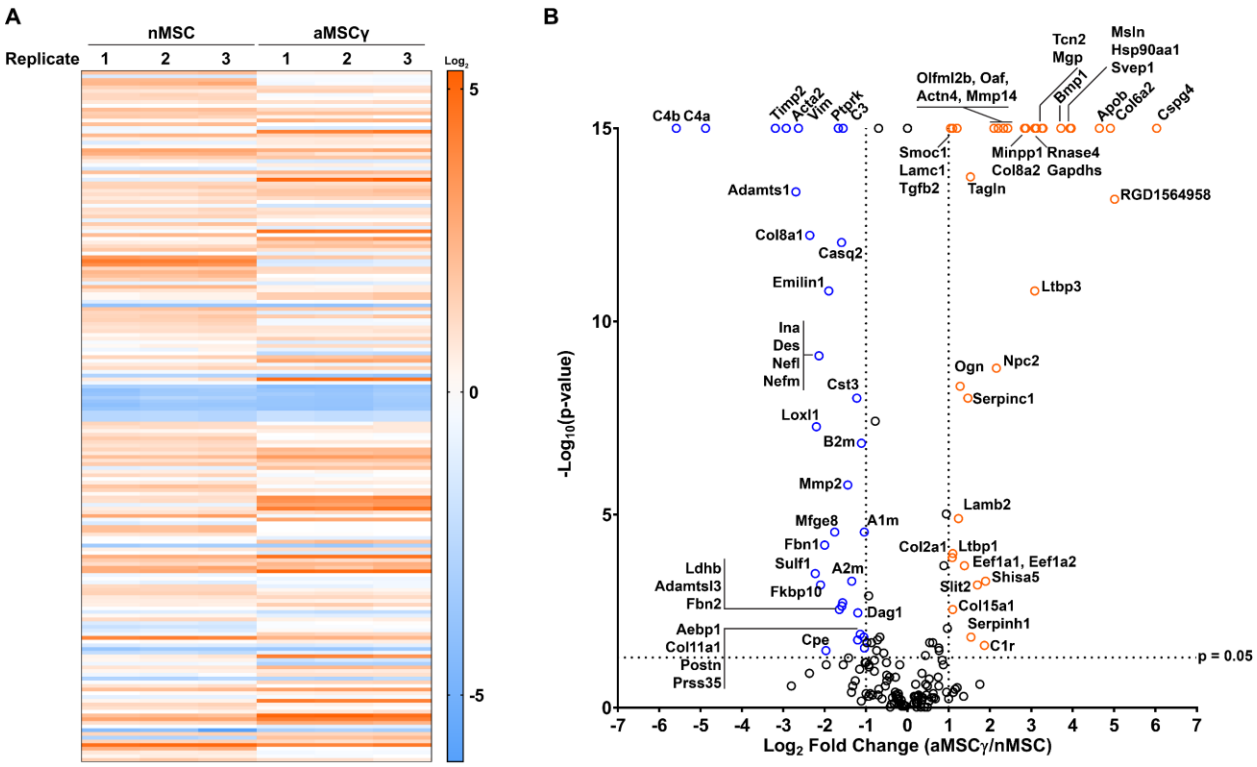

Figure 32. Quantitative proteomics analysis of MSC conditioned media. Mass spectrometry analysis of conditioned media from both nMSC and aMSCγ was performed to determine the protein composition of the media **A.** Heat map analysis of biological replicates from both nMSC and aMSCγ conditioned media. **B.** Volcano plot showing differentially secreted proteins between aMSCγ and nMSC. Positive fold changes indicate higher expression in aMSCγ and negative fold changes indicate higher expression in nMSC.

5. DISCUSSION

5.1. Characterization of changes in microglia and neural stem cell behavior after *in vitro* hypoxia

5.1.1. Microglia adopt a pro-inflammatory phenotype after exposure to hypoxia and negatively regulate neural stem cell proliferation

Cerebral ischemia significantly impacts the behavior of both microglia and neural stem cells. It is well documented that microglia acquire a pro-inflammatory phenotype after experimentally induced stroke, which is associated with increased infarct volume and reduced function (Barone, Arvin et al. 1997, Loddick, Turnbull et al. 1998, Shimakura, Kamanaka et al. 2000, Boutin, LeFeuvre et al. 2001, Herrmann, Tarabin et al. 2003, Gidday, Gasche et al. 2005, Yamashita, Sawamoto et al. 2005, Yilmaz, Arumugam et al. 2006, Lambertsen, Clausen et al. 2009, Konoeda, Shichita et al. 2010). The interaction between these two cell types after an ischemic insult, and the mechanisms underlying these changes, however, are not well understood. We hypothesized that ischemia would induce microglia to adopt a pro-inflammatory phenotype and that this change would negatively regulate neural stem cell characteristics and that ischemia would increase neural stem cell proliferation. To address this, we used several *in vitro* models to study the effect of hypoxia on both microglia and neural stem cells separately, and how microglia would regulate proliferation of neural stem cells.

We found that exposure to hypoxia is sufficient to induce microglia to take on a pro-inflammatory phenotype as determined by increased production of IL-6 and TNF-α. Furthermore, we found that conditioned media from both normoxia- and hypoxia-primed microglia causes an acute increase in neural stem cell proliferation but after 24 hours,

proliferation is decreased only in neural stem cells grown in media from hypoxia-primed microglia. This is consistent with previous literature demonstrating an increase in SVZ proliferation when exposed to pro-inflammatory molecules (Wu, Kuo et al. 2000). However, previous literature has also shown that when grown in culture, SVZ-derived neural stem cells exposed to pro-inflammatory cytokines have reduced proliferation (Ben-Hur, Ben-Menachem et al. 2003, Monje, Toda et al. 2003). These previous studies, in combination with our data suggests that inflammatory molecules produced by microglia can, in fact, regulate proliferation of neural stem cells but that this regulation is highly time dependent. Our studies suggest that the secreted molecules from microglia are sufficient to cause a rapid increase in neural stem cell proliferation, perhaps as a compensatory mechanism due increase in inflammatory mediators, but that exposure to these molecules for longer periods of time is ultimately detrimental.

5.1.2. Hypoxia is detrimental to neural stem cell health in the long term

Ischemia has been demonstrated to increase SVZ neurogenesis acutely (Liu, Solway et al. 1998, Arvidsson, Collin et al. 2002, Tonchev, Yamashima et al. 2003, Plane, Liu et al. 2004, Ong, Plane et al. 2005, Lichtenwalner and Parent 2006, Barks, Liu et al. 2008, Tonchev 2011, Tsai, Yang et al. 2011). These newly proliferating cells, however, do not survive long-term and provide no lasting functional benefit. To try to understand what is happening with these cells to prevent them from surviving and maturing *in vivo*, we studied their proliferative capacity *in vitro* after exposure to OGD. We found that neural stem cells do, in fact, have an acute increase in proliferation after an initial exposure to OGD. However, this increase is not sustained beyond the first 24 hours suggesting that

some intrinsic factor is responsible for these changes. To answer this, mRNA levels of several neurotrophic factors were examined. Interestingly, 24 hours after OGD, levels of BDNF, GDNF, IGF-1, NT3, and NGF were all significantly elevated in neural stem cells. By 48 hours, however, levels of BDNF, GDNF, and IGF-1 were reduced to below normal levels while NT3 and NGF remained increased. This suggests that the acute proliferative burst is caused by an increase in production of multiple neurotrophic factors and that loss of several of these factors in combination is sufficient to cause reductions in proliferation long-term.

5.2. Characterization of functional improvements after stroke and mesenchymal stem cell treatment

5.2.1. Mesenchymal stem cells improve sensorimotor function after stroke

There have been hundreds of preclinical animal studies and numerous human clinical trials examining the efficacy and safety of mesenchymal stem cells for the treatment of ischemic stroke. It is widely accepted that MSCs are an effective treatment option for ischemic stroke. What is largely unknown still are the mechanisms by which MSCs impart their benefit. Furthermore, the vast majority of clinical trials looking at MSC treatment for stroke have studied the affect of MSC therapy when administered in the subacute (1 week to 1 month)(Moniche, Gonzalez et al. 2012, Diez-Tejedor, Gutierrez-Fernandez et al. 2014, Moniche, Rosado-de-Castro et al. 2016) or chronic (>30 days after the ischemic event)(Suarez-Monteagudo, Hernandez-Ramirez et al. 2009, Battistella, de Freitas et al. 2011, Bhasin, Srivastava et al. 2011, Honmou 2016, Steinberg, Kondziolka et al. 2016) time frame. Only 2 trials (Savitz, Misra et al. 2011, Friedrich, Martins et al.

2012) have investigated the safety or efficacy of using MSCs for acute (<1 week) ischemic stroke patients. Therefore, we hypothesized that acute administration of bone marrow-derived MSCs would improve long-term functional recovery.

To study the effect of acute administration of MSCs after stroke, we utilized a rat model of ischemic stroke, the middle cerebral artery occlusion model. When administered 3 hours after the onset of reperfusion, animals treated with both nMSC and aMSCγ exhibit a more rapid and more sustained functional improvement compared to vehicle treated animals. When scored using a cumulative sensorimotor scoring system, the mNSS, MSC treated rats have significantly lower (i.e. better function) scores 1 day after stroke and this score rapidly declined and eventually returned to baseline levels by 3 weeks after stroke. Vehicle treated rats, in comparison, had a slow recovery over the first week and by 3 weeks after stroke still had higher mNSS scores and did not return to baseline. Additionally, when put through open field testing 1 day after stroke, vehicle treated rats performed significantly worse than sham animals and had reduced total ambulatory distance, ambulatory time, ambulatory episodes, and an increased proportion of clockwise turns. Further, they spent significantly more time in the center of the open field apparatus, suggesting non-treated animals are less anxious than sham animals. Compared to vehicle treated stroke animals, MSC treated animals demonstrated significantly increased performance in all of the above metrics of the open field testing. Interestingly, all animals moved at a similar velocity suggesting that the deficits seen in vehicle treated animals were not necessarily a result of the inability to ambulate but perhaps the inability to sustain ambulation. These changes persisted 7 days after stroke

as well, consistent with the mNSS data demonstrating that MSC treated animals have a more rapid and sustained functional improvement.

5.2.2. Mesenchymal stem cells reduce infarct volume following stroke

An important outcome measure of ischemic stroke is lesion size. This outcome measure is incredibly crucial, especially when investigating acute therapies, as it is a direct measure of efficacy of the therapy and its ability to prevent the lesion size from expanding. We hypothesized that acute treatment with MSCs would reduce infarct volume and infarct percent. To examine this, MRI analysis was performed 48 hours after surgery/treatment as this has previously been demonstrated to exhibit maximal MRI signal changes following MCAO. Not surprisingly, rats treated with both nMSC and aMSCγ had significantly reduced infarct volumes (i.e. total infarcted brain tissue) and infarct percentages (i.e. percent of infarcted brain tissue in a given coronal brain slice). Because treatment with MSCs was done acutely and because rats were imaged only 48 hours later, the reductions in infarct volume and infarct percent are likely due to prevention of infarct from developing altogether, rather than from tissue or cell replacement which would occur over a longer period of time.

5.3. Characterization of the effect of mesenchymal stem cells on microglia

5.3.1. Mesenchymal stem cells suppress pro-inflammatory signaling by microglia

It is well established that mesenchymal stem cells act as immunosuppressive agents and are effective at converting peripheral macrophages from a pro-inflammatory phenotype to a pro-regenerative phenotype. Consequently, we hypothesized that

microglia would behave similarly and that MSCs would cause microglia to adopt a pro-regenerative phenotype. To study this, cultured microglia were primed in OGD and then cultured in MSC conditioned media. Supernatants were then analyzed for various cytokines to determine the functional phenotype of the microglia. When grown in MSC conditioned media, microglia had significantly reduced production of IL-6 and TNF-α up to 48 hours after OGD and when grown specifically in aMSCγ conditioned media had increased production of IL-4 and IL-10 up to 1 week after OGD. These data suggest that much like peripheral macrophages, MSCs can interconvert microglia from a pro-inflammatory phenotype to a pro-regenerative phenotype.

5.3.2. Mesenchymal stem cells reduce microglia activation following stroke

Because of our *in vitro* data suggesting that MSCs convert microglia phenotypes, we hypothesized that MSC treatment following MCAO would cause reductions in microglia activation in brain tissue. We observed that microglia activation was significantly reduced in MSC treated animals 1 week after stroke, as measured by CD68 staining, and that this reduction persisted up to 3 weeks later. CD68, however, is expressed in low levels in quiescent, non-activated microglia as, which we saw in our animals as well. Therefore, we also examined morphology of microglia in vehicle treated and MSC treated animals. Consistent with the notion that MSCs are immunosuppressive and reduce microglia activation, microglia in MSC treated animals exhibit morphologies more typical of resting-state microglia rather than activated microglia which predominated in the vehicle treated animals. These data demonstrate that acute administration of MSCs following MCAO is sufficient to prevent microglia activation. These data, taken together

with the *in vitro* data, suggest that the reductions in infarct size and restoration of sensorimotor deficits associated with MSC treatment or, in large part, due to reductions in post-stroke inflammation.

5.4. Characterization of the effects of mesenchymal stem cells on neural stem cells

5.4.1. Mesenchymal stem cells rescue neurotrophic factor loss from neural stem cells

It is known that MSCs secrete a number of different neurotrophic factors (Moradi, Haji Ghasem Kashani et al. 2012, Sadan, Melamed et al. 2012, Sadan, Shemesh et al. 2012) and that this has beneficial effects in CNS disorders (Sadan, Melamed et al. 2012, Sadan, Shemesh et al. 2012). It is not known, however, how *ex vivo* activation of MSCs with IFN-γ alters expression of these molecules, and whether they would be beneficial for maintaining neural stem cell health following hypoxia or ischemia. We hypothesized that IFN-γ activation of MSCs would enhance neurotrophic factor expression by MSCs and that these increases would support neurotrophic factor expression in neural stem cells. To address this, expression of different neurotrophic factors by nMSC and aMSCγ was examined and our data shows that BDNF, GDNF, IGF-1, NT3, and NGF are all expressed in both cell types with IFN-γ activation significantly upregulating expression of GDNF and IGF-1. This suggests to us that secretion of these molecules from MSCs could help to either replace or sustain the neurotrophic factors that are lost from neural stem cells following oxygen-glucose deprivation. To answer this, we utilized a transwell co-culture model of neural stem cells and aMSCγ. Following OGD priming, neural stem cells grown in the presence of aMSCγ had significantly increased mRNA levels of BDNF, GDNF, and IGF-1 24 and 48 hours after oxygen-glucose deprivation. This suggests that the additional trophic support from paracrine mediators by aMSCγ is able to replace, and perhaps even

further increase, the neurotrophic factor support that is lost from the neural stem cells directly after OGD.

5.4.2. Mesenchymal stem cells increase myelin producing oligodendrocytes

Given previous literature suggesting that MSCs enhance proliferation in the SVZ (Yoo, Kim et al. 2008, van Velthoven, Sheldon et al. 2013) we hypothesized that treatment both *in vitro* and *in vivo* with MSCs would increase proliferation of neural stem cells after OGD and after cerebral ischemia. When we first designed *in vitro* experiments to answer this question, we noted an interesting morphological phenotype in neural stem cells grown in conditioned media from mesenchymal stem cells. These cells normally grow in suspension as three-dimensional spheres. However, when grown in MSC conditioned media, the cells did not grow in suspension but grew adherently and put out fine processes, a morphology typical of neural stem cells undergoing differentiation. It is important to note, though, that mesenchymal stem cells secrete numerous extracellular matrix components including various collagens, laminin, and fibronectin. Consequently, the morphological changes seen could be the result of one of two things: 1) because of the ECM components secreted from MSCs, it is possible that the neural stem cells have a substrate on which to grow, or 2) the neural stem cells are, in fact, differentiating.

Because of previous data showing that MSCs enhance proliferation of neural stem cells, we hypothesized that in our system, neural stem cells grown in MSC conditioned media would have enhanced proliferation. To answer this, we performed cell cycle analysis via BrdU flow cytometry and determined that, in fact, the opposite was true. Neural stem cells grown in both nMSC and aMSCγ conditioned media had significantly

fewer cells in the S phase of the cell cycle and significantly more cells in the G0/1 phase which suggests that cells are no longer proliferating and are exiting the cell cycle. These data, together with the morphological changes demonstrate that neural stem cells grown in the MSC conditioned media or actively differentiating rather than maintaining their stemness.

To determine the differentiation state of the neural stem cells, they were grown for 6 days in conditioned media from nMSC and aMSCγ and then protein lysates were collected to examine levels of lineage-specific markers. Interestingly, cells grown in both nMSC and aMSCg conditioned media had significant reductions in GFAP (astrocyte marker), Neurofilament-L (neuron marker), and Sox2 (stem cell marker). Additionally, nMSC caused a trending increase in levels of PDGFRα (oligodendrocyte progenitor cell [OPC] marker) while aMSCγ conditioned media significantly increased levels of PDGFRα. Together, these data show that neural stem cells grown in MSC, more specifically aMSCγ, conditioned media, differentiate into oligodendrocytes. There is some previous literature, albeit limited, demonstrating that in mouse models of multiple sclerosis (MS) bone marrow-derived MSCs recruit OPCs to MS lesions and induce remyelination (Rivera and Aigner 2012, Jaramillo-Merchan, Jones et al. 2013).

To determine how these *in vitro* effects carry over into MSC treated animals, we utilized a rat model of stroke followed by acute administration of mesenchymal stem cells and examined brain tissue 24 hours, 1 week, and 3 weeks afterwards. Interestingly, vehicle treated animals had decreased cell proliferation in the SVZ while MSC treatment significantly increased proliferation 24 hours later. Additionally, a small cohort of naïve animals that had intrastriatal transplantation of aMSCγ exhibited increased proliferation

as well. These data seem to contradict the *in vitro* data which showed reductions in neural stem cell proliferation grown in MSC conditioned media. However, *in vivo*, numbers of proliferating neuroblasts and proliferating OPCs were not changed with MSC treatment. This suggests that MSC conditioned media selectively decreases proliferation in neural stem cells specifically but increases proliferation of other cell types like astrocytes and microglia. The reduction of proliferation in the vehicle treated animals seems to go against many previous studies which demonstrate an increase in SVZ proliferation after ischemia. However, several studies have shown that ischemia plus increased inflammation (both of which have been shown to increase proliferation separately) is sufficient to prevent an increase in SVZ proliferation (Plane, Liu et al. 2004, Ong, Plane et al. 2005, Barks, Liu et al. 2008).

Furthermore, consistent with our *in vitro* studies, there was a significant increase in OPCs in the SVZ in aMSCγ treated animals with trending reductions in immature neurons 24 hours later. By 1 week after stroke, however, the numbers of these cells in the SVZ were similar between all groups. Given that there are increased OPCs in the SVZ after 24 hours, and no changes in OPC numbers between groups at 1 week, we hypothesized that the OPCs are further differentiating long-term. Therefore, we looked at brain tissue from animals after 3 weeks (a sufficient time for cells to terminally differentiate) to determine the numbers of mature oligodendrocytes. Interestingly, in these animals the numbers of $CNPase^{+}$ cells in both nMSC and aMSCγ treated animals was decreased compared to sham and vehicle treated animals. This suggests that OPCs are migrating out of the SVZ into the striatum towards the lesion site and perhaps differentiating into mature oligodendrocytes. Supporting this, analysis of OPCs and

mature oligodendrocytes in the striatum of rats 3 weeks after surgery showed that both nMSC and aMSCγ treated animals had significantly more OPCs and mature oligodendrocytes compared to vehicle treated animals.

It is important that aMSCγ increase the number of OPCs following stroke. However, the functional significance of this is even more important. Previous work has shown that MSC treatment in MS models enhances remyelination (Jaramillo-Merchan, Jones et al. 2013), therefore, we hypothesized that a similar occurrence would occur following stroke. Because there were increased numbers of OPCs 24 hours after treatment, we utilized another set of animals to determine levels of myelin in the ipsilateral hemisphere 1 week after treatment, a time point sufficient for OPCs to differentiate into mature, myelinating oligodendrocytes. Remarkably, animals treated with aMSCγ had significantly increased levels of MBP in the ipsilateral hemisphere compared to sham, vehicle treated, and nMSC treated animals. Collectively, these data show that treatment with aMSCγ after stroke induces differentiation of SVZ neural stem cells into mature, myelin-producing oligodendrocytes.

5.4.4. Potential effector molecules

In an effort to determine what some of the possible effector molecules secreted by MSCs are that could account for the effects they cause both *in vitro* and *in vivo*, we performed proteomics analysis of conditioned media to determine what proteins are secreted by MSCs and how quantities of these proteins change with IFN-γ activation. Not surprisingly, a large percentage of proteins identified were signaling molecules or extracellular matrix components. In our studies, the effect of nMSC and aMSCγ were both

similar and different. They were similar in that they both reduced microglia activation and suppressed inflammatory signaling to a similar extent and they were different in that the changes associated with oligodendrogenesis were mostly unique to aMSCγ treatment. Therefore, the protein identities and quantities associated with regulation of microglia and inflammation are likely similar between nMSC and aMSCγ while the protein identities and quantities associated with oligodendrogenesis are likely either unique protein hits to aMSCγ or are proteins that up or downregulated with IFN-γ activation.

One notable protein that was detected in conditioned media from both nMSC and aMSCg was MFGE8, also known as lactadherin. Previous studies have shown that treatment with recombinant MFGE8 after MCAO improves functional deficits (Cheyuo, Jacob et al. 2012, Deroide, Li et al. 2013). These improvements resulted from reductions in inflammatory signaling by microglia, reductions of neutrophil infiltration, and decreases in apoptosis (Cheyuo, Jacob et al. 2012). In another paper, improvements were attributed to reductions in inflammasome activation and reduced inflammasome -induced IL-1β production following MFGE8 treatment (Deroide, Li et al. 2013). Based on these previous data and our proteomics data showing that both nMSC and aMSCγ secrete MFGE8, it is possible that the reductions seen in microglia activation following MSC treatment after stroke could result from the presence of paracrine signaling by MFGE8.

Typically, oligodendrocyte differentiation, either from neural stem cells or OPC, results from exogenous signaling molecules like bFGF, PDGF, IGF-1, T3, and SHH agonists (Wang, Bates et al. 2013, Douvaras and Fossati 2015, Goldman and Kuypers 2015). These molecules, however, were not detected in the secreted proteome of the MSCs suggesting that the effects seen in these studies are a result of other proteins.

Previous studies have suggested a role for TGF-β signaling in both OPC migration (Fok-Seang, Mathews et al. 1995) and in inducing oligodendrocyte differentiation (McKinnon, Piras et al. 1993, Fok-Seang, Mathews et al. 1995, Schnadelbach, Mandl et al. 1998, Unsicker and Strelau 2000, Dobolyi, Vincze et al. 2012, Palazuelos, Klingener et al. 2014). Interestingly, two of the significantly upregulated proteins from the aMSCγ conditioned media were TGF-β2 and Ltbp3 suggesting that perhaps these proteins are, at least in part, responsible for the recruitment and differentiation of oligodendrocytes after aMSCγ treatment. Of course, it is possible that the changes seen after MSC treatment are not protein-mediated and are due to other non-protein effector molecules such as miRNAs. As an example, miR-219, in cooperation with miR-338, induce oligodendrocyte differentiation via inhibition of Lingo1 and Etv5 (Wang, Moyano et al. 2017). Most likely, however, a single effector molecule is not solely responsible for the cellular changes seen after MSC treatment and the effect is likely due to a combination of multiple molecules including both proteins and miRNAs.

6. CONCLUSIONS AND FUTURE DIRECTIONS

What happens both at the molecular and cellular level after stroke within the brain is necessary to adequately design and test new therapy options to be able to directly target these changes. Current therapies for ischemic stroke patients rely on oversimplified targets, i.e. “inflammation,” rather than specific molecules, cells, or cell events (e.g. differentiation of endogenous progenitor cells). The work in this thesis helps to bridge the knowledge gap between post-ischemic events and a potential therapeutic option for ischemic stroke patients, mesenchymal stem cell-based therapy.

Previous studies have demonstrated the relevance of post-stroke inflammation to brain repair but the results from these studies have been contradictory with some studies suggesting a beneficial role for inflammation while others demonstrate the detrimental effects inflammation has on brain repair. The data presented in this thesis suggests that acute inflammation is, in fact, detrimental to long-term recovery following stroke with untreated animals continuing to be significantly impaired long after stroke. Furthermore, animals continue to have increased levels inflammation even into the chronic stroke time periods demonstrating that even long after the initial injury, inflammation is sustained. Consequently, therapies aimed at reducing post-ischemic inflammation have been utilized to try to enhance recovery. However, almost all of these agents utilized in clinical trials have not demonstrated significant improvement over placebo suggesting that anti-inflammatory monotherapy may not be beneficial for stroke patients.

For various reasons, including delay to treatment and lack of recognizing stroke symptoms, no stroke therapy can be developed to completely regenerate infarcted tissue or prevent the formation of an infarct core. Consequently, therapies aimed at limiting the

size of the infarct and infarct penumbra are most clinically relevant. Related to this, preservation of the support structure within the penumbra is crucial for long-term functional recovery after stroke. A large part of this support structure is myelin which serves many functions within the brain to maintain a homeostatic state and it is known that stroke induces myelin loss in animal models (Irving, Bentley et al. 2001, McIver, Muccigrosso et al. 2010). Consequently, therapies that can promote remyelination or maintenance of exiting myelin structure within the penumbra is important to preserve normal neuron and brain function. From our data, MSCs, more specifically aMSCγ, have the capacity to induce oligodendrocyte differentiation after stroke. Not only that, they seem to recruit both OPCs and mature oligodendrocytes into the striatum towards the infarct location and which leads to increased levels of myelin in the ipsilateral hemisphere.

As demonstrated in this thesis, treatment with MSCs after ischemic stroke was incredibly beneficial and was successful in increasing lasting functional recovery in animals. Based on our data, the recovery seems to be the result of two things: 1) reduction in acute inflammation after stroke, leading to a reduced infarct size and core and 2) increases in myelin-producing oligodendrocytes which support the ischemic penumbra to help maintain normal brain homeostasis. While potential mediators of these changes have been identified via proteomics analysis, it is possible that the effects are the result of other molecules. Therefore, future work should include analysis of other molecules like miRNAs and other small molecules. Additionally, to prove that the beneficial effects result from identified molecules from the various -omics approaches, repeat studies are necessary to test specifically these molecules either singly or in a combined fashion to determine if they impart the same benefits as treatment with the cells themselves.

Second, while MSCs increase the numbers of myelin-producing cells, and increase myelin levels, the adequacy of this myelination needs to be determined. Therefore, additional future studies should be performed to measure extent of individual axon myelination (i.e. via g-ratio analysis) to determine whether or not new myelin is properly wrapping axon fibers. Lastly, the work in this thesis focuses on the effect of MSC treatment on SVZ-derived neurogenesis without examining the effect on hippocampal neurogenesis. Therefore, additional future studies should investigate how hippocampal neurogenesis is altered following stroke and how MSC therapy can alter those processes as well. Furthermore, additional behavior tests should be performed to more comprehensively address cognitive changes after stroke and MSC treatment.

In summary, the goal of this thesis was to determine some of the molecular and cellular changes that occur following ischemic stroke and to determine how treatment with mesenchymal stem cells can alter these changes to cause long-term functional recovery. We presented novel information showing that treatment with MSCs leads to reduction in microglia activation and induces remyelination via recruitment and differentiation of OPCs. Furthermore, while most clinical trials have examined efficacy of MSC treatment in chronic stroke patients with minimal benefit, we show that acute MSC therapy leads to rapid improvement with no lasting deficits.

LITERATURE CITED

Aarum, J., K. Sandberg, S. L. Haeberlein and M. A. Persson (2003). "Migration and differentiation of neural precursor cells can be directed by microglia." Proc Natl Acad Sci U S A **100**(26): 15983-15988.

Aguzzi, A., B. A. Barres and M. L. Bennett (2013). "Microglia: scapegoat, saboteur, or something else?" Science **339**(6116): 156-161.

Aktas, O., O. Ullrich, C. Infante-Duarte, R. Nitsch and F. Zipp (2007). "Neuronal damage in brain inflammation." Arch Neurol **64**(2): 185-189.

Amantea, D., G. Nappi, G. Bernardi, G. Bagetta and M. T. Corasaniti (2009). "Post-ischemic brain damage: pathophysiology and role of inflammatory mediators." FEBS J **276**(1): 13-26.

Arvidsson, A., T. Collin, D. Kirik, Z. Kokaia and O. Lindvall (2002). "Neuronal replacement from endogenous precursors in the adult brain after stroke." Nat Med **8**(9): 963-970.

Bachstetter, A. D., J. M. Morganti, J. Jernberg, A. Schlunk, S. H. Mitchell, K. W. Brewster, C. E. Hudson, M. J. Cole, J. K. Harrison, P. C. Bickford and C. Gemma (2011). "Fractalkine and CX 3 CR1 regulate hippocampal neurogenesis in adult and aged rats." Neurobiol Aging **32**(11): 2030-2044.

Barks, J. D., Y. Q. Liu, Y. Shangguan, J. Li, J. Pfau and F. S. Silverstein (2008). "Impact of indolent inflammation on neonatal hypoxic-ischemic brain injury in mice." Int J Dev Neurosci **26**(1): 57-65.

Barone, F. C., B. Arvin, R. F. White, A. Miller, C. L. Webb, R. N. Willette, P. G. Lysko and G. Z. Feuerstein (1997). "Tumor necrosis factor-alpha. A mediator of focal ischemic brain injury." Stroke **28**(6): 1233-1244.

Bath, P. M., R. Iddenden, F. J. Bath, J. M. Orgogozo and C. Tirilazad International Steering (2001). "Tirilazad for acute ischaemic stroke." Cochrane Database Syst Rev(4): CD002087.

Battistella, V., G. R. de Freitas, L. M. da Fonseca, D. Mercante, B. Gutfilen, R. C. Goldenberg, J. V. Dias, T. H. Kasai-Brunswick, E. Wajnberg, P. H. Rosado-de-Castro, S. V. Alves-Leon, R. Mendez-Otero and C. Andre (2011). "Safety of autologous bone marrow mononuclear cell transplantation in patients with nonacute ischemic stroke." Regen Med **6**(1): 45-52.

Ben-Hur, T., O. Ben-Menachem, V. Furer, O. Einstein, R. Mizrachi-Kol and N. Grigoriadis (2003). "Effects of proinflammatory cytokines on the growth, fate, and motility of multipotential neural precursor cells." Mol Cell Neurosci **24**(3): 623-631.

Bhasin, A., M. V. Srivastava, S. S. Kumaran, S. Mohanty, R. Bhatia, S. Bose, S. Gaikwad, A. Garg and B. Airan (2011). "Autologous mesenchymal stem cells in chronic stroke." Cerebrovasc Dis Extra **1**(1): 93-104.

Bonde, S., C. T. Ekdahl and O. Lindvall (2006). "Long-term neuronal replacement in adult rat hippocampus after status epilepticus despite chronic inflammation." Eur J Neurosci **23**(4): 965-974.

Borgens, R. B. and P. Liu-Snyder (2012). "Understanding secondary injury." Q Rev Biol **87**(2): 89-127.

Boutin, H., R. A. LeFeuvre, R. Horai, M. Asano, Y. Iwakura and N. J. Rothwell (2001). "Role of IL-1alpha and IL-1beta in ischemic brain damage." J Neurosci **21**(15): 5528-5534.

Bye, N., A. M. Turnley and M. C. Morganti-Kossmann (2012). "Inflammatory regulators of redirected neural migration in the injured brain." Neurosignals **20**(3): 132-146.

Cao, Z., A. Balasubramanian and S. P. Marrelli (2014). "Pharmacologically induced hypothermia via TRPV1 channel agonism provides neuroprotection following ischemic stroke when initiated 90 min after reperfusion." Am J Physiol Regul Integr Comp Physiol **306**(2): R149-156.

Chen, J. R., G. Y. Cheng, C. C. Sheu, G. F. Tseng, T. J. Wang and Y. S. Huang (2008). "Transplanted bone marrow stromal cells migrate, differentiate and improve motor function in rats with experimentally induced cerebral stroke." J Anat **213**(3): 249-258.

Cheyuo, C., A. Jacob, R. Wu, M. Zhou, L. Qi, W. Dong, Y. Ji, W. W. Chaung, H. Wang, J. Nicastro, G. F. Coppa and P. Wang (2012). "Recombinant human MFG-E8 attenuates cerebral ischemic injury: its role in anti-inflammation and anti-apoptosis." Neuropharmacology **62**(2): 890-900.

Choi, Y. S., M. Y. Lee, K. W. Sung, S. W. Jeong, J. S. Choi, H. J. Park, O. N. Kim, S. B. Lee and S. Y. Kim (2003). "Regional differences in enhanced neurogenesis in the dentate gyrus of adult rats after transient forebrain ischemia." Mol Cells **16**(2): 232-238.

Clarke, L. and D. van der Kooy (2011). "The adult mouse dentate gyrus contains populations of committed progenitor cells that are distinct from subependymal zone neural stem cells." Stem Cells **29**(9): 1448-1458.

Crain, J. M., M. Nikodemova and J. J. Watters (2013). "Microglia express distinct M1 and M2 phenotypic markers in the postnatal and adult central nervous system in male and female mice." J Neurosci Res **91**(9): 1143-1151.

Curtis, M. A., M. Kam, U. Nannmark, M. F. Anderson, M. Z. Axell, C. Wikkelso, S. Holtas, W. M. van Roon-Mom, T. Bjork-Eriksson, C. Nordborg, J. Frisen, M. Dragunow, R. L. Faull and P. S. Eriksson (2007). "Human neuroblasts migrate to the olfactory bulb via a lateral ventricular extension." Science **315**(5816): 1243-1249.

del Zoppo, G. J. and P. B. Gorelick (2010). "Innate inflammation as the common pathway of risk factors leading to TIAs and stroke." Ann N Y Acad Sci **1207**: 8-10.

Denes, A., R. Vidyasagar, J. Feng, J. Narvainen, B. W. McColl, R. A. Kauppinen and S. M. Allan (2007). "Proliferating resident microglia after focal cerebral ischaemia in mice." J Cereb Blood Flow Metab **27**(12): 1941-1953.

Deroide, N., X. Li, D. Lerouet, E. Van Vre, L. Baker, J. Harrison, M. Poittevin, L. Masters, L. Nih, I. Margaill, Y. Iwakura, B. Ryffel, M. Pocard, A. Tedgui, N. Kubis and Z. Mallat (2013). "MFGE8 inhibits inflammasome-induced IL-1beta production and limits postischemic cerebral injury." J Clin Invest **123**(3): 1176-1181.

Diez-Tejedor, E., M. Gutierrez-Fernandez, P. Martinez-Sanchez, B. Rodriguez-Frutos, G. Ruiz-Ares, M. L. Lara and B. F. Gimeno (2014). "Reparative therapy for acute ischemic stroke with allogeneic mesenchymal stem cells from adipose tissue: a safety assessment: a phase II randomized, double-blind, placebo-controlled, single-center, pilot clinical trial." J Stroke Cerebrovasc Dis **23**(10): 2694-2700.

Dobolyi, A., C. Vincze, G. Pal and G. Lovas (2012). "The neuroprotective functions of transforming growth factor beta proteins." Int J Mol Sci **13**(7): 8219-8258.

Donnan, G. A., M. Fisher, M. Macleod and S. M. Davis (2008). "Stroke." Lancet **371**(9624): 1612-1623.

Douvaras, P. and V. Fossati (2015). "Generation and isolation of oligodendrocyte progenitor cells from human pluripotent stem cells." Nat Protoc **10**(8): 1143-1154.

Edaravone Acute Infarction Study, G. (2003). "Effect of a novel free radical scavenger, edaravone (MCI-186), on acute brain infarction. Randomized, placebo-controlled, double-blind study at multicenters." Cerebrovasc Dis **15**(3): 222-229.

Eikelenboom, P., R. Veerhuis, W. Scheper, A. J. Rozemuller, W. A. van Gool and J. J. Hoozemans (2006). "The significance of neuroinflammation in understanding Alzheimer's disease." J Neural Transm **113**(11): 1685-1695.

Ekdahl, C. T., J. H. Claasen, S. Bonde, Z. Kokaia and O. Lindvall (2003). "Inflammation is detrimental for neurogenesis in adult brain." Proc Natl Acad Sci U S A **100**(23): 13632-13637.

Ekdahl, C. T., Z. Kokaia and O. Lindvall (2009). "Brain inflammation and adult neurogenesis: the dual role of microglia." Neuroscience **158**(3): 1021-1029.

Emsley, H. C., C. J. Smith, R. F. Georgiou, A. Vail, S. J. Hopkins, N. J. Rothwell, P. J. Tyrrell and I. Acute Stroke (2005). "A randomised phase II study of interleukin-1 receptor antagonist in acute stroke patients." J Neurol Neurosurg Psychiatry **76**(10): 1366-1372.

Enlimomab Acute Stroke Trial, I. (2001). "Use of anti-ICAM-1 therapy in ischemic stroke: results of the Enlimomab Acute Stroke Trial." Neurology **57**(8): 1428-1434.

Erices, A., P. Conget and J. J. Minguell (2000). "Mesenchymal progenitor cells in human umbilical cord blood." Br J Haematol **109**(1): 235-242.

Erlandsson, A., C. H. Lin, F. Yu and C. M. Morshead (2011). "Immunosuppression promotes endogenous neural stem and progenitor cell migration and tissue regeneration after ischemic injury." Exp Neurol **230**(1): 48-57.

Ernst, A., K. Alkass, S. Bernard, M. Salehpour, S. Perl, J. Tisdale, G. Possnert, H. Druid and J. Frisen (2014). "Neurogenesis in the striatum of the adult human brain." Cell **156**(5): 1072-1083.

Fiscus, R. R., J. P. Yuen, S. L. Chan, J. H. Kwong and S. B. Chew (2002). "Nitric oxide and cyclic GMP as pro- and anti-apoptotic agents." J Card Surg **17**(4): 336-339.

Fok-Seang, J., G. A. Mathews, C. ffrench-Constant, J. Trotter and J. W. Fawcett (1995). "Migration of oligodendrocyte precursors on astrocytes and meningeal cells." Dev Biol **171**(1): 1-15.

Friedenstein, A. J., U. F. Deriglasova, N. N. Kulagina, A. F. Panasuk, S. F. Rudakowa, E. A. Luria and I. A. Ruadkow (1974). "Precursors for fibroblasts in different populations of hematopoietic cells as detected by the in vitro colony assay method." Exp Hematol **2**(2): 83-92.

Friedenstein, A. J., J. F. Gorskaja and N. N. Kulagina (1976). "Fibroblast precursors in normal and irradiated mouse hematopoietic organs." Exp Hematol **4**(5): 267-274.

Friedrich, M. A., M. P. Martins, M. D. Araujo, C. Klamt, L. Vedolin, B. Garicochea, E. F. Raupp, J. Sartori El Ammar, D. C. Machado, J. C. Costa, R. G. Nogueira, P. H. Rosado-de-Castro, R. Mendez-Otero and G. R. Freitas (2012). "Intra-arterial infusion of autologous bone marrow mononuclear cells in patients with moderate to severe middle cerebral artery acute ischemic stroke." Cell Transplant **21 Suppl 1**: S13-21.

Ge, S., C. H. Yang, K. S. Hsu, G. L. Ming and H. Song (2007). "A critical period for enhanced synaptic plasticity in newly generated neurons of the adult brain." Neuron **54**(4): 559-566.

Gebara, E., S. Sultan, J. Kocher-Braissant and N. Toni (2013). "Adult hippocampal neurogenesis inversely correlates with microglia in conditions of voluntary running and aging." Front Neurosci **7**: 145.

Gidday, J. M., Y. G. Gasche, J. C. Copin, A. R. Shah, R. S. Perez, S. D. Shapiro, P. H. Chan and T. S. Park (2005). "Leukocyte-derived matrix metalloproteinase-9 mediates blood-brain barrier breakdown and is proinflammatory after transient focal cerebral ischemia." Am J Physiol Heart Circ Physiol **289**(2): H558-568.

Giunti, D., B. Parodi, C. Usai, L. Vergani, S. Casazza, S. Bruzzone, G. Mancardi and A. Uccelli (2012). "Mesenchymal stem cells shape microglia effector functions through the release of CX3CL1." Stem Cells **30**(9): 2044-2053.

Go, A. S., D. Mozaffarian, V. L. Roger, E. J. Benjamin, J. D. Berry, M. J. Blaha, S. Dai, E. S. Ford, C. S. Fox, S. Franco, H. J. Fullerton, C. Gillespie, S. M. Hailpern, J. A. Heit, V. J. Howard, M. D. Huffman, S. E. Judd, B. M. Kissela, S. J. Kittner, D. T. Lackland, J. H. Lichtman, L. D. Lisabeth, R. H. Mackey, D. J. Magid, G. M. Marcus, A. Marelli, D. B. Matchar, D. K. McGuire, E. R. Mohler, 3rd, C. S. Moy, M. E. Mussolino, R. W. Neumar, G. Nichol, D. K. Pandey, N. P. Paynter, M. J. Reeves, P. D. Sorlie, J. Stein, A. Towfighi, T. N. Turan, S. S. Virani, N. D. Wong, D. Woo, M. B. Turner, C. American Heart Association Statistics and S. Stroke Statistics (2014). "Heart disease and stroke statistics--2014 update: a report from the American Heart Association." Circulation **129**(3): e28-e292.

Goldman, S. A. and N. J. Kuypers (2015). "How to make an oligodendrocyte." Development **142**(23): 3983-3995.

Graeber, M. B., W. J. Streit, R. Kiefer, S. W. Schoen and G. W. Kreutzberg (1990). "New expression of myelomonocytic antigens by microglia and perivascular cells following lethal motor neuron injury." J Neuroimmunol **27**(2-3): 121-132.

Griffin, M. D., A. E. Ryan, S. Alagesan, P. Lohan, O. Treacy and T. Ritter (2013). "Anti-donor immune responses elicited by allogeneic mesenchymal stem cells: what have we learned so far?" Immunol Cell Biol **91**(1): 40-51.

Gronthos, S., M. Mankani, J. Brahim, P. G. Robey and S. Shi (2000). "Postnatal human dental pulp stem cells (DPSCs) in vitro and in vivo." Proc Natl Acad Sci U S A **97**(25): 13625-13630.

Gutierrez-Fernandez, M., B. Rodriguez-Frutos, J. Ramos-Cejudo, L. Otero-Ortega, B. Fuentes, M. T. Vallejo-Cremades, B. E. Sanz-Cuesta and E. Diez-Tejedor (2015). "Comparison between xenogeneic and allogeneic adipose mesenchymal stem cells in the treatment of acute cerebral infarct: proof of concept in rats." J Transl Med **13**: 46.

Hallbergson, A. F., C. Gnatenco and D. A. Peterson (2003). "Neurogenesis and brain injury: managing a renewable resource for repair." J Clin Invest **112**(8): 1128-1133.

Herrmann, O., V. Tarabin, S. Suzuki, N. Attigah, I. Coserea, A. Schneider, J. Vogel, S. Prinz, S. Schwab, H. Monyer, F. Brombacher and M. Schwaninger (2003). "Regulation of body temperature and neuroprotection by endogenous interleukin-6 in cerebral ischemia." J Cereb Blood Flow Metab **23**(4): 406-415.

Hickey, W. F., B. L. Hsu and H. Kimura (1991). "T-lymphocyte entry into the central nervous system." J Neurosci Res **28**(2): 254-260.

Hodges, H., P. Sowinski, D. Virley, A. Nelson, T. R. Kershaw, W. P. Watson, T. Veizovic, S. Patel, A. Mora, T. Rashid, S. J. French, A. Chadwick, J. A. Gray and J. D. Sinden (2000). "Functional reconstruction of the hippocampus: fetal versus conditionally immortal neuroepithelial stem cell grafts." Novartis Found Symp **231**: 53-65; discussion 65-59.

Hodges, H., T. Veizovic, N. Bray, S. J. French, T. P. Rashid, A. Chadwick, S. Patel and J. A. Gray (2000). "Conditionally immortal neuroepithelial stem cell grafts reverse age-associated memory impairments in rats." Neuroscience **101**(4): 945-955.

Honma, T., O. Honmou, S. Iihoshi, K. Harada, K. Houkin, H. Hamada and J. D. Kocsis (2006). "Intravenous infusion of immortalized human mesenchymal stem cells protects against injury in a cerebral ischemia model in adult rat." Exp Neurol **199**(1): 56-66.

Honmou, O. (2016). "[Phase III clinical trial using autologous mesenchymal stem cells for stroke patients]." Nihon Rinsho **74**(4): 649-654.

Horvath, R. J., N. Nutile-McMenemy, M. S. Alkaitis and J. A. Deleo (2008). "Differential migration, LPS-induced cytokine, chemokine, and NO expression in immortalized BV-2 and HAPI cell lines and primary microglial cultures." J Neurochem **107**(2): 557-569.

Huang, L., Z. B. Wu, Q. Zhuge, W. Zheng, B. Shao, B. Wang, F. Sun and K. Jin (2014). "Glial scar formation occurs in the human brain after ischemic stroke." Int J Med Sci **11**(4): 344-348.

Iadecola, C. and J. Anrather (2011). "The immunology of stroke: from mechanisms to translation." Nat Med **17**(7): 796-808.

In 't Anker, P. S., S. A. Scherjon, C. Kleijburg-van der Keur, W. A. Noort, F. H. Claas, R. Willemze, W. E. Fibbe and H. H. Kanhai (2003). "Amniotic fluid as a novel source of mesenchymal stem cells for therapeutic transplantation." Blood **102**(4): 1548-1549.

Iosif, R. E., H. Ahlenius, C. T. Ekdahl, V. Darsalia, P. Thored, S. Jovinge, Z. Kokaia and O. Lindvall (2008). "Suppression of stroke-induced progenitor proliferation in adult subventricular zone by tumor necrosis factor receptor 1." J Cereb Blood Flow Metab **28**(9): 1574-1587.

Iosif, R. E., C. T. Ekdahl, H. Ahlenius, C. J. Pronk, S. Bonde, Z. Kokaia, S. E. Jacobsen and O. Lindvall (2006). "Tumor necrosis factor receptor 1 is a negative regulator of progenitor proliferation in adult hippocampal neurogenesis." J Neurosci **26**(38): 9703-9712.

Irving, E. A., D. L. Bentley and A. A. Parsons (2001). "Assessment of white matter injury following prolonged focal cerebral ischaemia in the rat." Acta Neuropathol **102**(6): 627-635.

Jacobs, S. A., J. Pinxteren, V. D. Roobrouck, A. Luyckx, W. van't Hof, R. Deans, C. M. Verfaillie, M. Waer, A. D. Billiau and S. W. Van Gool (2013). "Human multipotent adult progenitor cells are nonimmunogenic and exert potent immunomodulatory effects on alloreactive T-cell responses." Cell Transplant **22**(10): 1915-1928.

Jakubs, K., S. Bonde, R. E. Iosif, C. T. Ekdahl, Z. Kokaia, M. Kokaia and O. Lindvall (2008). "Inflammation regulates functional integration of neurons born in adult brain." J Neurosci **28**(47): 12477-12488.

Janardhan, V. and A. I. Qureshi (2004). "Mechanisms of ischemic brain injury." Curr Cardiol Rep **6**(2): 117-123.

Jaramillo-Merchan, J., J. Jones, J. L. Ivorra, D. Pastor, M. C. Viso-Leon, J. A. Armengol, M. D. Molto, E. Geijo-Barrientos and S. Martinez (2013). "Mesenchymal stromal-cell transplants induce oligodendrocyte progenitor migration and remyelination in a chronic demyelination model." Cell Death Dis **4**: e779.

Jin, K., M. Minami, J. Q. Lan, X. O. Mao, S. Batteur, R. P. Simon and D. A. Greenberg (2001). "Neurogenesis in dentate subgranular zone and rostral subventricular zone after focal cerebral ischemia in the rat." Proc Natl Acad Sci U S A **98**(8): 4710-4715.

Jin, K., Y. Sun, L. Xie, A. Peel, X. O. Mao, S. Batteur and D. A. Greenberg (2003). "Directed migration of neuronal precursors into the ischemic cerebral cortex and striatum." Mol Cell Neurosci **24**(1): 171-189.

Jin, R., G. Yang and G. Li (2010). "Inflammatory mechanisms in ischemic stroke: role of inflammatory cells." J Leukoc Biol **87**(5): 779-789.

Kee, N. J., E. Preston and J. M. Wojtowicz (2001). "Enhanced neurogenesis after transient global ischemia in the dentate gyrus of the rat." Exp Brain Res **136**(3): 313-320.

Kim, J. and P. Hematti (2009). "Mesenchymal stem cell-educated macrophages: a novel type of alternatively activated macrophages." Exp Hematol **37**(12): 1445-1453.

Kingham, P. J., M. L. Cuzner and J. M. Pocock (1999). "Apoptotic pathways mobilized in microglia and neurones as a consequence of chromogranin A-induced microglial activation." J Neurochem **73**(2): 538-547.

Koh, S. H., K. S. Kim, M. R. Choi, K. H. Jung, K. S. Park, Y. G. Chai, W. Roh, S. J. Hwang, H. J. Ko, Y. M. Huh, H. T. Kim and S. H. Kim (2008). "Implantation of human umbilical cord-derived mesenchymal stem cells as a neuroprotective therapy for ischemic stroke in rats." Brain Res **1229**: 233-248.

Konoeda, F., T. Shichita, H. Yoshida, Y. Sugiyama, G. Muto, E. Hasegawa, R. Morita, N. Suzuki and A. Yoshimura (2010). "Therapeutic effect of IL-12/23 and their signaling pathway blockade on brain ischemia model." Biochem Biophys Res Commun **402**(3): 500-506.

Konsman, J. P., B. Drukarch and A. M. Van Dam (2007). "(Peri)vascular production and action of pro-inflammatory cytokines in brain pathology." Clin Sci (Lond) **112**(1): 1-25.

Kopen, G. C., D. J. Prockop and D. G. Phinney (1999). "Marrow stromal cells migrate throughout forebrain and cerebellum, and they differentiate into astrocytes after injection into neonatal mouse brains." Proc Natl Acad Sci U S A **96**(19): 10711-10716.

Krams, M., K. R. Lees, W. Hacke, A. P. Grieve, J. M. Orgogozo, G. A. Ford and A. S. Investigators (2003). "Acute Stroke Therapy by Inhibition of Neutrophils (ASTIN): an

adaptive dose-response study of UK-279,276 in acute ischemic stroke." Stroke **34**(11): 2543-2548.

Kriz, J. (2006). "Inflammation in ischemic brain injury: timing is important." Crit Rev Neurobiol **18**(1-2): 145-157.

Kunis, G., K. Baruch, N. Rosenzweig, A. Kertser, O. Miller, T. Berkutzki and M. Schwartz (2013). "IFN-gamma-dependent activation of the brain's choroid plexus for CNS immune surveillance and repair." Brain **136**(Pt 11): 3427-3440.

Kyritsis, N., C. Kizil, S. Zocher, V. Kroehne, J. Kaslin, D. Freudenreich, A. Iltzsche and M. Brand (2012). "Acute inflammation initiates the regenerative response in the adult zebrafish brain." Science **338**(6112): 1353-1356.

Lakhan, S. E., A. Kirchgessner and M. Hofer (2009). "Inflammatory mechanisms in ischemic stroke: therapeutic approaches." J Transl Med **7**: 97.

Lambertsen, K. L., B. H. Clausen, A. A. Babcock, R. Gregersen, C. Fenger, H. H. Nielsen, L. S. Haugaard, M. Wirenfeldt, M. Nielsen, F. Dagnaes-Hansen, H. Bluethmann, N. J. Faergeman, M. Meldgaard, T. Deierborg and B. Finsen (2009). "Microglia protect neurons against ischemia by synthesis of tumor necrosis factor." J Neurosci **29**(5): 1319-1330.

Lampl, Y., M. Boaz, R. Gilad, M. Lorberboym, R. Dabby, A. Rapoport, M. Anca-Hershkowitz and M. Sadeh (2007). "Minocycline treatment in acute stroke: an open-label, evaluator-blinded study." Neurology **69**(14): 1404-1410.

Lazarov, O., M. P. Mattson, D. A. Peterson, S. W. Pimplikar and H. van Praag (2010). "When neurogenesis encounters aging and disease." Trends Neurosci **33**(12): 569-579.

Lee, S., E. Szilagyi, L. Chen, K. Premanand, L. A. DiPietro, W. Ennis and A. M. Bartholomew (2013). "Activated mesenchymal stem cells increase wound tensile strength in aged mouse model via macrophages." J Surg Res **181**(1): 20-24.

Li, Y., J. Chen, X. G. Chen, L. Wang, S. C. Gautam, Y. X. Xu, M. Katakowski, L. J. Zhang, M. Lu, N. Janakiraman and M. Chopp (2002). "Human marrow stromal cell therapy for stroke in rat: neurotrophins and functional recovery." Neurology **59**(4): 514-523.

Li, Y., S. P. Yu, O. Mohamad, T. Genetta and L. Wei (2010). "Sublethal transient global ischemia stimulates migration of neuroblasts and neurogenesis in mice." Transl Stroke Res **1**(3): 184-196.

Lichtenwalner, R. J. and J. M. Parent (2006). "Adult neurogenesis and the ischemic forebrain." J Cereb Blood Flow Metab **26**(1): 1-20.

Lim, J. Y., C. H. Jeong, J. A. Jun, S. M. Kim, C. H. Ryu, Y. Hou, W. Oh, J. W. Chang and S. S. Jeun (2011). "Therapeutic effects of human umbilical cord blood-derived mesenchymal stem cells after intrathecal administration by lumbar puncture in a rat model of cerebral ischemia." Stem Cell Res Ther **2**(5): 38.

Liu, J., K. Solway, R. O. Messing and F. R. Sharp (1998). "Increased neurogenesis in the dentate gyrus after transient global ischemia in gerbils." J Neurosci **18**(19): 7768-7778.

Liu, N., Y. Zhang, L. Fan, M. Yuan, H. Du, R. Cheng, D. Liu and F. Lin (2011). "Effects of transplantation with bone marrow-derived mesenchymal stem cells modified by Survivin on experimental stroke in rats." J Transl Med **9**: 105.

Liu, X., J. Xia, L. Wang, Y. Song, J. Yang, Y. Yan, H. Ren and G. Zhao (2009). "Efficacy and safety of ginsenoside-Rd for acute ischaemic stroke: a randomized, double-blind, placebo-controlled, phase II multicenter trial." Eur J Neurol **16**(5): 569-575.

Liu, X. S., M. Chopp, R. L. Zhang and Z. G. Zhang (2013). "MicroRNAs in cerebral ischemia-induced neurogenesis." J Neuropathol Exp Neurol **72**(8): 718-722.

Liu, Y., L. Wang, T. Kikuiri, K. Akiyama, C. Chen, X. Xu, R. Yang, W. Chen, S. Wang and S. Shi (2011). "Mesenchymal stem cell-based tissue regeneration is governed by recipient T lymphocytes via IFN-gamma and TNF-alpha." Nat Med **17**(12): 1594-1601.

Lively, S., I. Moxon-Emre and L. C. Schlichter (2011). "SC1/hevin and reactive gliosis after transient ischemic stroke in young and aged rats." J Neuropathol Exp Neurol **70**(10): 913-929.

Loddick, S. A., A. V. Turnbull and N. J. Rothwell (1998). "Cerebral interleukin-6 is neuroprotective during permanent focal cerebral ischemia in the rat." J Cereb Blood Flow Metab **18**(2): 176-179.

Lohan, P., O. Treacy, M. D. Griffin, T. Ritter and A. E. Ryan (2017). "Anti-Donor Immune Responses Elicited by Allogeneic Mesenchymal Stem Cells and Their Extracellular Vesicles: Are We Still Learning?" Front Immunol **8**: 1626.

Lowrance, S. A., K. D. Fink, A. Crane, J. Matyas, N. D. Dey, J. J. Matchynski, T. Thibo, T. Reinke, J. Kippe, C. Hoffman, M. Sandstrom, J. Rossignol and G. L. Dunbar (2015). "Bone-marrow-derived mesenchymal stem cells attenuate cognitive deficits in an endothelin-1 rat model of stroke." Restor Neurol Neurosci **33**(4): 579-588.

Lyden, P. D., A. Shuaib, K. R. Lees, A. Davalos, S. M. Davis, H. C. Diener, J. C. Grotta, T. J. Ashwood, H. G. Hardemark, H. H. Svensson, L. Rodichok, W. W. Wasiewski, G. Ahlberg and C. T. Investigators (2007). "Safety and tolerability of NXY-059 for acute intracerebral hemorrhage: the CHANT Trial." Stroke **38**(8): 2262-2269.

Maffioli, E., S. Nonnis, R. Angioni, F. Santagata, B. Cali, L. Zanotti, A. Negri, A. Viola and G. Tedeschi (2017). "Proteomic analysis of the secretome of human bone marrow-derived mesenchymal stem cells primed by pro-inflammatory cytokines." J Proteomics **166**: 115-126.

Mantovani, A., A. Sica and M. Locati (2005). "Macrophage polarization comes of age." Immunity **23**(4): 344-346.

McIver, S. R., M. Muccigrosso, E. R. Gonzales, J. M. Lee, M. S. Roberts, M. S. Sands and M. P. Goldberg (2010). "Oligodendrocyte degeneration and recovery after focal cerebral ischemia." Neuroscience **169**(3): 1364-1375.

McKinnon, R. D., G. Piras, J. A. Ida, Jr. and M. Dubois-Dalcq (1993). "A role for TGF-beta in oligodendrocyte differentiation." J Cell Biol **121**(6): 1397-1407.

McTaggart, S. J. and K. Atkinson (2007). "Mesenchymal stem cells: immunobiology and therapeutic potential in kidney disease." Nephrology (Carlton) **12**(1): 44-52.

Ming, G. L. and H. Song (2011). "Adult neurogenesis in the mammalian brain: significant answers and significant questions." Neuron **70**(4): 687-702.

Minghetti, L. (2005). "Role of inflammation in neurodegenerative diseases." Curr Opin Neurol **18**(3): 315-321.

Mongiat, L. A., M. S. Esposito, G. Lombardi and A. F. Schinder (2009). "Reliable activation of immature neurons in the adult hippocampus." PLoS One **4**(4): e5320.

Moniche, F., A. Gonzalez, J. R. Gonzalez-Marcos, M. Carmona, P. Pinero, I. Espigado, D. Garcia-Solis, A. Cayuela, J. Montaner, C. Boada, A. Rosell, M. D. Jimenez, A. Mayol and A. Gil-Peralta (2012). "Intra-arterial bone marrow mononuclear cells in ischemic stroke: a pilot clinical trial." Stroke **43**(8): 2242-2244.

Moniche, F., P. H. Rosado-de-Castro, I. Escudero, E. Zapata, F. J. de la Torre Laviana, R. Mendez-Otero, M. Carmona, P. Pinero, A. Bustamante, L. Lebrato, J. A. Cabezas, A. Gonzalez, G. R. de Freitas and J. Montaner (2016). "Increasing Dose of Autologous Bone Marrow Mononuclear Cells Transplantation Is Related to Stroke Outcome: Results from a Pooled Analysis of Two Clinical Trials." Stem Cells Int **2016**: 8657173.

Monje, M. L., H. Toda and T. D. Palmer (2003). "Inflammatory blockade restores adult hippocampal neurogenesis." Science **302**(5651): 1760-1765.

Moradi, F., M. Haji Ghasem Kashani, M. T. Ghorbanian and T. Lashkarbolouki (2012). "Spontaneous Expression of Neurotrophic Factors and TH, Nurr1, Nestin Genes in Long-term Culture of Bone Marrow Mesenchymal Stem Cells." Cell J **13**(4): 243-250.

Morioka, T., A. N. Kalehua and W. J. Streit (1993). "Characterization of microglial reaction after middle cerebral artery occlusion in rat brain." J Comp Neurol **327**(1): 123-132.

Morrens, J., W. Van Den Broeck and G. Kempermann (2012). "Glial cells in adult neurogenesis." Glia **60**(2): 159-174.

Nakashiba, T., J. D. Cushman, K. A. Pelkey, S. Renaudineau, D. L. Buhl, T. J. McHugh, V. Rodriguez Barrera, R. Chittajallu, K. S. Iwamoto, C. J. McBain, M. S. Fanselow and S. Tonegawa (2012). "Young dentate granule cells mediate pattern separation, whereas old granule cells facilitate pattern completion." Cell **149**(1): 188-201.

Noh, M. Y., S. M. Lim, K. W. Oh, K. A. Cho, J. Park, K. S. Kim, S. J. Lee, M. S. Kwon and S. H. Kim (2016). "Mesenchymal Stem Cells Modulate the Functional Properties of Microglia via TGF-beta Secretion." Stem Cells Transl Med **5**(11): 1538-1549.

Nomura, T., O. Honmou, K. Harada, K. Houkin, H. Hamada and J. D. Kocsis (2005). "I.V. infusion of brain-derived neurotrophic factor gene-modified human mesenchymal stem cells protects against injury in a cerebral ischemia model in adult rat." Neuroscience **136**(1): 161-169.

Norris, J. W. and V. C. Hachinski (1986). "High dose steroid treatment in cerebral infarction." Br Med J (Clin Res Ed) **292**(6512): 21-23.

Nowicka, D., K. Rogozinska, M. Aleksy, O. W. Witte and J. Skangiel-Kramska (2008). "Spatiotemporal dynamics of astroglial and microglial responses after photothrombotic stroke in the rat brain." Acta Neurobiol Exp (Wars) **68**(2): 155-168.

Ohab, J. J., S. Fleming, A. Blesch and S. T. Carmichael (2006). "A neurovascular niche for neurogenesis after stroke." J Neurosci **26**(50): 13007-13016.

Ohtaki, H., J. H. Ylostalo, J. E. Foraker, A. P. Robinson, R. L. Reger, S. Shioda and D. J. Prockop (2008). "Stem/progenitor cells from bone marrow decrease neuronal death in global ischemia by modulation of inflammatory/immune responses." Proc Natl Acad Sci U S A **105**(38): 14638-14643.

Ong, J., J. M. Plane, J. M. Parent and F. S. Silverstein (2005). "Hypoxic-ischemic injury stimulates subventricular zone proliferation and neurogenesis in the neonatal rat." Pediatr Res **58**(3): 600-606.

Packer, M. A., Y. Stasiv, A. Benraiss, E. Chmielnicki, A. Grinberg, H. Westphal, S. A. Goldman and G. Enikolopov (2003). "Nitric oxide negatively regulates mammalian adult neurogenesis." Proc Natl Acad Sci U S A **100**(16): 9566-9571.

Palazuelos, J., M. Klingener and A. Aguirre (2014). "TGFbeta signaling regulates the timing of CNS myelination by modulating oligodendrocyte progenitor cell cycle exit through SMAD3/4/FoxO1/Sp1." J Neurosci **34**(23): 7917-7930.

Palmer, T. D., A. R. Willhoite and F. H. Gage (2000). "Vascular niche for adult hippocampal neurogenesis." J Comp Neurol **425**(4): 479-494.

Parent, J. M., Z. S. Vexler, C. Gong, N. Derugin and D. M. Ferriero (2002). "Rat forebrain neurogenesis and striatal neuron replacement after focal stroke." Ann Neurol **52**(6): 802-813.

Park, D. H., D. J. Eve, P. R. Sanberg, J. Musso, 3rd, A. D. Bachstetter, A. Wolfson, A. Schlunk, M. O. Baradez, J. D. Sinden and C. Gemma (2010). "Increased neuronal proliferation in the dentate gyrus of aged rats following neural stem cell implantation." Stem Cells Dev **19**(2): 175-180.

Pettigrew, L. C., S. E. Kasner, G. W. Albers, M. Gorman, J. C. Grotta, D. G. Sherman, Y. Funakoshi, H. Ishibashi and G. Arundic Acid Stroke Study (2006). "Safety and tolerability of arundic acid in acute ischemic stroke." J Neurol Sci **251**(1-2): 50-56.

Plane, J. M., R. Liu, T. W. Wang, F. S. Silverstein and J. M. Parent (2004). "Neonatal hypoxic-ischemic injury increases forebrain subventricular zone neurogenesis in the mouse." Neurobiol Dis **16**(3): 585-595.

Pluchino, S., L. Zanotti, B. Rossi, E. Brambilla, L. Ottoboni, G. Salani, M. Martinello, A. Cattalini, A. Bergami, R. Furlan, G. Comi, G. Constantin and G. Martino (2005). "Neurosphere-derived multipotent precursors promote neuroprotection by an immunomodulatory mechanism." Nature **436**(7048): 266-271.

Polchert, D., J. Sobinsky, G. Douglas, M. Kidd, A. Moadsiri, E. Reina, K. Genrich, S. Mehrotra, S. Setty, B. Smith and A. Bartholomew (2008). "IFN-gamma activation of mesenchymal stem cells for treatment and prevention of graft versus host disease." Eur J Immunol **38**(6): 1745-1755.

Porcheray, F., W. Wong, S. L. Saidman, J. De Vito, T. C. Girouard, M. Chittenden, J. Shaffer, N. Tolkoff-Rubin, B. R. Dey, T. R. Spitzer, R. B. Colvin, A. B. Cosimi, T. Kawai, D. H. Sachs, M. Sykes and E. Zorn (2009). "B-cell immunity in the context of T-cell tolerance after combined kidney and bone marrow transplantation in humans." Am J Transplant **9**(9): 2126-2135.

Qu, T., C. L. Brannen, H. M. Kim and K. Sugaya (2001). "Human neural stem cells improve cognitive function of aged brain." Neuroreport **12**(6): 1127-1132.

Quinones-Hinojosa, A., N. Sanai, O. Gonzalez-Perez and J. M. Garcia-Verdugo (2007). "The human brain subventricular zone: stem cells in this niche and its organization." Neurosurg Clin N Am **18**(1): 15-20, vii.

Quittet, M. S., O. Touzani, L. Sindji, J. Cayon, F. Fillesoye, J. Toutain, D. Divoux, L. Marteau, M. Lecocq, S. Roussel, C. N. Montero-Menei and M. Bernaudin (2015). "Effects of mesenchymal stem cell therapy, in association with pharmacologically active microcarriers releasing VEGF, in an ischaemic stroke model in the rat." Acta Biomater **15**: 77-88.

Rezai-Zadeh, K., D. Gate and T. Town (2009). "CNS infiltration of peripheral immune cells: D-Day for neurodegenerative disease?" J Neuroimmune Pharmacol **4**(4): 462-475.

Rivera, F. J. and L. Aigner (2012). "Adult mesenchymal stem cell therapy for myelin repair in multiple sclerosis." Biol Res **45**(3): 257-268.

Rocha, B., V. Calamia, V. Casas, M. Carrascal, F. J. Blanco and C. Ruiz-Romero (2014). "Secretome analysis of human mesenchymal stem cells undergoing chondrogenic differentiation." J Proteome Res **13**(2): 1045-1054.

Rolls, A., R. Shechter and M. Schwartz (2009). "The bright side of the glial scar in CNS repair." Nat Rev Neurosci **10**(3): 235-241.

Roy, N. S., A. Benraiss, S. Wang, R. A. Fraser, R. Goodman, W. T. Couldwell, M. Nedergaard, A. Kawaguchi, H. Okano and S. A. Goldman (2000). "Promoter-targeted selection and isolation of neural progenitor cells from the adult human ventricular zone." J Neurosci Res **59**(3): 321-331.

Ryan, J. M., F. P. Barry, J. M. Murphy and B. P. Mahon (2005). "Mesenchymal stem cells avoid allogeneic rejection." J Inflamm (Lond) **2**: 8.

Sadan, O., E. Melamed and D. Offen (2012). "Intrastriatal transplantation of neurotrophic factor-secreting human mesenchymal stem cells improves motor function and extends survival in R6/2 transgenic mouse model for Huntington's disease." PLoS Curr **4**: e4f7f6dc013d014e.

Sadan, O., N. Shemesh, R. Barzilay, M. Dadon-Nahum, T. Blumenfeld-Katzir, Y. Assaf, M. Yeshurun, R. Djaldetti, Y. Cohen, E. Melamed and D. Offen (2012). "Mesenchymal stem cells induced to secrete neurotrophic factors attenuate quinolinic acid toxicity: a potential therapy for Huntington's disease." Exp Neurol **234**(2): 417-427.

Sanai, N., A. D. Tramontin, A. Quinones-Hinojosa, N. M. Barbaro, N. Gupta, S. Kunwar, M. T. Lawton, M. W. McDermott, A. T. Parsa, J. Manuel-Garcia Verdugo, M. S. Berger and A. Alvarez-Buylla (2004). "Unique astrocyte ribbon in adult human brain contains neural stem cells but lacks chain migration." Nature **427**(6976): 740-744.

Savitz, S. I., V. Misra, M. Kasam, H. Juneja, C. S. Cox, Jr., S. Alderman, I. Aisiku, S. Kar, A. Gee and J. C. Grotta (2011). "Intravenous autologous bone marrow mononuclear cells for ischemic stroke." Ann Neurol **70**(1): 59-69.

Schilling, M., M. Besselmann, C. Leonhard, M. Mueller, E. B. Ringelstein and R. Kiefer (2003). "Microglial activation precedes and predominates over macrophage infiltration in transient focal cerebral ischemia: a study in green fluorescent protein transgenic bone marrow chimeric mice." Exp Neurol **183**(1): 25-33.

Schilling, M., M. Besselmann, M. Muller, J. K. Strecker, E. B. Ringelstein and R. Kiefer (2005). "Predominant phagocytic activity of resident microglia over hematogenous macrophages following transient focal cerebral ischemia: an investigation using green fluorescent protein transgenic bone marrow chimeric mice." Exp Neurol **196**(2): 290-297.

Schmidt-Hieber, C., P. Jonas and J. Bischofberger (2004). "Enhanced synaptic plasticity in newly generated granule cells of the adult hippocampus." Nature **429**(6988): 184-187.

Schnadelbach, O., C. Mandl and A. Faissner (1998). "Expression of DSD-1-PG in primary neural and glial-derived cell line cultures, upregulation by TGF-beta, and implications for cell-substrate interactions of the glial cell line Oli-neu." Glia **23**(2): 99-119.

Schwamm, L. H., S. F. Ali, M. J. Reeves, E. E. Smith, J. L. Saver, S. Messe, D. L. Bhatt, M. V. Grau-Sepulveda, E. D. Peterson and G. C. Fonarow (2013). "Temporal trends in patient characteristics and treatment with intravenous thrombolysis among acute ischemic stroke patients at Get With The Guidelines-Stroke hospitals." Circ Cardiovasc Qual Outcomes **6**(5): 543-549.

Schwartz, M., J. Kipnis, S. Rivest and A. Prat (2013). "How do immune cells support and shape the brain in health, disease, and aging?" J Neurosci **33**(45): 17587-17596.

Shimakura, A., Y. Kamanaka, Y. Ikeda, K. Kondo, Y. Suzuki and K. Umemura (2000). "Neutrophil elastase inhibition reduces cerebral ischemic damage in the middle cerebral artery occlusion." Brain Res **858**(1): 55-60.

Shuaib, A., K. R. Lees, P. Lyden, J. Grotta, A. Davalos, S. M. Davis, H. C. Diener, T. Ashwood, W. W. Wasiewski, U. Emeribe and S. I. T. Investigators (2007). "NXY-059 for the treatment of acute ischemic stroke." N Engl J Med **357**(6): 562-571.

Silva, N. A., J. Moreira, S. Ribeiro-Samy, E. D. Gomes, R. Y. Tam, M. S. Shoichet, R. L. Reis, N. Sousa and A. J. Salgado (2013). "Modulation of bone marrow mesenchymal stem cell secretome by ECM-like hydrogels." Biochimie **95**(12): 2314-2319.

Slepko, N. and G. Levi (1996). "Progressive activation of adult microglial cells in vitro." Glia **16**(3): 241-246.

Spalding, K. L., O. Bergmann, K. Alkass, S. Bernard, M. Salehpour, H. B. Huttner, E. Bostrom, I. Westerlund, C. Vial, B. A. Buchholz, G. Possnert, D. C. Mash, H. Druid and J. Frisen (2013). "Dynamics of hippocampal neurogenesis in adult humans." Cell **153**(6): 1219-1227.

Spite, M. and C. N. Serhan (2010). "Novel lipid mediators promote resolution of acute inflammation: impact of aspirin and statins." Circ Res **107**(10): 1170-1184.

Stansley, B., J. Post and K. Hensley (2012). "A comparative review of cell culture systems for the study of microglial biology in Alzheimer's disease." J Neuroinflammation **9**: 115.

Steinberg, G. K., D. Kondziolka, L. R. Wechsler, L. D. Lunsford, M. L. Coburn, J. B. Billigen, A. S. Kim, J. N. Johnson, D. Bates, B. King, C. Case, M. McGrogan, E. W. Yankee and N. E. Schwartz (2016). "Clinical Outcomes of Transplanted Modified Bone Marrow-Derived Mesenchymal Stem Cells in Stroke: A Phase 1/2a Study." Stroke **47**(7): 1817-1824.

Stenzel, W. and G. Alber (2008). Regulation of the inflammatory response in brain. Handbook of Neurochemistry and Molecular Neurobiology. A. Lajtha, A. Galoyan and H. O. Besedovsky, Springer US**:** 235-262.

Stevens, S. L., J. Bao, J. Hollis, N. S. Lessov, W. M. Clark and M. P. Stenzel-Poore (2002). "The use of flow cytometry to evaluate temporal changes in inflammatory cells following focal cerebral ischemia in mice." Brain Res **932**(1-2): 110-119.

Suarez-Monteagudo, C., P. Hernandez-Ramirez, L. Alvarez-Gonzalez, I. Garcia-Maeso, K. de la Cuetara-Bernal, L. Castillo-Diaz, M. L. Bringas-Vega, G. Martinez-Aching, L. M. Morales-Chacon, M. M. Baez-Martin, C. Sanchez-Catasus, M. Carballo-Barreda, R. Rodriguez-Rojas, L. Gomez-Fernandez, E. Alberti-Amador, C. Macias-Abraham, E. D. Balea, L. C. Rosales, L. Del Valle Perez, B. B. Ferrer, R. M. Gonzalez and J. A. Bergado (2009). "Autologous bone marrow stem cell neurotransplantation in stroke patients. An open study." Restor Neurol Neurosci **27**(3): 151-161.

Suh, H., W. Deng and F. H. Gage (2009). "Signaling in adult neurogenesis." Annu Rev Cell Dev Biol **25**: 253-275.

Takagi, Y., K. Nozaki, J. Takahashi, J. Yodoi, M. Ishikawa and N. Hashimoto (1999). "Proliferation of neuronal precursor cells in the dentate gyrus is accelerated after transient forebrain ischemia in mice." Brain Res **831**(1-2): 283-287.

Takasawa, K., K. Kitagawa, Y. Yagita, T. Sasaki, S. Tanaka, K. Matsushita, T. Ohstuki, T. Miyata, H. Okano, M. Hori and M. Matsumoto (2002). "Increased proliferation of neural progenitor cells but reduced survival of newborn cells in the contralateral hippocampus after focal cerebral ischemia in rats." J Cereb Blood Flow Metab **22**(3): 299-307.

Tanaka, R., M. Komine-Kobayashi, H. Mochizuki, M. Yamada, T. Furuya, M. Migita, T. Shimada, Y. Mizuno and T. Urabe (2003). "Migration of enhanced green fluorescent protein expressing bone marrow-derived microglia/macrophage into the mouse brain following permanent focal ischemia." Neuroscience **117**(3): 531-539.

Tanaka, R., K. Yamashiro, H. Mochizuki, N. Cho, M. Onodera, Y. Mizuno and T. Urabe (2004). "Neurogenesis after transient global ischemia in the adult hippocampus visualized by improved retroviral vector." Stroke **35**(6): 1454-1459.

Thored, P., U. Heldmann, W. Gomes-Leal, R. Gisler, V. Darsalia, J. Taneera, J. M. Nygren, S. E. Jacobsen, C. T. Ekdahl, Z. Kokaia and O. Lindvall (2009). "Long-term accumulation of microglia with proneurogenic phenotype concomitant with persistent neurogenesis in adult subventricular zone after stroke." Glia **57**(8): 835-849.

Thored, P., J. Wood, A. Arvidsson, J. Cammenga, Z. Kokaia and O. Lindvall (2007). "Long-term neuroblast migration along blood vessels in an area with transient angiogenesis and increased vascularization after stroke." Stroke **38**(11): 3032-3039.

Tobin, M. K., J. A. Bonds, R. D. Minshall, D. A. Pelligrino, F. D. Testai and O. Lazarov (2014). "Neurogenesis and inflammation after ischemic stroke: what is known and where we go from here." J Cereb Blood Flow Metab **34**(10): 1573-1584.

Tonchev, A. B. (2011). "Brain ischemia, neurogenesis, and neurotrophic receptor expression in primates." Arch Ital Biol **149**(2): 225-231.

Tonchev, A. B., T. Yamashima, L. Zhao, H. J. Okano and H. Okano (2003). "Proliferation of neural and neuronal progenitors after global brain ischemia in young adult macaque monkeys." Mol Cell Neurosci **23**(2): 292-301.

Towfighi, A. and J. L. Saver (2011). "Stroke declines from third to fourth leading cause of death in the United States: historical perspective and challenges ahead." Stroke **42**(8): 2351-2355.

Toyoshima, A., T. Yasuhara, M. Kameda, J. Morimoto, H. Takeuchi, F. Wang, T. Sasaki, S. Sasada, A. Shinko, T. Wakamori, M. Okazaki, A. Kondo, T. Agari, C. V. Borlongan and I. Date (2015). "Intra-Arterial Transplantation of Allogeneic Mesenchymal Stem Cells Mounts Neuroprotective Effects in a Transient Ischemic Stroke Model in Rats: Analyses of Therapeutic Time Window and Its Mechanisms." PLoS One **10**(6): e0127302.

Tsai, Y. W., Y. R. Yang, P. S. Wang and R. Y. Wang (2011). "Intermittent hypoxia after transient focal ischemia induces hippocampal neurogenesis and c-Fos expression and reverses spatial memory deficits in rats." PLoS One **6**(8): e24001.

Tureyen, K., R. Vemuganti, K. A. Sailor, K. K. Bowen and R. J. Dempsey (2004). "Transient focal cerebral ischemia-induced neurogenesis in the dentate gyrus of the adult mouse." J Neurosurg **101**(5): 799-805.

Unsicker, K. and J. Strelau (2000). "Functions of transforming growth factor-beta isoforms in the nervous system. Cues based on localization and experimental in vitro and in vivo evidence." Eur J Biochem **267**(24): 6972-6975.

Vallieres, L., I. L. Campbell, F. H. Gage and P. E. Sawchenko (2002). "Reduced hippocampal neurogenesis in adult transgenic mice with chronic astrocytic production of interleukin-6." J Neurosci **22**(2): 486-492.

van Velthoven, C. T., R. A. Sheldon, A. Kavelaars, N. Derugin, Z. S. Vexler, H. L. Willemen, M. Maas, C. J. Heijnen and D. M. Ferriero (2013). "Mesenchymal stem cell transplantation attenuates brain injury after neonatal stroke." Stroke **44**(5): 1426-1432.

Walton, N. M., B. M. Sutter, E. D. Laywell, L. H. Levkoff, S. M. Kearns, G. P. Marshall, 2nd, B. Scheffler and D. A. Steindler (2006). "Microglia instruct subventricular zone neurogenesis." Glia **54**(8): 815-825.

Wang, C., F. Liu, Y. Y. Liu, C. H. Zhao, Y. You, L. Wang, J. Zhang, B. Wei, T. Ma, Q. Zhang, Y. Zhang, R. Chen, H. Song and Z. Yang (2011). "Identification and characterization of neuroblasts in the subventricular zone and rostral migratory stream of the adult human brain." Cell Res **21**(11): 1534-1550.

Wang, H., A. L. Moyano, Z. Ma, Y. Deng, Y. Lin, C. Zhao, L. Zhang, M. Jiang, X. He, Z. Ma, F. Lu, M. Xin, W. Zhou, S. O. Yoon, E. R. Bongarzone and Q. R. Lu (2017). "miR-219 Cooperates with miR-338 in Myelination and Promotes Myelin Repair in the CNS." Dev Cell **40**(6): 566-582 e565.

Wang, S., J. Bates, X. Li, S. Schanz, D. Chandler-Militello, C. Levine, N. Maherali, L. Studer, K. Hochedlinger, M. Windrem and S. A. Goldman (2013). "Human iPSC-derived oligodendrocyte progenitor cells can myelinate and rescue a mouse model of congenital hypomyelination." Cell Stem Cell **12**(2): 252-264.

Wang, X., G. Chen, C. Huang, H. Tu, J. Zou and J. Yan (2017). "Bone marrow stem cells-derived extracellular matrix is a promising material." Oncotarget **8**(58): 98336-98347.

Watcharotayangul, J., L. Mao, H. Xu, F. Vetri, V. L. Baughman, C. Paisansathan and D. A. Pelligrino (2012). "Post-ischemic vascular adhesion protein-1 inhibition provides neuroprotection in a rat temporary middle cerebral artery occlusion model." J Neurochem **123 Suppl 2**: 116-124.

Wei, L., J. L. Fraser, Z. Y. Lu, X. Hu and S. P. Yu (2012). "Transplantation of hypoxia preconditioned bone marrow mesenchymal stem cells enhances angiogenesis and neurogenesis after cerebral ischemia in rats." Neurobiol Dis **46**(3): 635-645.

Wong, G., Y. Goldshmit and A. M. Turnley (2004). "Interferon-gamma but not TNF alpha promotes neuronal differentiation and neurite outgrowth of murine adult neural stem cells." Exp Neurol **187**(1): 171-177.

Wu, J. P., J. S. Kuo, Y. L. Liu and S. F. Tzeng (2000). "Tumor necrosis factor-alpha modulates the proliferation of neural progenitors in the subventricular/ventricular zone of adult rat brain." Neurosci Lett **292**(3): 203-206.

Xiao, B., F. Rao, Z. Y. Guo, X. Sun, Y. G. Wang, S. Y. Liu, A. Y. Wang, Q. Y. Guo, H. Y. Meng, Q. Zhao, J. Peng, Y. Wang and S. B. Lu (2016). "Extracellular matrix from human umbilical cord-derived mesenchymal stem cells as a scaffold for peripheral nerve regeneration." Neural Regen Res **11**(7): 1172-1179.

Xin, H., Y. Li, Z. Liu, X. Wang, X. Shang, Y. Cui, Z. G. Zhang and M. Chopp (2013). "MiR-133b promotes neural plasticity and functional recovery after treatment of stroke with multipotent mesenchymal stromal cells in rats via transfer of exosome-enriched extracellular particles." Stem Cells **31**(12): 2737-2746.

Xu, H. L., L. Salter-Cid, M. D. Linnik, E. Y. Wang, C. Paisansathan and D. A. Pelligrino (2006). "Vascular adhesion protein-1 plays an important role in postischemic inflammation and neuropathology in diabetic, estrogen-treated ovariectomized female rats subjected to transient forebrain ischemia." J Pharmacol Exp Ther **317**(1): 19-29.

Yagita, Y., K. Kitagawa, T. Ohtsuki, K. Takasawa, T. Miyata, H. Okano, M. Hori and M. Matsumoto (2001). "Neurogenesis by progenitor cells in the ischemic adult rat hippocampus." Stroke **32**(8): 1890-1896.

Yamashita, T., K. Sawamoto, S. Suzuki, N. Suzuki, K. Adachi, T. Kawase, M. Mihara, Y. Ohsugi, K. Abe and H. Okano (2005). "Blockade of interleukin-6 signaling aggravates ischemic cerebral damage in mice: possible involvement of Stat3 activation in the protection of neurons." J Neurochem **94**(2): 459-468.

Yamauchi, T., Y. Kuroda, T. Morita, H. Shichinohe, K. Houkin, M. Dezawa and S. Kuroda (2015). "Therapeutic effects of human multilineage-differentiating stress enduring (MUSE) cell transplantation into infarct brain of mice." PLoS One **10**(3): e0116009.

Yang, C., H. Liu and D. Liu (2014). "Mutant hypoxia-inducible factor 1alpha modified bone marrow mesenchymal stem cells ameliorate cerebral ischemia." Int J Mol Med **34**(6): 1622-1628.

Yang, H., Z. Xie, L. Wei, H. Yang, S. Yang, Z. Zhu, P. Wang, C. Zhao and J. Bi (2013). "Human umbilical cord mesenchymal stem cell-derived neuron-like cells rescue memory deficits and reduce amyloid-beta deposition in an AbetaPP/PS1 transgenic mouse model." Stem Cell Res Ther **4**(4): 76.

Yilmaz, G., T. V. Arumugam, K. Y. Stokes and D. N. Granger (2006). "Role of T lymphocytes and interferon-gamma in ischemic stroke." Circulation **113**(17): 2105-2112.

Yilmaz, G. and D. N. Granger (2010). "Leukocyte recruitment and ischemic brain injury." Neuromolecular Med **12**(2): 193-204.

Yoo, S. W., S. S. Kim, S. Y. Lee, H. S. Lee, H. S. Kim, Y. D. Lee and H. Suh-Kim (2008). "Mesenchymal stem cells promote proliferation of endogenous neural stem cells and survival of newborn cells in a rat stroke model." Exp Mol Med **40**(4): 387-397.

Zhang, Q., T. Gao, Y. Luo, X. Chen, G. Gao, X. Gao, Y. Zhou and J. Dai (2012). "Transient focal cerebral ischemia/reperfusion induces early and chronic axonal changes in rats: its importance for the risk of Alzheimer's disease." PLoS One **7**(3): e33722.

Zhang, R. L., M. Chopp, S. R. Gregg, Y. Toh, C. Roberts, Y. Letourneau, B. Buller, L. Jia, P. N. D. S and Z. G. Zhang (2009). "Patterns and dynamics of subventricular zone neuroblast migration in the ischemic striatum of the adult mouse." J Cereb Blood Flow Metab **29**(7): 1240-1250.

Zhao, C., E. M. Teng, R. G. Summers, Jr., G. L. Ming and F. H. Gage (2006). "Distinct morphological stages of dentate granule neuron maturation in the adult mouse hippocampus." J Neurosci **26**(1): 3-11.

Zhao, L. R., W. M. Duan, M. Reyes, C. D. Keene, C. M. Verfaillie and W. C. Low (2002). "Human bone marrow stem cells exhibit neural phenotypes and ameliorate neurological deficits after grafting into the ischemic brain of rats." Exp Neurol **174**(1): 11-20.

Zhao, S., R. Wehner, M. Bornhauser, R. Wassmuth, M. Bachmann and M. Schmitz (2010). "Immunomodulatory properties of mesenchymal stromal cells and their therapeutic consequences for immune-mediated disorders." Stem Cells Dev **19**(5): 607-614.

Ziv, Y., H. Avidan, S. Pluchino, G. Martino and M. Schwartz (2006). "Synergy between immune cells and adult neural stem/progenitor cells promotes functional recovery from spinal cord injury." Proc Natl Acad Sci U S A **103**(35): 13174-13179.

Ziv, Y., N. Ron, O. Butovsky, G. Landa, E. Sudai, N. Greenberg, H. Cohen, J. Kipnis and M. Schwartz (2006). "Immune cells contribute to the maintenance of neurogenesis and spatial learning abilities in adulthood." Nat Neurosci **9**(2): 268-275.

Zuk, P. A., M. Zhu, H. Mizuno, J. Huang, J. W. Futrell, A. J. Katz, P. Benhaim, H. P. Lorenz and M. H. Hedrick (2001). "Multilineage cells from human adipose tissue: implications for cell-based therapies." Tissue Eng **7**(2): 211-228.

APPENDIX 1

Gene	Forward	Reverse	RefSeq No.
GDNF	CGAAGAGAGAGGAACCG	TAGCCCAAACCCAAGTC	NM_019139.1
IGF-1	TACTTCAACAAGCCCACAG	TACATCTCCAGCCTCCTC	NM_001082478.1
BDNF	ACCCTGAGTTCCACCAG	AAGTTGCCTTGTCCGTG	NM_001270630.1
NTF3	TAATGATGAGTGGCTGCG	CCGTATGACTATTTCCAGGG	NM_031073.3
NGF	CGCATCGCTCTCCTTCA	GCCCAGACACTGAGGTG	NM_001277055.1
RPLP0	TTCTCCTTCGGGCTGAT	ATTGCGGACACCCTCTA	NM_022402.2

Table A1. Primer sequences for qRT-PCR. All primer sets used in this dissertation were designed against rat genes. Abbreviations: GNDF – glial derived neurotrophic factor; IGF-1 – insulin-like growth factor 1; BDNF – brain derived neurotrophic factor; NTF3 – neurotrophin 3; NGF – nerve growth factor; RPLP0 – ribosomal protein lateral stalk subunit P0.

APPENDIX 2

Target	Conjugate	Supplier	Catalog No.	Application(s)	Concentration
Sox2	-	Santa Cruz	sc-17320	WB	0.4 µg/mL
GFAP	-	Dako	Z0334	WB	5.8 µg/mL
PDGFRα	-	Santa Cruz	sc-338	IHC WB	0.4 µg/mL 0.2 µg/mL
Actin	-	ThermoFisher Scientific	MA5-11869	WB	0.04 µg/mL
B-III-tubulin	-	ThermoFisher Scientific	32-2600	WB	0.1 µg/mL
BrdU	-	Abcam	ab6326	IHC	2 µg/mL
DCX	-	Santa Cruz	sc-8066	IHC WB	0.2 µg/mL 0.2 µg/mL
Cyclin D1	-	Abcam	ab74646	WB	5 µg/mL
Iba1	-	Wako	019-19741	IHC	0.5 µg/mL
CD68	-	Bio-Rad	MCA341R	IHC	2 µg/mL
CNPase	-	Gift from Dr. Ernesto Bongarzone	-	IHC	1:10 dilution
MBP	-	Santa Cruz	sc-376995	WB	0.4 µg/mL
CD11b	Biotin	BioLegend	201803	MSC Purification	10 µg/mL
CD45	Biotin	BioLegend	202203	MSC Purification	10 µg/mL
CD11b	V450	BD Biosciences	562108	FC	0.5 µg/test
RT1D	FITC	BD Biosciences	550982	FC	0.5 µg/test
CD29	PE	BD Biosciences	562154	FC	0.5 µg/test
CD45	PE-Cy7	BD Biosciences	561588	FC	0.5 µg/test
CD90	APC	eBioscience	17-0900	FC	0.5 µg/test
Ms IgA	V450	BD Biosciences	5262142	FC	0.5 µg/test
Ms IgG1	FITC	BD Biosciences	550616	FC	0.5 µg/test
Hm IgM	PE	BD Biosciences	562114	FC	0.5 µg/test
Ms IgG1	PE-Cy7	BD Biosciences	561588	FC	0.5 µg/test
Ms IgG2a	APC	eBioscience	17-4724	FC	0.5 µg/test

Rabbit IgG	IRDye 800CW	LI-COR	925-32213	WB	0.05 µg/mL
Goat IgG	IRDye 800 CW	LI-COR	925-32214	WB	0.05 µg/mL
Mouse IgG	IRDye 680RD	LI-COR	925-68072	WB	0.05 µg/mL
Mouse IgG	IRDye 680LT	LI-COR	925-68022	WB	0.05 µg/mL
Rabbit IgG	Biotin	Jackson ImmunoResearch	711-065-152	IHC	6 µg/mL
Streptavidin	AF488	Jackson ImmunoResearch	016-540-084	IHC	1.5 µg/mL
Goat IgG	AF488	Jackson ImmunoResearch	705-545-147	IHC	3 µg/mL
Rat IgG	Cy3	Jackson ImmunoResearch	712-165-153	IHC	3 µg/mL
Rabbit IgG	Cy3	Jackson ImmunoResearch	711-585-152	IHC	3 µg/mL
Mouse IgG	Cy3	Jackson ImmunoResearch	715-165-151	IHC	3 µg/mL
Goat IgG	Cy5	Jackson ImmunoResearch	705-175-147	IHC	6 µg/mL

Table A2. Antibodies. Primary antibodies are listed above the black line and secondary antibodies are listed below the black line. Abbreviations: Sox2 – SRY box 2; GFAP – glial fibrillary acidic protein; PDGFRα – platelet derived growth factor receptor α; BrdU – 5-bromo-2'-deoxyuridine; DCX – doublecortin; Iba1 – ionized calcium-binding adapter molecule 1; CD – cluster of differentiation; RT1D – MHC class II RT1D alpha chain; Ig – immunoglobulin; Ms – mouse; Hm – hamster; WB – Western blot; IHC – immunohistochemistry; MSC – mesenchymal stem cell; FC – flow cytometry.

APPENDIX 3

Motor tests	
Raising rat by tail	CumMax:3
Flexion of forelimb	1
Flexion of hindlimb	1
Head moved >10° to vertical axis within 30 s	1
	SCORE:
Placing rat on floor (normal=0; maximum=3)	RangeMax:3
Normal walk	0
Inability to walk straight	1
Circling toward paretic side	2
Falls down to paretic side	3
	SCORE:
Sensory tests	CumMax:2
Placing test	1
Proprioceptive test	1
	SCORE:
Beam balance tests (normal=0; maximum=6)	RangeMax:6
Balances with steady posture	0
Grasps side of beam	1
Hugs beam and 1 limb falls down from beam	2
Hugs beam and 2 limbs fall down from beam, or spins on beam (>60 s)	3
Attempts to balance on beam but falls off (>40 s)	4
Attempts to balance on beam but falls off (>20 s)	5
Falls off; no attempt to balance or hang on to beam (<20 s)	6
	SCORE:
Reflex absence and abnormal movements	CumMax:4
Pinna reflex	1
Corneal reflex	1
Startle reflex	1
Seizures, myoclonus, myodystony	1
	SCORE:
Cumulative Score (maximum = 18)	SCORE:

APPENDIX 4

Protein Descriptions	UniProt Accession ID	Gene Symbol
72 kDa type IV collagenase OS=Rattus norvegicus GN=Mmp2 PE=2 SV=2	P33436	Mmp2
78 kDa glucose-regulated protein OS=Rattus norvegicus GN=Hspa5 PE=1 SV=1	P06761	Hspa5
A disintegrin and metalloproteinase with thrombospondin motifs 1 OS=Rattus norvegicus GN=Adamts1 PE=2 SV=1	Q9WUQ1	Adamts1
Actin, aortic smooth muscle OS=Rattus norvegicus GN=Acta2 PE=2 SV=1	P62738	Acta2
Actin, beta-like 2 OS=Rattus norvegicus GN=Actbl2 PE=1 SV=1	D3ZRN3	[y]Actbl2
Actinin alpha 2 OS=Rattus norvegicus GN=Actn2 PE=1 SV=1	D3ZCV0	Actn2
Actinin alpha 3 OS=Rattus norvegicus GN=Actn3 PE=1 SV=1	Q8R4I6	[n]Actn3
Actn1 protein OS=Rattus norvegicus GN=Actn1 PE=1 SV=1	Q6GMN8	Actn1
ADAM metallopeptidase with thrombospondin type 1 motif, 12 OS=Rattus norvegicus GN=Adamts12 PE=4 SV=2	D3ZTJ3	Adamts12
ADAMTS-like 3 OS=Rattus norvegicus GN=Adamtsl3 PE=4 SV=3	D4ADD4	Adamtsl3
Adipocyte enhancer-binding protein 1 OS=Rattus norvegicus GN=Aebp1 PE=2 SV=1	A2RUV9	Aebp1
Aggrecan core protein OS=Rattus norvegicus GN=Acan PE=1 SV=2	P07897; D4A7Y1	Acan
AHNAK nucleoprotein OS=Rattus norvegicus GN=Ahnak PE=1 SV=1	A0A0G2JU96	[n]Ahnak
Alpha 4 type V collagen OS=Rattus norvegicus GN=Col5a3 PE=2 SV=1	Q9JI04	Col5a3
Alpha-1-macroglobulin OS=Rattus norvegicus GN=A1m PE=1 SV=1	Q63041	A1m
Alpha-2 antiplasmin OS=Rattus norvegicus GN=Serpinf1 PE=1 SV=1	Q80ZA3	Serpinf1
Alpha-2-macroglobulin OS=Rattus norvegicus GN=A2m PE=2 SV=2	P06238	A2m
Alpha-actinin-4 OS=Rattus norvegicus GN=Actn4 PE=1 SV=2	Q9QXQ0	Actn4
Alpha-internexin OS=Rattus norvegicus GN=Ina PE=1 SV=2	P23565;G3V8Q2	[n]Ina
Amyloid beta A4 protein OS=Rattus norvegicus GN=App PE=1 SV=2	P08592	App
Apolipoprotein B-100 OS=Rattus norvegicus GN=Apob PE=1 SV=1	Q7TMA5	Apob
Beta-2-glycoprotein 1 OS=Rattus norvegicus GN=Apoh PE=2 SV=2	P26644	Apoh
Beta-2-microglobulin OS=Rattus norvegicus GN=B2m PE=1 SV=1	P07151	B2m
Biglycan OS=Rattus norvegicus GN=Bgn PE=2 SV=1	P47853	Bgn

Protein Descriptions	UniProt Accession ID	Gene Symbol
C1r protein OS=Rattus norvegicus GN=C1r PE=1 SV=1	B5DEH7	C1r
Cadherin 13 OS=Rattus norvegicus GN=Cdh13 PE=2 SV=1	Q8R490	Cdh13
Calreticulin OS=Rattus norvegicus GN=Calr PE=1 SV=1	P18418	Calr
Calsequestrin OS=Rattus norvegicus GN=Casq2 PE=1 SV=2	F1M944	Casq2
Calsyntenin-1 OS=Rattus norvegicus GN=Clstn1 PE=2 SV=1	Q6Q0N0	Clstn1
Carboxypeptidase E OS=Rattus norvegicus GN=Cpe PE=1 SV=1	P15087;D4A8X4	Cpe
Carboxypeptidase OS=Rattus norvegicus GN=Ctsa PE=1 SV=1	Q6AYS3	^{n}Ctsa
Carboxypeptidase Q OS=Rattus norvegicus GN=Cpq PE=1 SV=1	Q6IRK9	Cpq
Cartilage oligomeric matrix protein OS=Rattus norvegicus GN=Comp PE=1 SV=1	P35444	Comp
Catenin beta-1 OS=Rattus norvegicus GN=Ctnnb1 PE=1 SV=1	Q9WU82	^{n}Ctnnb1
Cathepsin B OS=Rattus norvegicus GN=Ctsb PE=1 SV=1	Q6IN22	Ctsb
Cathepsin L1 OS=Rattus norvegicus GN=Ctsl PE=1 SV=2	P07154	Ctsl
CD44 antigen OS=Rattus norvegicus GN=Cd44 PE=1 SV=2	P26051	Cd44
Chondroitin sulfate proteoglycan 4 OS=Rattus norvegicus GN=Cspg4 PE=1 SV=2	Q00657	Cspg4
Class I histocompatibility antigen, Non-RT1.A alpha-1 chain OS=Rattus norvegicus GN=RT1-Aw2 PE=1 SV=1	P15978	^{Y}RT1-Aw2
Coiled-coil domain-containing protein 80 OS=Rattus norvegicus GN=Ccdc80 PE=1 SV=1	Q6QD51	Ccdc80
Collagen alpha-1(I) chain OS=Rattus norvegicus GN=Col1a1 PE=1 SV=5	P02454	Col1a1
Collagen alpha-1(II) chain OS=Rattus norvegicus GN=Col2a1 PE=1 SV=2	P05539	Col2a1
Collagen alpha-1(III) chain OS=Rattus norvegicus GN=Col3a1 PE=2 SV=3	P13941	Col3a1
Collagen alpha-1(V) chain OS=Rattus norvegicus GN=Col5a1 PE=1 SV=1	Q9JI03;A0A0G2JX47	Col5a1
Collagen alpha-1(XI) chain OS=Rattus norvegicus GN=Col11a1 PE=1 SV=2	P20909	Col11a1
Collagen alpha-1(XII) chain (Fragment) OS=Rattus norvegicus GN=Col12a1 PE=2 SV=1	P70560;A0A0G2KAJ7	Col12a1
Collagen alpha-2(I) chain OS=Rattus norvegicus GN=Col1a2 PE=1 SV=3	P02466;A0A0G2K5E8	Col1a2
Collagen type IV alpha 1 chain OS=Rattus norvegicus GN=Col4a1 PE=1 SV=1	F1MA59	Col4a1
Collagen type IV alpha 2 chain OS=Rattus norvegicus GN=Col4a2 PE=1 SV=3	F1M6Q3	Col4a2
Collagen type IV alpha 5 chain OS=Rattus norvegicus GN=Col4a5 PE=3 SV=3	F1LUN5	Col4a5
Collagen type V alpha 2 chain OS=Rattus norvegicus GN=Col5a2 PE=1 SV=3	F1LQ00	Col5a2

Protein Descriptions	UniProt Accession ID	Gene Symbol
Collagen type VI alpha 1 chain OS=Rattus norvegicus GN=Col6a1 PE=1 SV=1	D3ZUL3	Col6a1
Collagen type VI alpha 2 chain OS=Rattus norvegicus GN=Col6a2 PE=1 SV=2	F1LNH3	Col6a2
Collagen type VIII alpha 1 chain OS=Rattus norvegicus GN=Col8a1 PE=1 SV=3	D4AC70	Col8a1
Collagen type VIII alpha 2 chain OS=Rattus norvegicus GN=Col8a2 PE=4 SV=1	D4ADG9	Col8a2
Collagen type XV alpha 1 chain OS=Rattus norvegicus GN=Col15a1 PE=1 SV=1	A0A0G2JV12	Col15a1
Collagen type XVI alpha 1 chain OS=Rattus norvegicus GN=Col16a1 PE=1 SV=2	F1LND0	Col16a1
Collagen type XVIII alpha 1 chain OS=Rattus norvegicus GN=Col18a1 PE=1 SV=2	F1LR02	Col18a1
Complement C1q tumor necrosis factor-related protein 5 OS=Rattus norvegicus GN=C1qtnf5 PE=2 SV=1	Q5FVH0	C1qtnf5
Complement C1s subcomponent OS=Rattus norvegicus GN=C1s PE=1 SV=1	G3V7L3;D4A1S0	^{y}C1s
Complement C2 OS=Rattus norvegicus GN=C2 PE=1 SV=1	Q6MG73;A0A0U1RRP9	C2
Complement C3 OS=Rattus norvegicus GN=C3 PE=1 SV=3	P01026;M0RBF1	C3
Complement C4B (Chido blood group) OS=Rattus norvegicus GN=C4b PE=1 SV=1	Q6MG90	C4b
Complement component 4A (Rodgers blood group) OS=Rattus norvegicus GN=C4a PE=1 SV=2	M0RB00	C4a
Connective tissue growth factor OS=Rattus norvegicus GN=Ctgf PE=2 SV=1	Q9R1E9	Ctgf
Cystatin-C OS=Rattus norvegicus GN=Cst3 PE=1 SV=2	P14841	Cst3
Cysteine and glycine-rich protein 1 OS=Rattus norvegicus GN=Csrp1 PE=1 SV=2	P47875	^{n}Csrp1
Desmin OS=Rattus norvegicus GN=Des PE=1 SV=2	P48675	Des
Dystroglycan 1 OS=Rattus norvegicus GN=Dag1 PE=1 SV=1	F1M8K0	Dag1
EGF-containing fibulin-like extracellular matrix protein 2 OS=Rattus norvegicus GN=Efemp2 PE=1 SV=1	A0A0G2K2R5	Efemp2
Elastin microfibril interfacer 1 OS=Rattus norvegicus GN=Emilin1 PE=1 SV=1	D3Z9E1	Emilin1
Elastin OS=Rattus norvegicus GN=Eln PE=1 SV=2	Q99372	Eln
Elongation factor 1-alpha 1 OS=Rattus norvegicus GN=Eef1a1 PE=2 SV=1	P62630	Eef1a1
Elongation factor 1-alpha 2 OS=Rattus norvegicus GN=Eef1a2 PE=1 SV=1	P62632	^{y}Eef1a2
Elongation factor 2 OS=Rattus norvegicus GN=Eef2 PE=1 SV=4	P05197	Eef2
Endothelial differentiation-related factor 1 OS=Rattus norvegicus GN=Edf1 PE=1 SV=1	P69736	Edf1
Extracellular matrix protein 1 OS=Rattus norvegicus GN=Ecm1 PE=1 SV=2	Q62894	Ecm1
Extracellular sulfatase Sulf-1 OS=Rattus norvegicus GN=Sulf1 PE=1 SV=1	Q8VI60	Sulf1

Protein Descriptions	UniProt Accession ID	Gene Symbol
FAT atypical cadherin 1 OS=Rattus norvegicus GN=Fat1 PE=1 SV=1	A0A0G2K5L1	Fat1
Fibrillin 1 OS=Rattus norvegicus GN=Fbn1 PE=1 SV=1	G3V9M6	Fbn1
Fibrillin 2 OS=Rattus norvegicus GN=Fbn2 PE=4 SV=3	F1M5Q4	Fbn2
Fibronectin OS=Rattus norvegicus GN=Fn1 PE=1 SV=3	F1LST1;A0A096P6L8	Fn1
Fibulin 2 OS=Rattus norvegicus GN=Fbln2 PE=1 SV=1	G3V6X1	Fbln2
Fibulin-1 OS=Rattus norvegicus GN=Fbln1 PE=1 SV=1	D3ZQ25	Fbln1
Fibulin-5 OS=Rattus norvegicus GN=Fbln5 PE=2 SV=1	Q9WVH8	Fbln5
Filamin A OS=Rattus norvegicus GN=Flna PE=1 SV=1	C0JPT7	Flna
Follistatin-related protein 1 OS=Rattus norvegicus GN=Fstl1 PE=1 SV=1	Q62632;F8WG88	Fstl1
Follistatin-related protein 3 OS=Rattus norvegicus GN=Fstl3 PE=2 SV=1	Q99PW7	Fstl3
Fructose-bisphosphate aldolase OS=Rattus norvegicus GN=Aldoart2 PE=2 SV=1	Q6AY07	Aldoart2
Galectin-3-binding protein OS=Rattus norvegicus GN=Lgals3bp PE=1 SV=2	O70513	Lgals3bp
Gelsolin OS=Rattus norvegicus GN=Gsn PE=1 SV=1	Q68FP1	Gsn
Gliomedin OS=Rattus norvegicus GN=Gldn PE=1 SV=1	Q80WL1	[n]Gldn
Glyceraldehyde-3-phosphate dehydrogenase, testis-specific OS=Rattus norvegicus GN=Gapdhs PE=1 SV=1	Q9ESV6	[n]Gapdhs
Glypican 4 OS=Rattus norvegicus GN=Gpc4 PE=1 SV=1	Q642B0	Gpc4
GM2 ganglioside activator OS=Rattus norvegicus GN=Gm2a PE=1 SV=1	Q6IN37	Gm2a
Granulin, isoform CRA_c OS=Rattus norvegicus GN=Grn PE=4 SV=1	G3V8V1	Grn
Haptoglobin OS=Rattus norvegicus GN=Hp PE=1 SV=3	P06866	Hp
Heat shock protein HSP 90-alpha OS=Rattus norvegicus GN=Hsp90aa1 PE=1 SV=3	P82995	Hsp90aa1
Heat shock protein HSP 90-beta OS=Rattus norvegicus GN=Hsp90ab1 PE=1 SV=4	P34058	[Y]Hsp90ab1
Hemicentin 1 OS=Rattus norvegicus GN=Hmcn1 PE=1 SV=3	F1M4Q3	Hmcn1
Hepatoma-derived growth factor-related protein 3 OS=Rattus norvegicus GN=Hdgfrp3 PE=1 SV=1	Q923W4	Hdgfl3
Heterogeneous nuclear ribonucleoprotein K OS=Rattus norvegicus GN=Hnrnpk PE=1 SV=1	P61980	[Y]Hnrnpk
Histone cluster 1 H1 family member c OS=Rattus norvegicus GN=Hist1h1c PE=1 SV=1	A0A0G2K654	Hist1h1c
Histone H1.0 OS=Rattus norvegicus GN=H1f0 PE=2 SV=2	P43278	H1f0
Histone H1.1 OS=Rattus norvegicus GN=Hist1h1a PE=1 SV=1	D4A3K5	Hist1h1a

Protein Descriptions	UniProt Accession ID	Gene Symbol
Histone H1.4 OS=Rattus norvegicus GN=Hist1h1e PE=1 SV=3	P15865	Hist1h1e
Histone H1.5 OS=Rattus norvegicus GN=Hist1h1b PE=1 SV=1	D3ZBN0	Hist1h1b
Histone H1t OS=Rattus norvegicus GN=Hist1h1t PE=1 SV=2	P06349	Hist1h1t
Histone H2B OS=Rattus norvegicus GN=Hist1h2bo PE=3 SV=1	A0A0G2JXI9	Hist1h2bo
Histone H2B OS=Rattus norvegicus GN=Hist2h2be PE=3 SV=3	D4A817	^{Y}Hist2h2be
Histone H2B OS=Rattus norvegicus GN=LOC102549061 PE=3 SV=1	A0A0G2JXE0	^{Y}LOC102549061
Inactive serine protease 35 OS=Rattus norvegicus GN=Prss35 PE=2 SV=1	Q5R212	Prss35
Insulin-like growth factor binding protein 7, isoform CRA_b OS=Rattus norvegicus GN=Igfbp7 PE=1 SV=2	F1M9B2	Igfbp7
Inter-alpha-trypsin inhibitor heavy chain H3 OS=Rattus norvegicus GN=Itih3 PE=2 SV=1	Q63416	Itih3
Interleukin-1 receptor-like 1 OS=Rattus norvegicus GN=Il1rl1 PE=2 SV=1	Q62611;F1LR63	Il1rl1
Lactadherin OS=Rattus norvegicus GN=Mfge8 PE=2 SV=1	P70490;Q1PBJ1	Mfge8
Laminin subunit alpha 4 OS=Rattus norvegicus GN=Lama4 PE=1 SV=3	F1LTF8	Lama4
Laminin subunit alpha 5 OS=Rattus norvegicus GN=Lama5 PE=1 SV=2	F1MAN8	Lama5
Laminin subunit beta 1 OS=Rattus norvegicus GN=Lamb1 PE=1 SV=3	D3ZQN7	Lamb1
Laminin subunit beta-2 OS=Rattus norvegicus GN=Lamb2 PE=2 SV=1	P15800	Lamb2
Laminin subunit gamma 1 OS=Rattus norvegicus GN=Lamc1 PE=1 SV=1	F1MAA7	Lamc1
Latent-transforming growth factor beta-binding protein 1 OS=Rattus norvegicus GN=Ltbp1 PE=1 SV=1	Q00918	Ltbp1
Latent-transforming growth factor beta-binding protein 2 OS=Rattus norvegicus GN=Ltbp2 PE=1 SV=1	O35806;A0A0G2K1G5	Ltbp2
Latent-transforming growth factor beta-binding protein 3 OS=Rattus norvegicus GN=Ltbp3 PE=4 SV=1	F1LRT0	Ltbp3
Lipocalin 7, isoform CRA_a OS=Rattus norvegicus GN=Tinagl1 PE=1 SV=1	Q4V8N0;Q9EQT5	Tinagl1
L-lactate dehydrogenase A chain OS=Rattus norvegicus GN=Ldha PE=1 SV=1	P04642	Ldha
L-lactate dehydrogenase B chain OS=Rattus norvegicus GN=Ldhb PE=1 SV=2	P42123	Ldhb
Lumican OS=Rattus norvegicus GN=Lum PE=1 SV=1	P51886	Lum
Lysyl oxidase homolog 2 OS=Rattus norvegicus GN=Loxl2 PE=2 SV=2	B5DF27;A0A0G2K4P0	Loxl2
Lysyl oxidase-like 1 OS=Rattus norvegicus GN=Loxl1 PE=2 SV=1	Q5FWS5	Loxl1
Lysyl oxidase-like 3 OS=Rattus norvegicus GN=Loxl3 PE=4 SV=1	D3ZP82	Loxl3
Lysyl oxidase-like 4 OS=Rattus norvegicus GN=Loxl4 PE=4 SV=1	D4A9V5	Loxl4

Protein Descriptions	UniProt Accession ID	Gene Symbol
Macrophage colony-stimulating factor 1 OS=Rattus norvegicus GN=Csf1 PE=2 SV=1	Q8JZQ0	Csf1
Mannan-binding lectin serine protease 1 OS=Rattus norvegicus GN=Masp1 PE=1 SV=2	Q8CHN8	Masp1
Matrix Gla protein OS=Rattus norvegicus GN=Mgp PE=1 SV=2	P08494	Mgp
Matrix metallopeptidase 19 OS=Rattus norvegicus GN=Mmp19 PE=2 SV=1	C0M4B0	^{n}Mmp19
Matrix metalloproteinase-14 OS=Rattus norvegicus GN=Mmp14 PE=2 SV=2	Q10739	Mmp14
Matrix metalloproteinase-23 OS=Rattus norvegicus GN=Mmp23 PE=1 SV=1	O88272	Mmp23
Mesothelin OS=Rattus norvegicus GN=Msln PE=2 SV=2	Q9ERA7	Msln
Metalloendopeptidase OS=Rattus norvegicus GN=Bmp1 PE=3 SV=2	F1M798	Bmp1
Metalloendopeptidase OS=Rattus norvegicus GN=Tll1 PE=3 SV=3	D3Z8U5	Tll1
Metalloproteinase inhibitor 1 OS=Rattus norvegicus GN=Timp1 PE=1 SV=2	P30120	Timp1
Metalloproteinase inhibitor 2 OS=Rattus norvegicus GN=Timp2 PE=1 SV=3	P30121	Timp2
Multiple inositol polyphosphate phosphatase 1 OS=Rattus norvegicus GN=Minpp1 PE=1 SV=3	O35217	Minpp1
Myosin, heavy polypeptide 9, non-muscle OS=Rattus norvegicus GN=Myh9 PE=1 SV=1	G3V6P7;Q62812	Myh9
Neurofilament heavy polypeptide OS=Rattus norvegicus GN=Nefh PE=1 SV=4	P16884;F1LRZ7	Nefh
Neurofilament light polypeptide OS=Rattus norvegicus GN=Nefl PE=1 SV=3	P19527	^{Y}Nefl
Neurofilament medium polypeptide OS=Rattus norvegicus GN=Nefm PE=1 SV=3	G3V7S2	Nefm
Nidogen-1 OS=Rattus norvegicus GN=Nid1 PE=1 SV=1	F1LM84	Nid1
Nidogen-2 OS=Rattus norvegicus GN=Nid2 PE=2 SV=1	B5DFC9	Nid2
Non-muscle caldesmon OS=Rattus norvegicus GN=Cald1 PE=1 SV=1	Q62736;A0A0G2JTV2	Cald1
NPC intracellular cholesterol transporter 2 OS=Rattus norvegicus GN=Npc2 PE=1 SV=1	F7FJQ3	Npc2
Nuclear ubiquitous casein and cyclin-dependent kinase substrate 1 OS=Rattus norvegicus GN=Nucks1 PE=1 SV=1	Q9EPJ0	Nucks1
Nucleobindin-1 OS=Rattus norvegicus GN=Nucb1 PE=1 SV=1	Q63083	Nucb1
Nucleobindin-2 OS=Rattus norvegicus GN=Nucb2 PE=1 SV=1	Q9JI85	Nucb2
Nucleoside diphosphate kinase A OS=Rattus norvegicus GN=Nme1 PE=1 SV=1	Q05982	^{Y}Nme1
Nucleoside diphosphate kinase B OS=Rattus norvegicus GN=Nme2 PE=1 SV=1	P19804	^{Y}Nme2
Olfactomedin-like 2B OS=Rattus norvegicus GN=Olfml2b PE=4 SV=1	D4A0J7	Olfml2b
Olfactomedin-like protein 3 OS=Rattus norvegicus GN=Olfml3 PE=2 SV=2	B0BNI5	Olfml3

Protein Descriptions	UniProt Accession ID	Gene Symbol
Osteoglycin OS=Rattus norvegicus GN=Ogn PE=1 SV=1	D3ZVB7	Ogn
Osteopontin OS=Rattus norvegicus GN=Spp1 PE=1 SV=2	P08721	Spp1
Out at first protein homolog OS=Rattus norvegicus GN=Oaf PE=2 SV=1	Q6AYE5	Oaf
Pappalysin 2 OS=Rattus norvegicus GN=Pappa2 PE=4 SV=2	D3ZQ32	Pappa2
Peptidyl-glycine alpha-amidating monooxygenase OS=Rattus norvegicus GN=Pam PE=1 SV=1	P14925	Pam
Peptidyl-prolyl cis-trans isomerase A OS=Rattus norvegicus GN=Ppia PE=1 SV=2	P10111	Ppia
Peptidyl-prolyl cis-trans isomerase B OS=Rattus norvegicus GN=Ppib PE=1 SV=3	P24368	Ppib
Peptidylprolyl isomerase OS=Rattus norvegicus GN=Fkbp10 PE=1 SV=1	Q5U2V1;A0A096MJW1	Fkbp10
Periostin OS=Rattus norvegicus GN=Postn PE=1 SV=1	D3ZAF5;A0A097BW25	Postn
Peroxidasin OS=Rattus norvegicus GN=Pxdn PE=4 SV=1	A0A0G2JWB6	Pxdn
Peroxiredoxin-1 OS=Rattus norvegicus GN=Prdx1 PE=1 SV=1	Q63716	[Y]Prdx1
Plasma protease C1 inhibitor OS=Rattus norvegicus GN=Serping1 PE=2 SV=1	Q6P734	[Y]Serping1
Plasminogen activator inhibitor 1 OS=Rattus norvegicus GN=Serpine1 PE=2 SV=1	P20961	Serpine1
Platelet-derived growth factor receptor-like protein OS=Rattus norvegicus GN=Pdgfrl PE=2 SV=1	Q5RJP7	[n]Pdgfrl
Plexin domain containing 2 OS=Rattus norvegicus GN=Plxdc2 PE=1 SV=1	B5DEZ8	[n]Plxdc2
Procollagen C-endopeptidase enhancer 1 OS=Rattus norvegicus GN=Pcolce PE=1 SV=1	O08628	Pcolce
Procollagen-lysine,2-oxoglutarate 5-dioxygenase 1 OS=Rattus norvegicus GN=Plod1 PE=2 SV=1	Q63321	Plod1
Procollagen-lysine,2-oxoglutarate 5-dioxygenase 2 OS=Rattus norvegicus GN=Plod2 PE=2 SV=1	Q811A3	[n]Plod2
Procollagen-lysine,2-oxoglutarate 5-dioxygenase 3 OS=Rattus norvegicus GN=Plod3 PE=2 SV=1	Q5U367	Plod3
Profilin-1 OS=Rattus norvegicus GN=Pfn1 PE=1 SV=2	P62963	Pfn1
Pro-neuropeptide Y OS=Rattus norvegicus GN=Npy PE=1 SV=1	P07808	Npy
Prosaposin OS=Rattus norvegicus GN=Psap PE=1 SV=1	P10960;F7EPE0	Psap
Protein CYR61 OS=Rattus norvegicus GN=Cyr61 PE=2 SV=1	Q9ES72	Cyr61
Protein disulfide-isomerase A3 OS=Rattus norvegicus GN=Pdia3 PE=1 SV=2	P11598	Pdia3
Protein NOV homolog OS=Rattus norvegicus GN=Nov PE=1 SV=1	Q9QZQ5	Nov
Protein S100-A11 OS=Rattus norvegicus GN=S100a11 PE=3 SV=1	Q6B345	S100a11
Protein shisa-5 OS=Rattus norvegicus GN=Shisa5 PE=1 SV=1	A0A0G2K447	Shisa5
Protein tyrosine phosphatase receptor type K OS=Rattus norvegicus GN=Ptprk PE=1 SV=1	A5I9F0	Ptprk

Protein Descriptions	UniProt Accession ID	Gene Symbol
Protein tyrosine phosphatase, receptor type, D OS=Rattus norvegicus GN=Ptprd PE=1 SV=2	M0RB22	Ptprd
Protein tyrosine phosphatase, receptor type, G OS=Rattus norvegicus GN=Ptprg PE=1 SV=1	A0A0G2K561	[Y]Ptprg
Protein-lysine 6-oxidase OS=Rattus norvegicus GN=Lox PE=1 SV=2	P16636	Lox
Putative uncharacterized protein RGD1565772_predicted OS=Rattus norvegicus GN=Ssc5d PE=4 SV=1	D3ZPK4	Ssc5d
Pyruvate kinase PKM OS=Rattus norvegicus GN=Pkm PE=1 SV=3	P11980	[Y]Pkm
Q6AYQ9|Q6AYQ9_RAT	Q6AYQ9	Ppic
RCG41803, isoform CRA_a OS=Rattus norvegicus GN=RT1-N2 PE=3 SV=1	Q6MFZ8	[Y]RT1-N2
RCG45259 OS=Rattus norvegicus GN=LOC684828 PE=1 SV=2	M0R7B4	LOC684828
RCG55135, isoform CRA_b OS=Rattus norvegicus GN=Tln1 PE=1 SV=1	G3V852	Tln1
Ribonuclease 4 OS=Rattus norvegicus GN=Rnase4 PE=1 SV=1	O55004	Rnase4
RT1 class I histocompatibility antigen, AA alpha chain OS=Rattus norvegicus PE=1 SV=2	P16391	[Y]
RT1 class I, N3 OS=Rattus norvegicus GN=RT1-N3 PE=2 SV=1	Q6MG01	[Y]RT1-N3
RT1 class Ia, locus A1 OS=Rattus norvegicus GN=RT1-A1 PE=1 SV=1	A0A0G2K1E1	[Y]RT1-A1
Rtf1, Paf1/RNA polymerase II complex component, homolog (S. cerevisiae) OS=Rattus norvegicus GN=Rtf1 PE=1 SV=1	D3ZLH8	[Y]Rtf1
Sema domain, immunoglobulin domain (Ig), and GPI membrane anchor, (Semaphorin) 7A (Predicted) OS=Rattus norvegicus GN=Sema7a PE=3 SV=1	D3ZQP6	Sema7a
Semaphorin 3C OS=Rattus norvegicus GN=Sema3c PE=3 SV=1	F7FHT4	Sema3c
Semaphorin 3D OS=Rattus norvegicus GN=Sema3d PE=3 SV=1	F1MAG8	[n]Sema3d
Serine (Or cysteine) peptidase inhibitor, clade C (Antithrombin), member 1 OS=Rattus norvegicus GN=Serpinc1 PE=1 SV=1	Q5M7T5	Serpinc1
Serine protease 23 OS=Rattus norvegicus GN=Prss23 PE=4 SV=1	A0A0G2JU46	Prss23
Serine protease HTRA1 OS=Rattus norvegicus GN=Htra1 PE=2 SV=1	Q9QZK5	Htra1
Serpin H1 OS=Rattus norvegicus GN=Serpinh1 PE=1 SV=1	P29457	Serpinh1
Similar to glyceraldehyde-3-phosphate dehydrogenase OS=Rattus norvegicus GN=LOC303448 PE=1 SV=1	Q498M9	[Y]LOC303448
Similar to RIKEN cDNA 1300017J02 OS=Rattus norvegicus GN=RGD1310507 PE=1 SV=3	E9PST1;A0A0G2K896	[n]RGD1310507
Similar to RT1 class I, CE11 OS=Rattus norvegicus GN=LOC683761 PE=3 SV=3	F1MAQ9	[Y]RT1-CE7
Slit homolog 1 protein OS=Rattus norvegicus GN=Slit1 PE=1 SV=1	O88279	[Y]Slit1

Protein Descriptions	UniProt Accession ID	Gene Symbol
Slit homolog 2 protein OS=Rattus norvegicus GN=Slit2 PE=4 SV=2	F1MA79	Slit2
SPARC OS=Rattus norvegicus GN=Sparc PE=1 SV=4	P16975	Sparc
SPARC-related modular calcium binding protein 1 OS=Rattus norvegicus GN=Smoc1 PE=1 SV=1	Q6IE50	Smoc1
Sulfhydryl oxidase 1 OS=Rattus norvegicus GN=Qsox1 PE=1 SV=1	Q6IUU3	Qsox1
Sushi domain containing 5 (Predicted) OS=Rattus norvegicus GN=Susd5 PE=4 SV=1	D3ZSC1	Susd5
Sushi repeat-containing protein SRPX2 OS=Rattus norvegicus GN=Srpx2 PE=1 SV=1	B5DF94	[n]Srpx2
Sushi, von Willebrand factor type A, EGF and pentraxin domain-containing protein 1 OS=Rattus norvegicus GN=Svep1 PE=1 SV=1	P0C6B8	Svep1
Tenascin C OS=Rattus norvegicus GN=Tnc PE=1 SV=1	A0A0G2K1L0	Tnc
Thrombospondin 2 OS=Rattus norvegicus GN=Thbs2 PE=4 SV=2	D4A2G6	Thbs2
Thrombospondin 3 OS=Rattus norvegicus GN=Thbs3 PE=4 SV=1	A0A0G2JZH3	Thbs3
Transcobalamin-2 OS=Rattus norvegicus GN=Tcn2 PE=2 SV=1	Q9R0D6	Tcn2
Transforming growth factor beta-2 OS=Rattus norvegicus GN=Tgfb2 PE=2 SV=2	Q07257	Tgfb2
Transforming growth factor beta-3 OS=Rattus norvegicus GN=Tgfb3 PE=2 SV=2	Q07258	Tgfb3
Transgelin OS=Rattus norvegicus GN=Tagln PE=1 SV=1	A0A0G2JWK7	Tagln
Transgelin-2 OS=Rattus norvegicus GN=Tagln2 PE=1 SV=1	Q5XFX0	Tagln2
Triosephosphate isomerase OS=Rattus norvegicus GN=Tpi1 PE=1 SV=2	P48500	[Y]Tpi1
Tubulointerstitial nephritis antigen-like OS=Rattus norvegicus GN=Tinagl1 PE=2 SV=1	Q9EQT5	[n]Tinagl1
Uncharacterized protein OS=Rattus norvegicus GN=Gm5414 PE=3 SV=1	A0A0G2JUG1	[Y]Gm5414
Uncharacterized protein OS=Rattus norvegicus GN=Itih2 PE=1 SV=3	D3ZFH5	Itih2
Uncharacterized protein OS=Rattus norvegicus GN=RGD1559534 PE=4 SV=1	F1M9V3	[Y]RGD1559534
Uncharacterized protein OS=Rattus norvegicus GN=RGD1564958 PE=1 SV=1	A0A0G2K8S2	RGD1564958
Uncharacterized protein OS=Rattus norvegicus GN=RT1-CE2 PE=3 SV=3	D3ZQG9;A0A0G2K8R6	[Y]RT1-CE2
Uncharacterized protein OS=Rattus norvegicus GN=Thbs1 PE=1 SV=2	M0R979;A0A0G2JV24	Thbs1
Uncharacterized protein OS=Rattus norvegicus PE=1 SV=2	F1M2N4	N/A
Uncharacterized protein OS=Rattus norvegicus PE=1 SV=3	F1LTJ5	N/A
Uncharacterized protein OS=Rattus norvegicus PE=4 SV=3	F1M8C7	N/A
Uncharacterized protein OS=Rattus norvegicus PE=4 SV=3	F1LUI2	N/A

Protein Descriptions	UniProt Accession ID	Gene Symbol
Versican core protein (Fragments) OS=Rattus norvegicus GN=Vcan PE=2 SV=2	Q9ERB4;D3Z9N6	Vcan
Vimentin OS=Rattus norvegicus GN=Vim PE=1 SV=2	P31000	Vim
Vinculin OS=Rattus norvegicus GN=Vcl PE=1 SV=1	P85972	Vcl
Vitamin K-dependent protein S OS=Rattus norvegicus GN=Pros1 PE=2 SV=1	P53813	Pros1
V-type proton ATPase subunit S1 OS=Rattus norvegicus GN=Atp6ap1 PE=2 SV=1	O54715	Atp6ap1

Table A3. Protein IDs from MSC mass spectrometry. Gene Symbols marked with n denote proteins unique to nMSC, gene symbols marked with γ denote proteins unique to aMSCγ.

APPENDIX 5

Matthew Kyle Tobin

From: permissions (US) <permissions@sagepub.com>
Sent: Monday, October 02, 2017 6:23 PM
To: Matthew Kyle Tobin
Subject: RE: Permission clarification

Hello Matt,

Thank you for your query. Per the SAGE Journal Author Guidelines (https://us.sagepub.com/en-us/nam/journal-author-archiving-policies-and-re-use) you are allowed to include up to one full article that you have authored in your dissertation.

Please note that this permission does not cover any third party material you included in your article and you must credit the original source, SAGE Publications. Please contact us for any further use of the material and good luck on your thesis/dissertation!

All the Best,
Yvonne
--
Yvonne McDuffee
Rights Coordinator
SAGE Publications Inc.
2455 Teller Road
Thousand Oaks, CA 91320

www.sagepublishing.com

Los Angeles | London | New Delhi
Singapore | Washington DC | Melbourne

The natural home for authors, editors & societies

From: Matthew Kyle Tobin [mailto:mktobin2@uic.edu]
Sent: Monday, October 2, 2017 1:25 PM
To: permissions (US) <permissions@sagepub.com>
Subject: Permission clarification

To Whom It May Concern:

I am in the process of writing my PhD dissertation and want to clarify whether I need permission to reuse an article I published in my dissertation. The article is:

Tobin et al., Neurogenesis and inflammation after ischemic stroke: what is known and were we go from here. J Cereb Blood Flow Metab, 2014, 34(10):1573-84.

Please advise if there is anything else required.

APPENDIX 6

T2-weighted MR imaging from MCAO animals. Left panel is vehicle treated, middle panel is nMSC treated, and right panel is aMSCγ treated animals.

CURRICULUM VITAE

MATTHEW K. TOBIN, B.S.

University of Illinois at Chicago
Medical Scientist Training Program
Graduate Program in Neuroscience
Department of Anatomy and Cell Biology

Email: mktobin2@uic.edu

Education

M.D., Ph.D:	University of Illinois at Chicago, College of Medicine Medical Scientist Training Program, Chicago, Illinois
B.S.:	University of Michigan, Literature, Science, and the Arts Neuroscience, Ann Arbor, Michigan, 2011

Awards

Jul. 2014 to Jul. 2015	Predoctoral NIH Training Grant #T32 HL007692-25 University of Illinois at Chicago, College of Medicine
2012	OptumHealth Presidential Student Mentor Grant American Society of Transplant Surgeons
2012	Dr. C.M. Craig Fellowship University of Illinois at Chicago, College of Medicine
2007 – 2008	William S. Bradford, D.D.S Scholarship University of Michigan, Ann Arbor, Michigan
2007 – 2008	Illinois State Scholar Illinois Student Assistance Commission
2007	Summer Research Fellowship Evanston Northwestern Healthcare, Evanston, Illinois

Licenses and Certifications

2010 – 2012	Phlebotomy Technician, State of Michigan
2008 – 2012	Emergency Medical Technician, State of Illinois
2008 – 2011	Emergency Medical Technician, State of Michigan
2008 – 2011	Emergency Medical Technician, National Registry of Emergency Medical Technicians
2008	Brain Trauma Foundation Certificate for Prehospital Care of Traumatic Brain Injury
2008	International Trauma Life Support (ITLS)

Research Support

AHA Predoctoral Fellowship 15PRE25080088 (Tobin, PI) 2015 – 2017
Mesenchymal stem cell promoted neuroregeneration following ischemic stroke
Goal: The goal of this project is to determine the potential of mesenchymal stem cells to promote long-term functional recovery following ischemic stroke via modulation of microglia and induction of neurogenesis.

Memberships in Professional Societies

2013 to present	American Association of Neurological Surgeons
2013 to present	Society for Neuroscience
2012 to present	Congress of Neurological Surgeons
2012 to present	American Physician Scientists Association
2012 to present	American College of Wound Healing and Tissue Repair
2011 to present	American Medical Association
2011 to present	American Medical Student Association

Research Experience

Jun. 2013 to present — *University of Illinois at Chicago, Anatomy and Cell Biology*
Graduate Student, Orly Lazarov, Ph.D.
- Developed a rodent model of ischemic stroke to investigate the interaction between inflammation and neurogenesis following ischemic injury.

Oct. 2011 to present — *University of Illinois at Chicago, Neurosurgery*
Graduate Research Assistant
- Performed data collection and analysis for multiple basic science and clinical research projects.
- Co-authored both manuscripts and abstracts.

Oct. 2011 to May 2013 — *University of Illinois at Chicago, Surgery*
Graduate Research Assistant, Amelia Bartholomew, M.D.
- Developed a murine model of acute kidney injury and chronic renal fibrosis to test nanoparticle and mesenchymal stem cell therapies.
- Helped develop a non-human primate model of renal transplantation to study allograft tolerance.

Oct. 2007 to Jul. 2011	*University of Michigan, Neurology* *Research Assistant, John Fink, M.D.* – Developed RNAi-based therapy against multiple forms of hereditary spastic paraplegia for both *in vitro* and *in vivo* applications.
Jun. 2008 to Aug. 2008	*Northwestern University, Otolaryngology* *Research Assistant, Donna Whitlon, Ph.D.* – Characterized morphology of cochlear spiral ganglion nerve fibers after treatment with different growth mediums.
Jun. 2007 to Aug. 2007	*Evanston Northwestern Healthcare, Behavior Genetics Unit* *Research Fellow, Alan Sanders, M.D.* – Performed DNA fragmentation analysis on isolated patient samples for studies on male sexual orientation.

Student Mentoring

Student	Current Position
Stacey Podkovik	Neurosurgery Resident, Riverside County Regional Medical Center
Terilyn Stephen	M.D./Ph.D. Candidate, University of Illinois at Chicago
Cindy Nahhas	M.D. Candidate, University of Illinois at Chicago
Zhan Yu	Research Assistant, University of Illinois at Chicago
Eric Gehrke	Post-baccalaureate Student, Northwestern University
Kianna Musaraca	Research Assistant, University of Illinois at Chicago
David Moore	B.S. Candidate, University of Illinois at Chicago
Kyra Lopez	Research Assistant, University of Illinois at Chicago
Amna Ali	B.S. Candidate, University of Illinois at Chicago
Christina Griffin	B.S. Candidate, University of Illinois at Chicago
Nakisa Dashti	B.S. Candidate, Northwestern University

Bibliography

Original Reports

1. **Tobin MK**, Lopez K, Pergande MR, Bartholomew AM, Cologna SM, Lazarov O. Mesenchymal stem cells induce recovery after stroke by regulation of inflammation and oligodendrogenesis. *J Am Heart Assoc*, 2019, in revision.
2. **Tobin MK**, Gragnaniello C, Sun F, Rangwala SD, Birk DM, Neckrysh S. Safety and efficacy of skipping C7 instrumentation in posterior cervicothoracic fusion. *World Neurosurg*, 2019. [Epub ahead of print]. PMID: 31154099.
3. **Tobin MK**, Musaraca K, Disouky A, Shetti A, Bheri A, Honer WG, Kim N, Bennett DA, Lazarov O. Human hippocampal neurogenesis persists in aged adults and Alzheimer's disease patients. *Cell Stem Cell*, 2019, 24(6):974-982. PMID: 31130513.
4. Tang T, Dong L, Ridgley DM, Ghura S, **Tobin MK**, Sun GY, LaDu MJ, Lee, JC. Cytosolic phospholipase A_2 facilitates oligomeric amyloid-β peptide association with microglia. *Mol Neurobiol*, 2019, 56(5):3222-3234. PMID: 30112630.

5. Hollands C, **Tobin MK**, Hsu M, Musaraca K, Yu T-S, Mishra R, Kernie SG, Lazarov O. Depletion of adult neurogenesis exacerbates cognitive deficits in Alzheimer's disease by compromising hippocampal inhibition. *Mol Neurodegener*. 2017, 12(1):64. PMID: 28886753.
6. **Tobin MK**, Birk D, Siemionow K, Neckrysh S, Schizas C. T1 pedicle subtraction osteotomy for the treatment of rigid cervical kyphotic deformity: clinical series of four patients and review of the literature. *J Neurosurg Spine*. 2017, 27(5):487-493. PMID: 28841105
7. Rangwala SD, **Tobin MK**, Birk DM, Butts JT, Nikas DC, Hahn YS. Pica in a child with anterior cingulate gyrus oligodendroglioma: Case report. *Pediatr Neurosurg*. 2017, 52(4):279-283. PMID: 28704833.
8. Rangwala SD, Birk DM, **Tobin MK**, Hahn YS, Nikas DC. Spontaneous resolution of spinal epidural hematoma resulting from domestic child abuse: Case report. *Pediatr Neurosurg*. 2017, 52(1):51-54. PMID: 27644085.
9. Bonds JA, Kuttner-Hirshler Y, Bartolotti N, **Tobin MK**, Pizzi M, Marr R, Lazarov O. Presenilin-1 dependent neurogenesis regulates hippocampal learning and memory. *PLoS One*. 2015, 10(6):e0131266. PMID: 26098332.
10. Birk DM, **Tobin MK**, Moss HE, Feinstein E, Charbel FT, Alaraj A. Improvement in venous outflow following superior sagittal sinus decompression after a gunshot wound to the head: Case report. *J Neurosurg*. 2015, 123(1):81-85. PMID: 25839927.
11. Alaraj A, **Tobin M**, Birk D, Aletich V. Role of argatroban during neurointerventional procedures in patients with heparin-induced thrombocytopenia. *J Neurointerv Surg*. 2014, 6(8):630-632. PMID: 24062254.

Book Chapters

1. **Tobin MK,** Denyer S, Kheirkhah P, Mehta AI. Intramedullary spinal cord tumors: Research areas and future therapies, in: *Tumors of the Spinal Canal: Surgical Approaches and Future Therapies*. 2019, manuscript in preparation.
2. **Tobin MK**, Testai FD: Rare genetic causes of stroke, in Caplan LR, Biller J, Leary MC, Lo EH, Thomas AJ, Yenari M, Zhang JH (eds): *Primer on Cerebrovascular Diseases, Second Edition*. Academic Press, 2017, pp. 545-554.
3. Birk DM, **Tobin MK**, Slavin KV: Neurosurgical options for control of chronic and malignant abdominal pain, in Kapural L (ed): *Chronic Abdominal pain: An Evidence Based, Comprehensive Guide to Clinical Management*. Springer, 2014, pp. 239-244.
4. Alaraj A, **Tobin MK**, Birk DM, Charbel FT: Simulation for neurosurgery and neurosurgical procedures, in Levine AI, DeMaria S, Schwartz AD, Sim AJ (eds): *The Comprehensive Textbook of Healthcare Simulation*. Springer, 2013, pp. 415-423.

Reviews

1. Skeoch GD, **Tobin MK**, Khan S, Linninger AA, Mehta AI. Corticosteroid treatment for metastatic spinal cord compression: A review. *Global Spine J*. 2017, 7(3):272-279. PMID: 28660111.

2. Genev IK[*], **Tobin MK[*]**, Zaidi S, Khan S, Amirouche F, Metha AI. Spinal compression fracture management: A review of current treatment strategies and possible future avenues. *Global Spine J*. 2017, 7(1):71-82. PMID: 28451512. [*]These authors contributed equally to the work.
3. Hobbs JG, Desai B, Young JS, Polster SP, **Tobin MK**, Geraghty JR, Linninger AA, Oyelese AA, Shin JH, Bydon M, Mehta AI. Intramedullary spinal cord tumors: A review and discussion of surgical rationale. *World Spinal Column J*. 2016, 7(2):65-83.
4. **Tobin MK[*]**, Geraghty JR[*], Engelhard HH, Linninger AA, Mehta AI. Intramedullary spinal cord tumors: A review of current and future treatment strategies. *Neurosurg Focus*. 2015, 39(2):E14. PMID: 26235012. [*]These authors contributed equally to the work.
5. **Tobin MK**, Bonds JA, Minshall RD, Pelligrino DA, Testai FD, Lazarov O. Neurogenesis and inflammation following ischemic stroke: what is known and where we go from here. *J Cereb Blood Flow Metab*. 2014, 34(10):1573-1584. PMID: 25074747.
6. Antony AK, Rodby K, **Tobin MK**, O'Connor MI, Pearl RK, DiPietro LA, Breidenbach WC, Bartholomew AM. Composite tissue allotransplantation and dysregulation in tissue repair and regeneration: a role for mesenchymal stem cells. *Front Immunol*. 2013, 4:188. PMID: 23847625.
7. Alaraj, A, Charbel FT, Birk D, **Tobin M**, Luciano C, Banerjee PP, Rizzi S, Sorenson J, Foley K, Slavin K, Roitberg B. Role of cranial and spinal virtual and augmented reality simulation using Immersive Touch modules in neurosurgical training. *Neurosurgery*. 2013, 72(Suppl 1):A115-A123. PMID: 23254799.

Abstracts

1. **Tobin MK**, Gragnaniello C, Rangwala SD, Sun F, Birk DM, Neckrysh S. Safety and efficacy of skipping C7 instrumentation in posterior cervicothoracic fusion. [abstract]. In: 2019 Congress of Neurological Surgeons Annual Meeting; 19-23 Oct 2019; San Francisco. Schaumburg, IL: Congress of Neurological Surgeons.
2. Gragnaniello C, **Tobin MK**, Chaudhry N, Neckrysh S. Secular trends in lumbar spinal canal dimensions in a modern U.S. population. [abstract]. In: 2019 Congress of Neurological Surgeons Annual Meeting; 19-23 Oct 2019; San Francisco. Schaumburg, IL: Congress of Neurological Surgeons.
3. Chaudhry N, **Tobin MK**, Gragnaniello C, Neckrysh S. Secular trends in cervical spinal canal dimensions in a modern U.S. population. [abstract]. In: 2019 Congress of Neurological Surgeons Annual Meeting; 19-23 Oct 2019; San Francisco. Schaumburg, IL: Congress of Neurological Surgeons.
4. **Tobin MK**, Lopez K, Pergande MR, Bartholomew AM, Cologna SM, Lazarov O. Treatment with activated mesenchymal stem cells increases long-term functional recovery following ischemic stroke via reduction of microglia activation and induction of oligodendrogenesis. [abstract]. In: Society for Neuroscience Annual Meeting; 4-7 Nov 2018; San Diego. Washington, DC: Society for Neurosocience.
5. Lazarov O, Musaraca K, Bheri A, Kim N, Bennett DA, **Tobin MK**. Persistence of adult hippocampal neurogenesis through aging and cognitive dysfunction.

[abstract]. In: Society for Neuroscience Annual Meeting; 4-7 Nov 2018; San Diego. Washington, DC: Society for Neurosocience.

6. **Tobin MK**, Bartholomew AM, Lazarov O. Treatment with activated mesenchymal stem cells increase long-term recovery following ischemic stroke via reduction of microglia activation and induction of oligodendrogenesis. [abstract]. In: 2018 Translational Science; 19-21 Apr 2018; Washington, DC. Washington, DC: Association for Clinical and Translation Science.
7. **Tobin MK**, Bartholomew AM, Lazarov O. Activated mesenchymal stem cells increase long-term recovery following ischemic stroke via reduction of microglia activation and induction of oligodendrogenesis. [abstract]. In: Society for Neuroscience Chicago Chapter Annual Meeting; 23 Mar 2018; Chicago. Washington, DC: Society for Neurosocience.
8. **Tobin MK**, Bartholomew AM, Lazarov O. Hypoxia-induced changes in neural stem cell and microglia characteristics. [abstract]. In: Society for Neuroscience Annual Meeting; 12-16 Nov 2016; San Diego. Washington, DC: Society for Neurosocience.
9. Rangwala SD, **Tobin MK**, Birk DM, Neckrysh S. Safety and efficacy of skipping C7 instrumentation in posterior cervicothoracic fusion. [abstract]. In: 84th AANS Annual Scientific Meeting; 30 Apr-4 May 2016; Chicago. Rolling Meadows: American Association of Neurological Surgeons.
10. **Tobin MK**, Bonds JA, Szilagyi E, Bartholomew AM, Pelligrino DA, Lazarov O. Changes in microglia and neural stem cell characteristics after exposure to hypoxia. [abstract]. In: Society for Neuroscience Annual Meeting; 17-21 Oct 2015; Chicago. Washington, DC: Society for Neuroscience.
11. Bonds JA, **Tobin MK**, Minshall R, Pelligrino D, Lazarov O. Endothelial caveolin-1 regulates the neurogenic vascular niche. [abstract]. In: Society for Neuroscience Annual Meeting; 17-21 Oct 2015; Chicago. Washington, DC: Society for Neuroscience.
12. **Tobin MK**, Rangwala S, Birk DM, Neckrysh S. Safety and efficacy of skipping C7 instrumentation in posterior cervicothoracic fusion. *Global Spine J*. 2015, S1(5):A023.
13. **Tobin MK**, Birk D, Siemionow K, Neckrysh S, Schizas C. T1 pedicle subtraction osteotomy for the treatment of rigid cervical kyphotic deformity. [abstract]. In: 82nd AANS Annual Scientific Meeting; 5-9 Apr 2014; San Francisco. Rolling Meadows: American Association of Neurological Surgeons.
14. **Tobin M**, O'Connor M, Szilagyi E, Capezio N, Nuñez L, Spretz R, Noriega, S, Bartholomew A. The effect of EGF and FSP1 targeting of nanoparticle delivery of IL-10 and GM-CSF following acute kidney injury. *Am J Transplant*. 2013, 13(S5):415. Abstract #C1302.
15. **Tobin M**, O'Connor M, Szilagyi E, Capezio N, Nuñez L, Spretz R, Noriega, S, Bartholomew A. Nanoparticle directed changes in kidney inflammation following acute ischemia. [abstract]. In: ASCI/AAP Joint Meeting; 26-28 Apr 2013; Chicago. Belleville: Association of American Physicians; Ann Arbor: The American Society of Clinical Investigation.
16. Neckrysh S, Siemionow K, Birk D, **Tobin M**, Schizas C. T1 pedicle subtraction osteotomy for the treatment of rigid cervical kyphotic deformity. [abstract]. In: 29th

Annual Meeting of the AANS/CNS Section on Disorders of the Spine and Peripheral Nerves; 6-9 Mar 2013; Phoenix. Rolling Meadows: American Association of Neurological Surgeons; Schaumburg: Congress of Neurological Surgeons.

17. **Tobin MK**, O'Connor MI, Szilagyi E, Capezio NE, Nuñez L, Spretz R, Bartholomew AM. The effect of EGF targeting on nanoparticle delivery of IL-10 and GM-CSF following acute kidney injury. [abstract]. In: University of Illinois at Chicago College of Medicine Research Forum; 16 Nov 2012; Chicago.
18. Rainier S, Bentley B, Siman-Tov T, **Tobin M**, Moore J, Brown, Jr. RH, Fink JK. 2009 Neuropathy target esterase mutations in individuals with sporadic ALS. [abstract]. In: American Society of Human Genetics 59th Annual Meeting; 20-24 Oct 2009; Honolulu. Bethesda: The American Society of Human Genetics.
19. **Tobin MK**, Rainier SR, Fink JK. 2009. Developing therapy for hereditary spastic paraplegia. [abstract]. In: Michigan Chapter Society for Neuroscience 40th Annual Meeting; 15 May 2009; Kalamazoo. Washington (DC): Society for Neuroscience.
20. **Tobin MK**, Moore J, Rainier SR, Bentley BA, Fink JK. 2008. Effects of spastin and atlastin mutations using a knockout mouse model of hereditary spastic paraplegia. [abstract]. In: University of Michigan Undergraduate Research Opportunity Program Symposium; 4 Apr 2008; Ann Arbor.

Presentations

Oral

1. **Tobin MK**, Lopez K, Pergande MR, Bartholomew AM, Cologna SM, Lazarov O. Treatment with activated mesenchymal stem cells increases long-term functional recovery following ischemic stroke via reduction of microglia activation and induction of oligodendrogenesis. Presented at the Society for Neuroscience Annual Meeting, 4-7 Nov 2018.
2. Lazarov O, Musaraca K, Bheri A, Kim N, Bennett DA, **Tobin MK**. Persistence of adult hippocampal neurogenesis through aging and cognitive dysfunction. Presented at the Society for Neuroscience Annual Meeting, 4-7 Nov 2018.
3. **Tobin MK**, Bartholomew AM, Lazarov O. Activated mesenchymal stem cells increase long-term recovery following ischemic stroke via reduction of microglia activation and induction of oligodendrogenesis. Presented at the University of Illinois at Chicago Graduate Program in Neuroscience Research Symposium, 22 Feb 2018, Chicago.
4. **Tobin MK**, Bartholomew AM, Lazarov O. Hypoxia-induced changes in neural stem cell and microglia characteristics. Presented at the University of Illinois at Chicago GEMS Research Symposium, 16 Sep 2016, Chicago.
5. **Tobin MK**, Rangwala S, Birk DM, Neckrysh S. Safety and efficacy of skipping C7 instrumentation in posterior cervicothoracic fusion. Presented at the Global Spine Congress, 20-23 May 2015, Buenos Aires.

Posters

1. **Tobin MK**, Gragnaniello C, Rangwala SD, Sun F, Birk DM, Neckrysh S. Safety and efficacy of skipping C7 instrumentation in posterior cervicothoracic fusion.

2019 Congress of Neurological Surgeons Annual Meeting, 19-23 Oct 2019, San Francisco.

2. Gragnaniello C, **Tobin MK**, Chaudhry N, Neckrysh S. Secular trends in lumbar spinal canal dimensions in a modern U.S. population. 2019 Congress of Neurological Surgeons Annual Meeting, 19-23 Oct 2019, San Francisco.
3. Chaudhry N, **Tobin MK**, Gragnaniello C, Neckrysh S. Secular trends in cervical spinal canal dimensions in a modern U.S. population. 2019 Congress of Neurological Surgeons Annual Meeting, 19-23 Oct 2019, San Francisco.
4. **Tobin MK**, Bartholomew AM, Lazarov O. Treatment with activated mesenchymal stem cells increase long-term recovery following ischemic stroke via reduction of microglia activation and induction of oligodendrogenesis. 2018 Translational Science, 19-21 Apr 2018, Washington, DC.
5. **Tobin MK**, Bartholomew AM, Lazarov O. Activated mesenchymal stem cells increase long-term recovery following ischemic stroke via reduction of microglia activation and induction of oligodendrogenesis. Society for Neuroscience Chicago Chapter Annual Meeting, 23 Mar 2018, Chicago.
6. **Tobin MK**, Bartholomew AM, Lazarov O. Mesenchymal stem cells promote the regenerative capacity of neural stem cells. University of Illinois at Chicago Annual Neuroscience Day, 13 Oct 2017, Chicago.
7. **Tobin MK**, Bartholomew AM, Lazarov O. Hypoxia-induced changes in neural stem cell and microglia characteristics. Society for Neuroscience Annual Meeting, 12-16 Nov 2016, San Diego.
8. **Tobin MK**, Bartholomew AM, Lazarov O. Hypoxia-induced changes in neural stem cell and microglia characteristics. University of Illinois at Chicago GEMS Research Symposium, 16 Sep 2016; Chicago.
9. Rangwala SD, **Tobin MK**, Birk DM, Neckrysh S. Safety and efficacy of skipping C7 instrumentation in posterior cervicothoracic fusion. 84th AANS Annual Scientific Meeting; 30 Apr-4 May 2016; Chicago.
10. **Tobin MK**, Bonds JA, Szilagyi E, Bartholomew AM, Pelligrino DA, Lazarov O. Changes in microglia and neural stem cell characteristics after exposure to hypoxia. Society for Neuroscience Annual Meeting, 17-21 Oct 2015, Chicago.
11. **Tobin MK**, Szilagyi E, Bartholomew AM, Lazarov O. Mesenchymal stem cells promote the regenerative capacity of microglia and neural stem cells after hypoxia. University of Illinois at Chicago College of Medicine Research Forum, 21 Nov 2014, Chicago.
12. **Tobin MK**, Szilagyi E, Bartholomew AM, Lazarov O. Mesenchymal stem cells promote the regenerative capacity of microglia and neural stem cells after hypoxia. University of Illinois at Chicago Annual Neuroscience Day, 18 Sep 2014, Chicago.
13. **Tobin MK**, Birk D, Siemionow K, Neckrysh S, Schizas C. T1 pedicle subtraction osteotomy for the treatment of rigid cervical kyphotic deformity. American Association of Neurological Surgeons Annual Scientific Meeting, 5-9 Apr 2014, San Francisco.
14. **Tobin M**, O'Connor M, Szilagyi E, Capezio N, Nuñez L, Spretz R, Noriega, S, Bartholomew A. The effect of EGF and FSP1 targeting of nanoparticle delivery of IL-10 and GM-CSF following acute kidney injury. American Transplant Congress

Annual Meeting, 18-22 May 2013, Seattle. – *Listed as a "Poster of Distinction" placing it in the top 10% of posters reviewed and scored.*

15. **Tobin MK**, O'Connor M, Capezio NE, Bartholomew AM. The effect of EGF targeting on nanoparticle delivery of IL-10 and GM-CSF following acute kidney injury. University of Illinois at Chicago College of Medicine Research Forum, 16 Nov 2012, Chicago.
16. Szilagyi E, Sears ML, Polchert D, Douglas GW, Wang H, Salomon DR, O'Connor M, **Tobin MK**, Bartholomew AM. Activated 3rd party MSC overcome MHC matching effects to potentiate heart transplant survival. American Transplant Congress Annual Meeting, 2-6 Jun 2012, Boston.
17. Szilagyi E, Premanand K, Willman MA, DiPietro LA, Salomon DR, Kenyon NS, Zhu J, **Tobin MK**, Bartholomew AM. Potentiating marrow derived mesenchymal stem cells via interferon gamma: results of form and functional changes. American Transplant Congress Annual Meeting, 2-6 Jun 2012, Boston.
18. **Tobin MK**, Rainier S, Fink JK. Developing RNA Interference as therapy for SPG6 hereditary spastic paraplegia. Michigan Chapter Society for Neuroscience Annual Meeting, 2009, Kalamazoo.
19. **Tobin MK**, Moore J, Bentley BA, Clark MC, Rainier S, Fink JK. Effects of spastin and atlastin mutations using a knockout mouse model of hereditary spastic paraplegia. University of Michigan Undergraduate Research Opportunity Program Symposium, 2008, Ann Arbor.